ORDER REDUCTION AND EIGENSTRUCTURE ASSIGNMENT FOR NONSMOOTH VIBRATING SYSTEMS: A NONLINEAR NORMAL MODES APPROACH

by

Rongdong Lu

RECOMMENDED:

Advisory Committee Chair

Department Head

APPROVED:

Dean, College of Science, Engineering and Mathematics

Dean of the Graduate School

8-13-02

Date

ORDER REDUCTION AND EIGENSTRUCTURE ASSIGNMENT FOR NONSMOOTH VIBRATING SYSTEMS: A NONLINEAR NORMAL MODES APPROACH

A

THESIS

Presented to the Faculty

of the University of Alaska Fairbanks

In Partial Fulfillment of the Requirements

for the Degree of

MASTER OF SCIENCE

By

Rongdong Lu

Fairbanks, Alaska

August 2002

ABSTRACT

Two related problems are addressed in this thesis.

The first one is for order reduction of conservative vibrating systems with piecewise linear nonsmooth nonlinearities of arbitrary dimension. Linear-based, PMM-based and LELSM-based order reduction transformations are applied. The technique is applied to multi-degree-of-freedom systems with nonsmooth clearance, deadzone, bang-bang, and saturation nonlinearities. The resulting approximate frequencies are compared with those obtained from numerical simulations.

The second technique is eigenstructure assignment of n-degree-of-freedom conservative vibrating systems with nonsmooth nonlinearities. Three distinct control strategies which utilize methods for approximating the NNM frequencies and mode shapes are employed. First, PMM for approximating NNM frequencies is used to determine n constant actuator gains for eigenvalue placement. Second, an approximate single-degree-of-freedom reduced model is found with one actuator gain for the mode to be controlled. The third strategy allows the frequencies and mode shapes (eigenstructure) to be placed by using a full $n \times n$ matrix of actuator gains and employing LELSM for approximating NNM frequencies and mode shapes.

LIST OF FIGURES

LIST OF TABLE

ACKNOWLEGEMENTS

I want to thank those many people who made this thesis possible.

This work was carried out under financial support of Graduate school of UAF and Air Force Office of Scientific Research, monitored by Dr. Dean Mook, under contract number F49620-01-1-0388.

I am indebted to Dr. Butcher who as my advisor, provided great ideas, suggestions and encouragements whenever I needed help, and devoted his valuable time for the discussions and comments during the writing phase of this thesis. Also I very appreciate the kind help from my other committee members, Dr. Lee and Dr. Lin.

CHAPTER 1

INTRODUCTION

Nonsmooth nonlinearities exist in many mechanical systems either by design or as the result of wear or failure. In particular, nonlinear systems in which the force-displacement curves are piecewise linear include bilinear systems with a nonvanishing clearance (i.e. gap between the equilibrium and crossing boundaries) and systems with symmetric nonlinearities such as deadzone, saturation, and bang-bang. These systems are of great importance in the modeling of such phenomena as joint dynamics (Gaul and Lenz, 1997), turbines and compressors subjected to casing rub (Choy *et al*, 1989), rotor-bearing systems with deadzone (Flowers and Wu, 1996), and transmission gears with backlash (Slotine and Li, 1991). Two problems related to these systems are addressed here: order reduction and eigenstructure assignment. Accurate reduced order models of large dimensional nonsmooth systems are an invaluable aid in the design and control of many vibrating systems. In such systems, periodic motions take place on curved invariant manifolds and are called nonlinear normal modes (NNMs). Such reduced order models are approximations to the actual NNMs of the full model. Important contributions to the subject of NNMs in nonsmooth systems include the studies of Zuo and Curnier (1994), Chen and Shaw (1996), Chati *et al.* (1997), and Butcher (1999). In the latter paper the BNM frequencies of a nonsmooth bilinear system with nonvanishing clearance were approximated using three analytical techniques which are based on the well-known bilinear frequency relation. The results were compared with those obtained from

numerical simulations of the actual NNM motions.

The subject of order reduction of nonsmooth systems has received little attention, however. Rhee and Burton (2000) applied a previously-developed linear-based Guyan-like reduction procedure which preserves the exact eigenstructure of the linearized model (Burton and Young, 1994; Burton and Rhee, 2000) to the cases of deadzone and bang-bang nonlinearities in a two degree-of-freedom vibrating system. The frequencies of the reduced models were compared with those of the actual NNMs in the full model obtained by direct numerical simulation. The method has the advantages that the coordinates of the reduced order model are a subset of the original physical coordinates and the form of the nonsmooth nonlinearity is retained in the reduced model. However, the nonlinearity is not accounted for in the transformation since it is linear-based. Consequently, the reduced models' frequencies were shown to differ significantly from the NNM frequencies of the full model. An alternate method pursued by Jiang et al (2001) and based on the concept of invariant manifolds involves obtaining a nonsmooth Galerkin-based order reduction transformation which utilizes the NNMs. This had been previously accomplished for smooth nonlinearities (Shaw and Pierre, 1993; Shaw *et al*, 1999; Burton and Rhee, 2000; Pesheck *et al.*, 2002). For vibrating systems with a nonsymmetric clearance nonlinearity, which have been studied by R. J. Comparin and R. Singh (1900), M. D. Todd and L. N. Virgin (1996), two different methods for obtaining reduced order models which more accurately track the original modes of the full systems than does the linear-based reduced model were applied by Butcher (2001). The resulting reduced models were improved from the linear-based versions for certain parameter ranges.

Here, a technique for order reduction of vibrating systems with symmetric nonsmooth nonlinearities of arbitrary dimension is proposed. First, the linear-based order reduction transformation used by Rhee and Burton (2000) is applied. It is shown that when only one master coordinate is retained, the exact frequency of the reduced order model may be derived analytically and used to approximate the nonlinear normal mode (NNM) frequency of the full model. In this context, the linear-based order reduction procedure serves as yet another method for approximating the true NNM frequencies as in (Butcher, 1999), and the resulting frequencies are compared with those obtained from the previous techniques based on the bilinear frequency relation and the exact ones obtained by numerical simulation of the full model. Second, this result is in turn used to construct improved reduced order models whose frequencies are much closer approximations to the NNM frequencies for the full model than those obtained via the linear-based transformation. For this purpose, two of the previous approximation techniques (called the piecewise modal method and local equivalent linear stiffness method) are utilized to obtain more accurate frequencies than those obtained from the linear-based order reduction. The technique is applied to systems with symmetric deadzone, bang-bang, and saturation nonlinearities. It is shown via direct simulation that the dynamics of the improved reduced models are much better at tracking the NNMs of the full models than those obtained via the linear-based transformation.

The problem of eigenstructure assignment for linear multi-degree-of-freedom vibrating systems has been covered by Inman (1989). The two problems considered were eigenvalue (pole) placement, in which the frequencies are shifted to preselected values via

constant-gain proportional feedback, and eigenstructure assignment, in which the use of feedback allows the eigenfrequencies as well as the mode shapes (eigenvectors) to be specified. If one desires to implement these techniques for nonsmooth piecewise linear systems, however, the application of constant-gain proportional feedback is not straightforward due to the fact that the exact NNM manifolds and frequencies of the uncontrolled system are not known. While it may be possible to implement gain switching (Stengel, 1994) at the crossing boundaries or various nonlinear control strategies that have been suggested for such systems (Slotine and Li, 1991), these may be difficult to accomplish in practice because of the inaccuracies caused by control delays or sensor errors. Also, constant-gain linear controllers are much easier to implement and are more cost-effective in practical applications. These issues are at the heart of a need to reconsider possible strategies for implementing constant-gain proportional state feedback control for systems with nonsmooth nonlinearities, and this issue is addressed here by considering the special case of conservative vibrating systems and position feedback.

Here, three strategies for eigenstructure assignment (the first two result in eigenvalue placement only) of such systems are proposed which utilize two of the methods, the piecewise modal method (PMM) and the local equivalent linear stiffness method (LELSM), for approximating the NNM frequencies and mode shapes used by Butcher (1999). The first strategy requires determining n constant actuator gains for an n degree-of-freedom system while the second involves finding an approximate single-degree-of-freedom reduced order model with one actuator gain for the mode to be controlled. The order reduction method used here is that of Rhee and Burton (2000) and preserves the

exact eigenstructure of one of the linear subregions. The third strategy allows the designer to specify the entire eigenstructure (frequencies and mode shapes) by using a full $n \times n$ matrix of constant actuator gains. These techniques are applied to a two degree-of-freedom system with a bilinear clearance nonlinearity and the controlled system is numerically simulated. The resulting frequencies and mode shapes are then compared for accuracy with the desired ones.

Chapter 2

Nonlinear Normal Modes

Since the first investigations of nonlinear normal modes (NNMs) by R. M. Rosenberg (1962), it has been a subject of much investigation for various nonlinear systems (Vakakis *et al,* 1996). In nonlinear vibrating systems, nonlinear normal modes are motions that are periodic in time and occur along the invariant manifolds in the configuration or phase space. NNMs are the nonlinear equivalent of linear normal modes, but unlike linear systems, superposition does not apply. It's important to know NNM frequencies since the forced system is resonant at these frequencies. For n-degree-of-freedom linear systems, normal modes are represented as orthogonal eigenvectors (straight perpendicular lines which intersect at the origin) in the n-dimensional configuration space, Fig.1(a) shows a 2-degree-of-freedom linear system in configuration space. For n-degree-of-freedom nonlinear systems, the NNMs are represented as closed curves in the n-dimensional configuration space. These curves are the projections of higher dimensional invariant manifolds in the 2n-dimensional phase space. The curves are tangent to the linearized system's eigenvectors at the origin as in Fig.1(b). In general, the NNM frequencies depend on the total energy or amplitude. All motions that are not NNMs are generally quasiperiodic as in Fig.2. It is shown in this thesis that NNMs enable a reduced order model to be obtained which is more accurate than one obtained via a linear-based order reduction transformation.

If the phase space manifold or the vector field are differentiable everywhere, then the

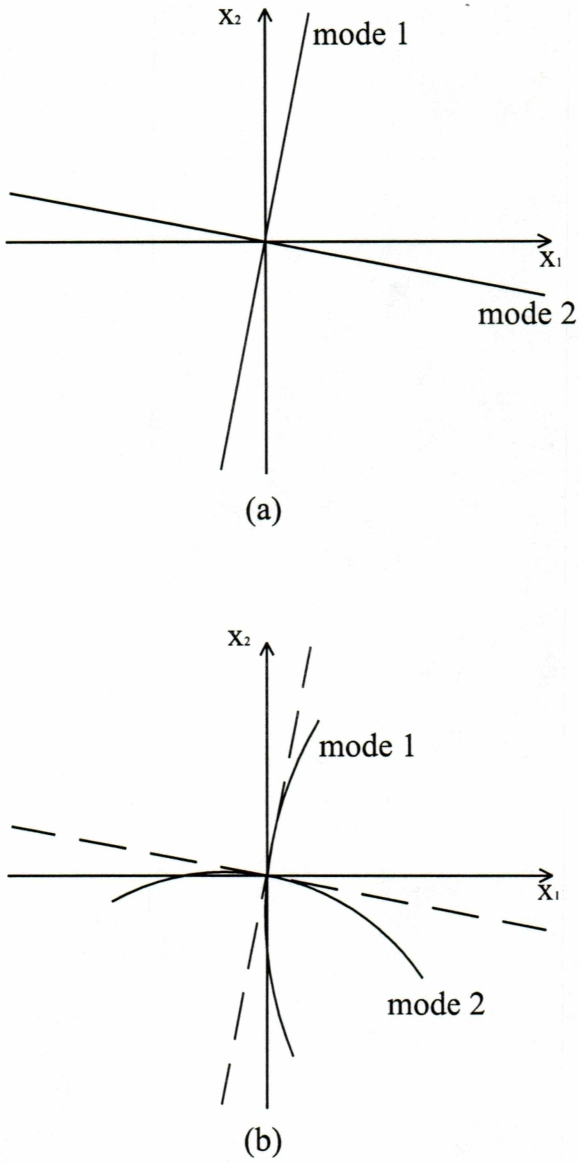

Figure 1: a) Normal modes of a linear system in configuration space.
(b)Normal modes of a smooth nonlinear system in configuration space.

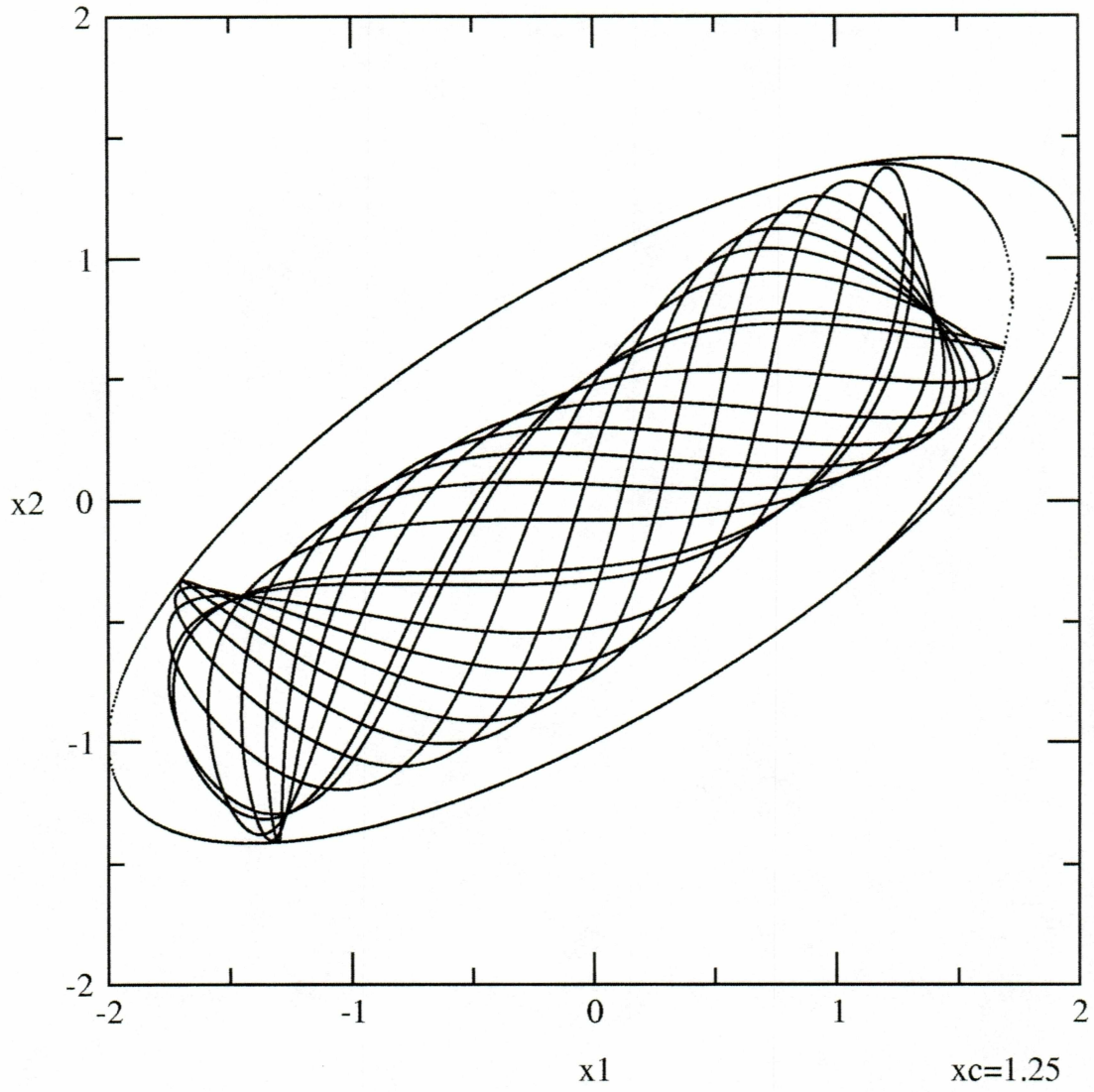

Figure 2: A quasiperiodic vibrating system with clearance nonlinearity

dynamical system is smooth (e.g. quadratic or cubic nonlinearities); otherwise it is nonsmooth.

Consider the following equations of motion for a smooth nonlinear system:

$$\begin{cases} \dfrac{d^2x}{dt^2} = -\dfrac{\partial V}{\partial x} \\ \dfrac{d^2y}{dt^2} = -\dfrac{\partial V}{\partial y} \end{cases} \tag{1}$$

The potential energy of this conservative system is $V = V(x, y)$, and the total energy is given by

$$\frac{1}{2}\left[\left(\frac{dx}{dt}\right)^2 + \left(\frac{dy}{dt}\right)^2\right] + V(x, y) = h \tag{2}$$

Let y=f(x) represent the invariant NNM manifold. Using the chain rule,

$$\frac{dy}{dt} = \frac{dy}{dx}\frac{dx}{dt} \qquad \frac{d^2y}{dt^2} = \frac{d^2y}{dx^2}\left(\frac{dx}{dt}\right)^2 + \left(\frac{dy}{dx}\right)\frac{d^2x}{dt^2} \tag{3}$$

Substituting (1) into the second of (3), we obtain

$$-\frac{\partial V}{\partial y} = \frac{d^2y}{dx^2}\left(\frac{dx}{dt}\right)^2 - \frac{dy}{dx}\frac{\partial V}{\partial x} \tag{4}$$

Substituting the first of (3) into (2), yields

$$\frac{1}{2}\left(\frac{dx}{dt}\right)^2\left[1 + \left(\frac{dy}{dx}\right)^2\right] + V(x, y) = h \tag{5}$$

Solving (5) for $\left(\frac{dx}{dt}\right)^2$ and substituting into (4), we obtain

$$2(h-V)\frac{d^2y}{dx^2}+\left[1+\left(\frac{dy}{dx}\right)^2\right]\left(\frac{\partial V}{\partial y}-\frac{dy}{dx}\frac{\partial V}{\partial x}\right) = 0 \tag{6}$$

Equation (6)(a 2nd order nonlinear o.d.e.) can be used to find the invariant manifold y=f(x).

Fig.3 shows an example of a smooth nonlinear system (Month and Rand, 1977). For spring k_3, k_1, $f = \delta + k\delta^3$, k_2 is coupling spring, $f = \delta^3$. Therefore, the total potential energy is

$$V(x,y) = \frac{1}{2}x^2+\frac{1}{4}kx^4+\frac{1}{4}(x-y)^4+\frac{1}{2}y^2+\frac{1}{4}ky^4 \tag{7}$$

For this system, the NNM plot as straight line segment as y=cx. This is called "similar normal mode", substituting y=cx and (7) in (6) yields

$$\frac{\partial V}{\partial y}-\frac{dy}{dx}\frac{\partial V}{\partial x} = -x^3(1-c)^3+cx+kc^3x^3-c(x+kx^3+x^3(1-c)^3) = 0 \tag{8}$$

or

$$c^4+(k-2)(c^3-c)-1 = 0 \tag{9}$$

which gives

$$\begin{aligned} &c^4+(k-2)(c^3-c)-1 = 0 \\ &c = 1,-1,1-\frac{k}{2}\pm\sqrt{\frac{k(k-4)}{2}} \end{aligned} \tag{10}$$

If k<4, then only two similar NNMs are present with slopes of ± 1 in the x-y configuration

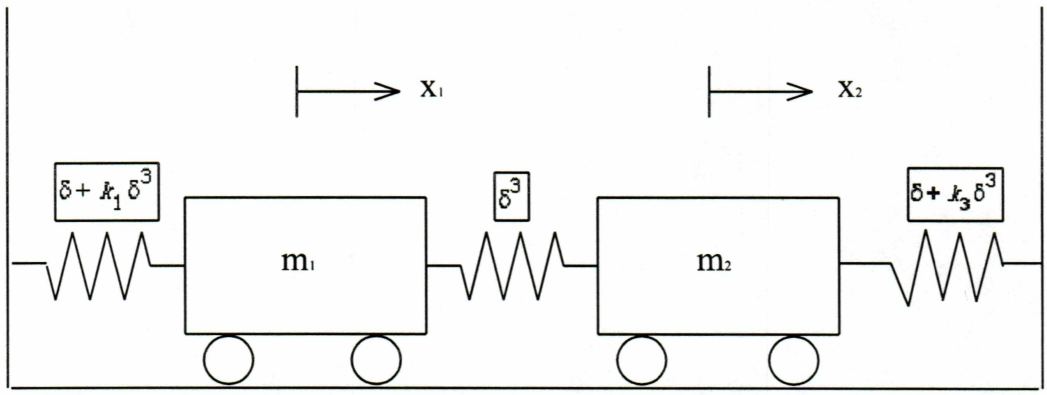

Figure 3: A smooth nonlinear vibrating system.

space. If k>4, then two additional NNMs are present.

From the example above, we can find out some additional characteristics of NNMs for smooth systems:

1. Frequency depends upon amplitude A and the slope of the line segment corresponding to the NNM depends upon the amplitude of vibration (although this is not true above).

2. The presence of higher harmonics will generally cause NNM to plot as curved lines segment through origin (called a "nonsimilar normal mode").

3. The shape of curved line segment which represent NNM will typically change with amplitude of vibration.

4. The end point of the line segment (curved or straight) represents places where the kinetic energy is zero.

5. x and y vanish simultaneously twice per cycle (corresponding to passage through the origin of x-y plan)

6. Both $\frac{dx}{dt}$ and $\frac{dy}{dt}$ vanish twice/cycle (corresponding to end point of line segment).

Nonlinear nonsmooth systems maybe piecewise linear. Such a system is comprised of separate linear subregions. If there are two linear subregions, the system is bilinear with one switching boundary. If there are three linear subregions, the system is trilinear with two switching boundaries.

NNMs for nonsmooth systems have different characteristics from those for smooth systems. For a bilinear system, some of the differences are listed as follows:

1. While the motions associated with most initial conditions of bilinear systems are

quasiperiodic or even chaotic, the motions of bilinear normal modes (BNMs) are periodic in time. Hence, resonance occurs when the system is forced at the associated frequencies or, since the motions are in general not sinusoidal, integral multiples of these frequencies.

2. The trajectories of BNMs in the configuration space are open curves (instead of straight lines as in the linear case), which, in contrast to NNMs of smooth nonlinear systems, neither pass through the origin nor are orthogonal at their intersection. Although the displacements do not vanish simultaneously, they do reach their maxima and minima at the same time, however.

3. If the clearance is zero, then the BNM frequencies are constant and independent of the energy level since the nonlinearity is concentrated at the origin. For a non-zero clearance, however, the frequencies depend on the energy (initial amplitude).

4. For weak non-linearities, the number of structurally stable BNMs is generally equal to the number of linear modes for non-resonant cases. Unlike the case for smooth non-linear systems, sufficient conditions for the existence and uniqueness of normal modes for bilinear systems are not available (although a necessary condition is given by Chen and Shaw(1996). As the strength of non-linearity increases, therefore, additional BNMS which have increasingly more complicated motions may occur along with regions of chaotic behavior.

CHAPTER 3

EXAMPLES OF NONSMOOTH NONLINEARITIES

Four nonlinearities are considered in this paper.

3.1 Bilinear Clearance Nonlinearity

A n-degree-of-freedom system with clearance nonlinearity is shown in Fig.4 and can be described by the equations below. It's a bilinear system, $f(x_1)$ is the nonlinear term.

$$\begin{aligned} & m_1\ddot{x}_1 + k_1x_1 - k_1x_2 + f(x_1) = 0 \\ & m_2\ddot{x}_2 + (k_1 + k_2)x_2 - k_1x_1 - k_2x_3 = 0 \\ & \quad \cdots \\ & m_n\ddot{x}_n + (k_{n-1} + k_n)x_n - k_{n-1}x_{n-1} = 0 \end{aligned} \qquad f(x_1) = \begin{cases} 0; & (x_1 < x_c) \\ k_c(x_1 - x_c); & (x_1 > x_c) \end{cases} \tag{11}$$

The asymmetric bilinear stiffness of the first mass is plotted in Fig.5 in which it is seen that the overall domain is divided into two distinct linear subregions in which the total energy is always conserved. Since the clearance x_c is *not* restricted to be positive, a negative clearance, or interference, is also allowed. Since the masses' positions are measured from equilibrium, penetration into the second subregion is made only when the energy of the system is sufficient such that the clearance is traversed by the first mass, i.e. $x_1 > x_c$. Otherwise if the energy is insufficient for contact with the free spring, then the system remains in the first linear subregion. In the case of interference, the energy must be sufficient for the first subregion to be obtained (i.e. $x_1 < x_c$); otherwise the system remains continuously in contact with the free spring.

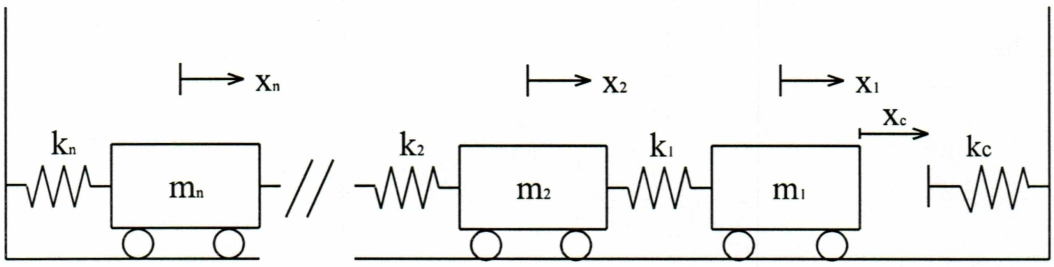

Figure 4: An *n*-degree-of-freedom Bilinear Vibrating System With a Clearance Nonlinearity

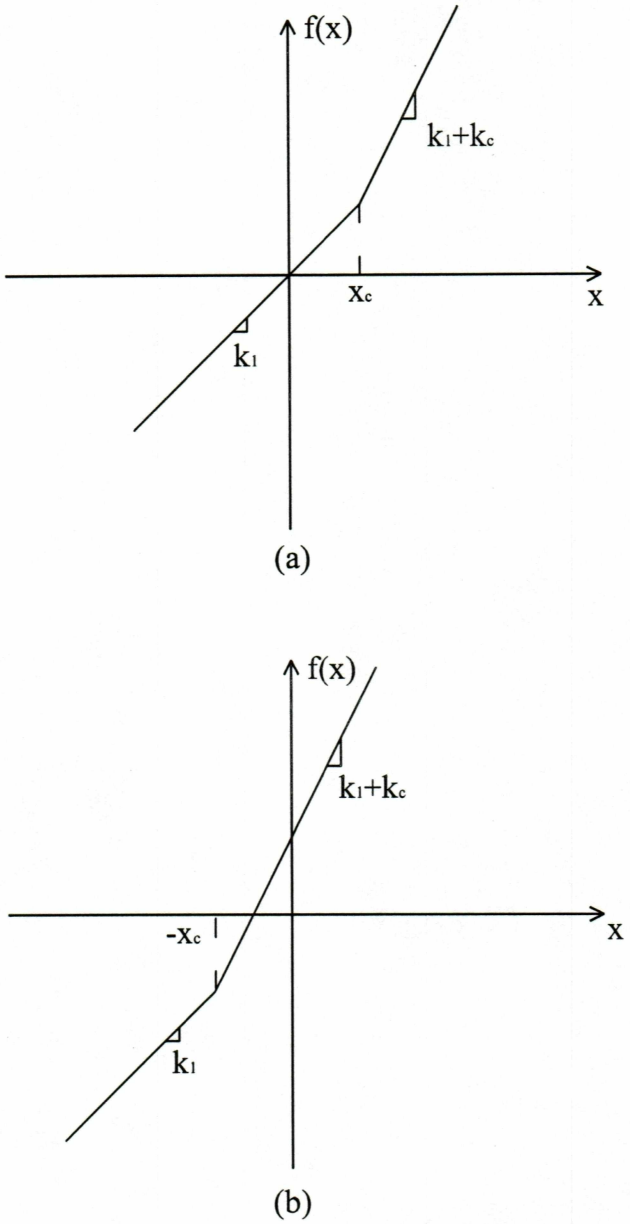

Figure 5: Force versus displacement of the first mass for the cases of a) clearance and b) interference

The scaled variables

$$\kappa_c = \frac{k_c}{k_1} \qquad \omega_- = \sqrt{\frac{k_1}{m_1}} \qquad \omega_+ = \sqrt{\frac{k_1 + k_c}{m_1}}$$

$$\alpha = \frac{\omega_+}{\omega_-} = \sqrt{1 + \kappa_c} \tag{12}$$

are now introduced where ω_- and ω_+ are the linear frequencies of vibration of m_1 (with m_2 held still) in the first and second linear subregions, respectively. As was explained by Butcher (1999), the total period of the single degree-of-freedom version of equation (11)

$$m\ddot{x}_1 + kx_1 + f(x_1) = 0 \qquad f(x_1) = \begin{cases} 0; & x_1 < x_c \\ k_c(x_1 - x_c); & x_1 > x_c \end{cases} \tag{13}$$

can be found by integrating over the closed path Γ as

$$T = \oint_\Gamma dt = 2\int_{-x_0}^{x_c} \frac{1}{\dot{x}_-} dx_- + 2\int_{x_c}^{x_c + D_+} \frac{1}{\dot{x}_+} dx_+ \tag{14}$$

in terms of the closed orbits in the phase plane $x_-^2 + \dot{x}_-^2 = x_0^2$ and $\alpha^2(x_+ - x_e)^2 + \dot{x}_+^2 = x_0^2 - x_c x_e$ where $x_e = (1 - 1/\alpha^2)x_c$ from which the velocities in the above integrals are determined. The initial displacement magnitude is x_0 and

$$D_+ = \frac{x_0}{\alpha}\sqrt{1 - \rho^2\left(1 - \frac{1}{\alpha^2}\right)} - \frac{x_c}{\alpha^2} \tag{15}$$

is the penetration distance into the second subregion (Butcher, 1999). The dimensionless parameter $\rho = x_c/x_0$ must lie in the interval [-1,1] if the clearance boundary is crossed.

Evaluation of these integrals yields the oscillation period from which the frequency is found as

$$\Omega = 2\omega_- \omega_+ \left[\omega_+\left(1+\frac{2}{\pi}\sin^{-1}\rho\right) + \omega_- \left(1-\frac{2}{\pi}\sin^{-1}\left(\frac{\rho}{\alpha\sqrt{1-\rho^2\left(1-\frac{1}{\alpha^2}\right)}} \right) \right) \right]^{-1} \tag{16}$$

When the clearance vanishes (ρ =0), equation (16) becomes the well-known "bilinear frequency relation" (BFR)

$$\Omega = \frac{2\omega_-\omega_+}{\omega_+ + \omega_-} \tag{17}$$

which has appeared in several studies of bilinear systems which do not contain a clearance (Shaw and Holmes, 1983). Fig. 6 shows the numerical simulations in configuration space of first and second BNMs with $\alpha^2 = 2$ and x_c=-2, -1.5, -1, -0.5, 0, 0.5, 1, 1.5, 2, for the two-degree-of-freedom system with clearance nonlinearity. The 1st and last cases are linear, the solid closed curves are the equipotential boundaries with and without the nonlinear spring. In a few of the cases, 3 NNMs are present simultaneously.

3.2 Symmetric Deadzone and Saturation Nonlinearities

Next, consider the *n*-degree-of-freedom vibrating system in Fig. 4 where the clearance is replaced with a symmetric deadzone or saturation nonlinearity of the form

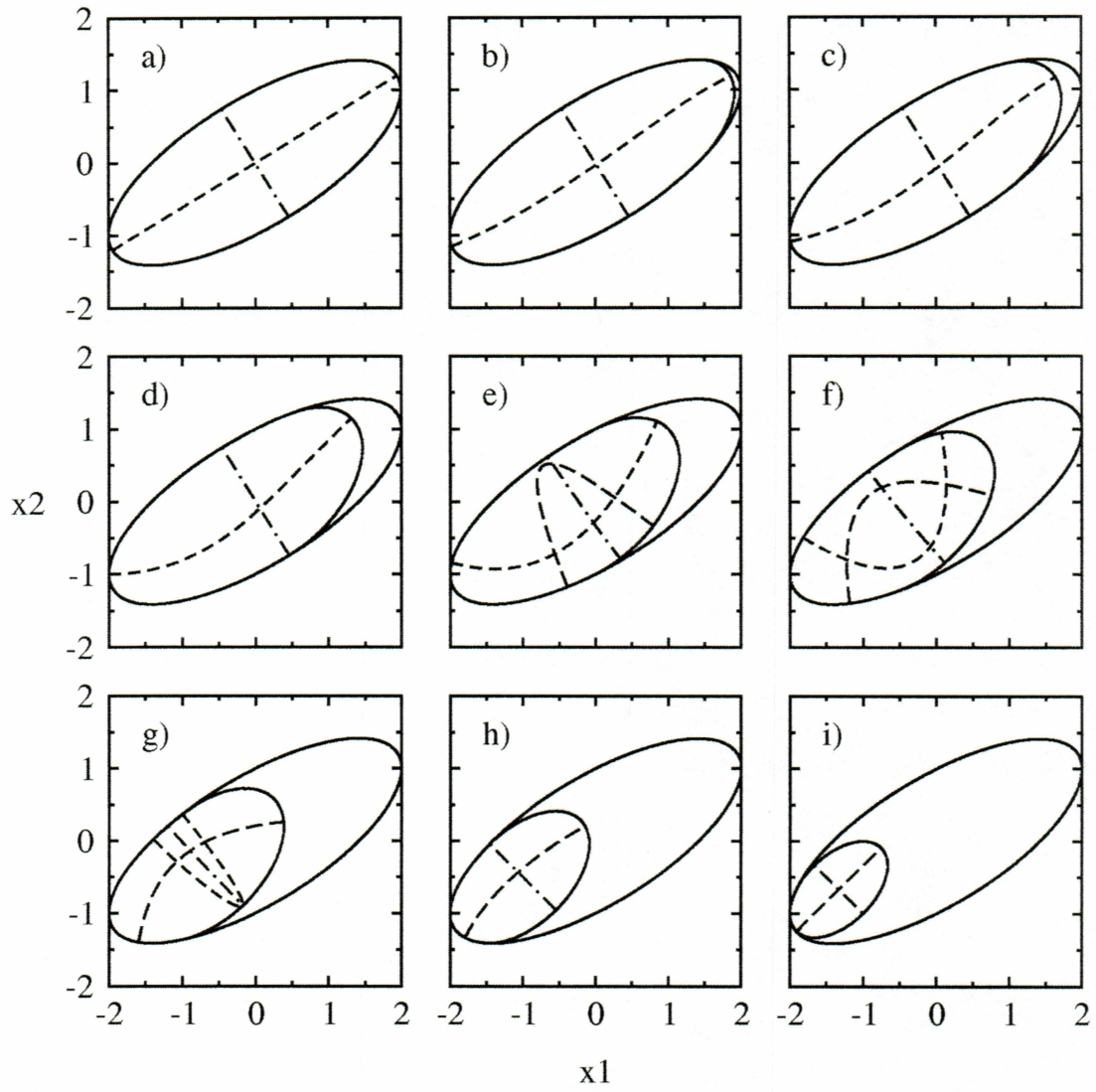

Figure 6: Numerical simulations in configuration space of BNMs for the two-degree-of-freedom system with clearance nonlinearity with α^2 =2 and xc=a) 2.0 (linear) b) 1.5 c) 1.0 d) 0.5 e) 0.0 f) -0.5 g) -1.0 h) -1.5 i) -2.0 (linear). The solid closed curves are the equipotential boundaries with and without the nonlinear spring.

$$f(x_1) = \begin{cases} 0; & |x_1| < x_c \\ k_c(x_1 - x_c); & x_1 > x_c \\ k_c(x_1 + x_c); & x_1 < -x_c \end{cases} \quad or \quad f(x_1) = \begin{cases} k_c x_1; & |x_1| < x_c \\ k_c x_c; & x_1 > x_c \\ -k_c x_c; & x_1 < -x_c \end{cases} \tag{18}$$

respectively. The stiffness of the first mass is plotted in Fig. 7 for both cases in which it is seen that the overall domain is divided into three distinct linear subregions. Since the masses' positions are measured from equilibrium, penetration of the first mass into the first and third subregion is made only when the energy of the system is sufficient such that the clearance is traversed by the first mass, i.e. $x_1 > x_c$ or $x_1 < -x_c$. Otherwise if the energy is insufficient for m_1 to reach x_c or $-x_c$, then the system remains in the second linear subregion and the solution is easily obtained. The scaled variables in equation (12) are now introduced where ω_- (or ω_+) is the linear frequency of m_1 (with m_2 held still) in the second subregion and ω_+ (or ω_-) is the frequency in the first and third subregions for deadzone (or saturation, respectively).

The total period of the single degree-of-freedom version of equation (11) and (18) can again be found by integrating over the closed path Γ as

$$T = \oint_{\Gamma} dt = 4\int_0^{x_c} \frac{1}{\dot{x}_-} dx_- + 4\int_{x_c}^{x_c + D_+} \frac{1}{\dot{x}_+} dx_+ \tag{19}$$

where the velocities are found from the phase plane $x_-^2 + \dot{x}_-^2 = \alpha^2(x_0 - x_e)^2$ and $\alpha^2(x_+ - x_e)^2 + \dot{x}_+^2 = \alpha^2(x_0 - x_e)^2$ where $x_e = (1 - 1/\alpha^2)x_c$ for deadzone. This yields the exact frequency as

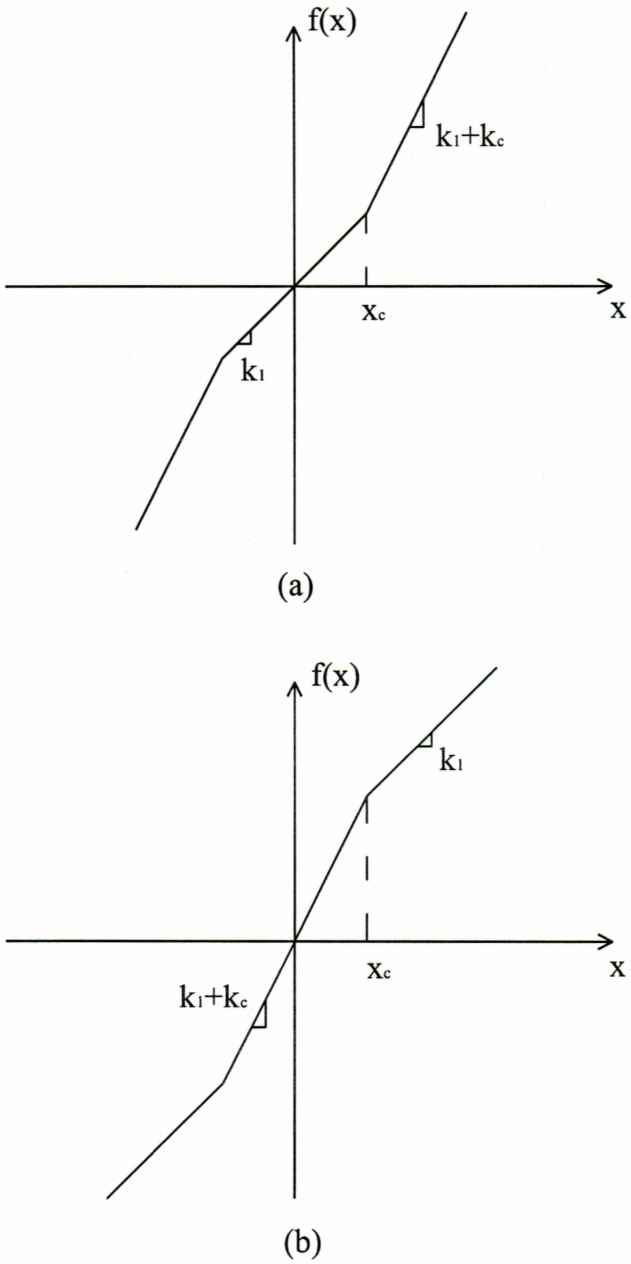

Figure 7: Force versus displacement of the first mass for
a) deadzone and b) saturation nonlinearities

$$\Omega = \omega_{-}\ \omega_{+}\left[\frac{2\omega_{+}}{\pi}\sin^{-1}\frac{\rho}{\sqrt{(\rho-1)^2\alpha^2+\rho(2-\rho)}}+\omega_{-}\left(1-\frac{2}{\pi}\sin^{-1}\left(\frac{\rho}{\alpha^2-\rho(\alpha^2-1)}\right)\right)\right]^{-1} \tag{20}$$

where $\rho = x_c/x_0$, x_0 is the initial displacement magnitude, and ρ lies in the interval [0,1]. For saturation, the substitutions $\omega_{+} \leftrightarrow \omega_{-}$ and $\alpha \rightarrow 1/\alpha$ are made in equation (20) to obtain

$$\Omega = \omega_{-}\ \omega_{+}\left[\frac{2\omega_{-}}{\pi}\sin^{-1}\frac{\rho}{\sqrt{\rho(2-\rho)+\frac{(\rho-1)^2}{\alpha^2}}}+\omega_{+}\left(1-\frac{2}{\pi}\sin^{-1}\left(\frac{\rho}{\frac{1}{\alpha^2}-\rho\left(\frac{1}{\alpha^2}-1\right)}\right)\right)\right]^{-1} \tag{21}$$

Fig. 8 shows the Numerical simulations in configuration space of first and second NNMs for the 2 dof system with deadzone nonlinearity($\alpha^2 = 2$) at $x_c = 0, 0.5, 1.25$ and 2.0. Fig. 9 shows the Numerical simulations in configuration space of first and second NNMs for the saturation nonlinearity at $x_c = 0, 0.25, 0.75$ and 1.25, the 1st and last figures in each case are purely linear.

3.3 Bang-bang Nonlinearity

Finally, consider the system in Fig. 4 where a bang-bang nonlinearity defined by

$$f(x_1) = \begin{cases} -\delta; & (x_1 < 0) \\ \delta; & (x_1 > 0) \end{cases} \tag{22}$$

replaces the clearance. The discontinuous stiffness of the first mass (with the others held still) is shown in Fig. 10 in which it is seen that the linear frequency is the same in both subregions. However, crossing of the discontinuity will occur regardless of the amplitude

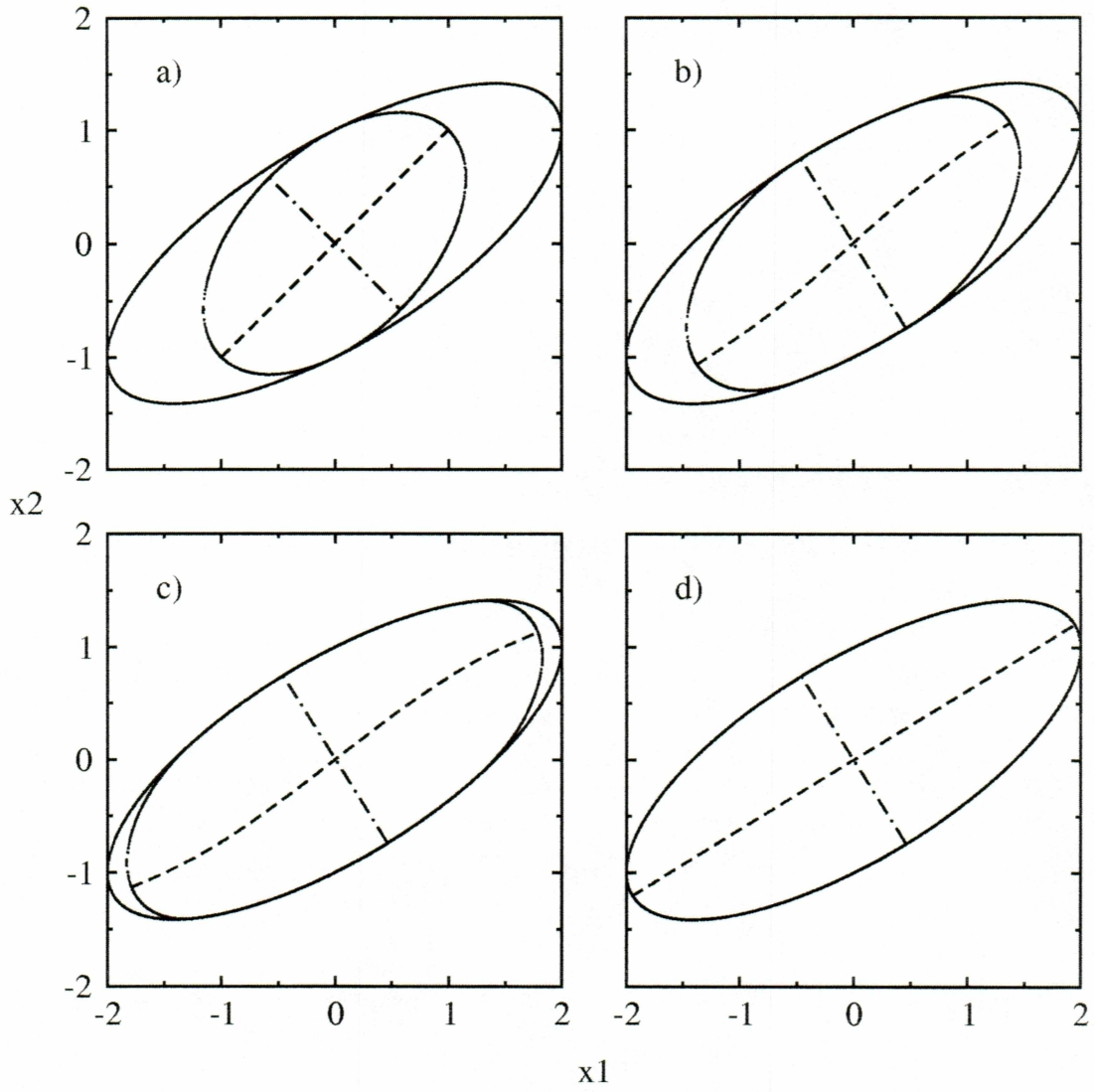

Figure 8: Numerical simulations in configuration space of NNMs for the two degree-of-freedom system with deadzone nonlinearity with α^2 =2 and xc= a) 0.0 (linear) b) 0.5 c) 1.25 d) 2.0 (linear). The solid closed curves are the equipotential boundaries with and without the nonlinear spring.

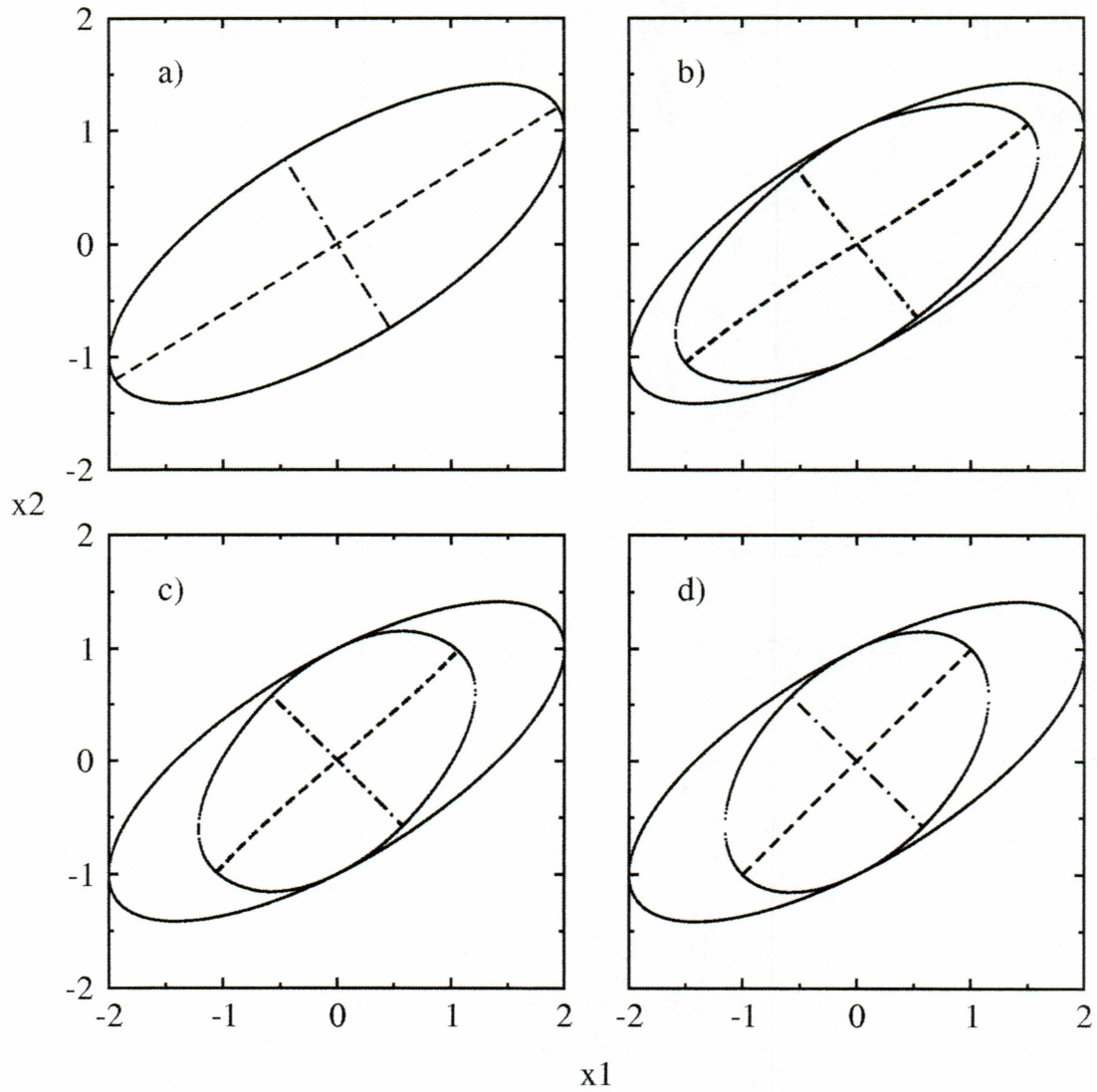

Figure 9: Numerical simulations in configuration space of NNMs for the two degree-of-freedom system with saturation nonlinearity with $\alpha^2 = 2$ and xc= a) 0.0 (linear) b) 0.25 c) 0.75 d) 1.25 (linear). The solid closed curves are the equipotential boundaries with and without the nonlinear spring.

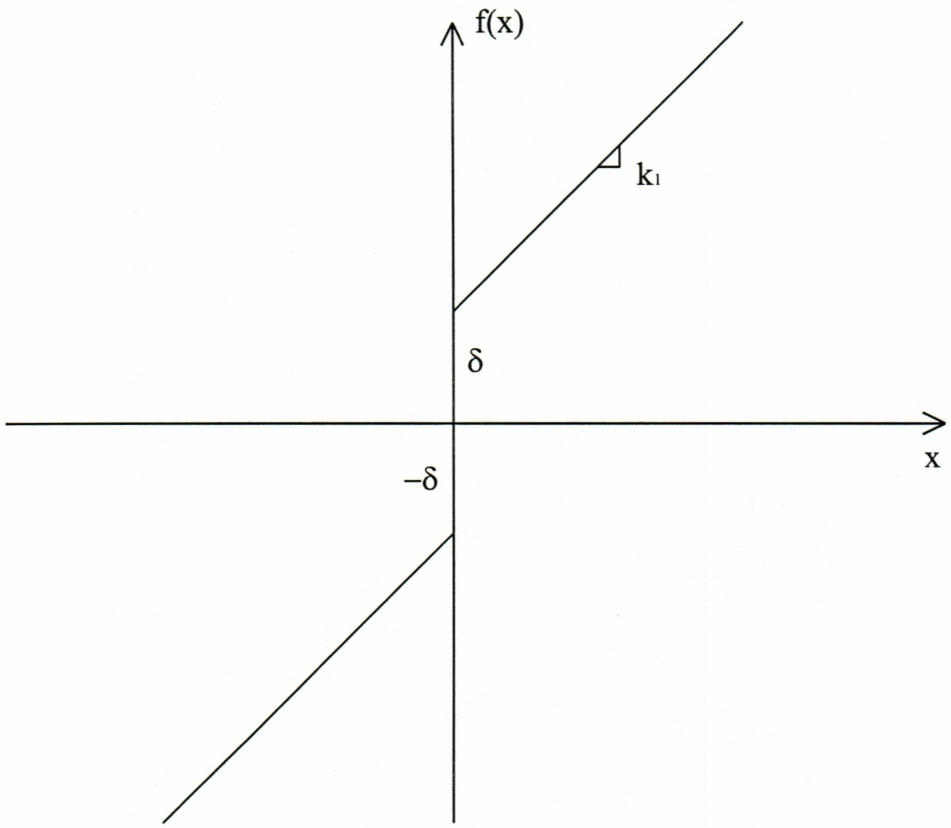

Figure 10: Force versus displacement for bang-bang nonlinearity

of oscillation. By integrating over the closed path as

$$T = \oint_{\Gamma} dt = 4\int_{0}^{x_0} \frac{1}{\dot{x}_-} dx_- \tag{23}$$

in terms of the closed orbits $(x_- - \delta/\omega^2)^2 + \dot{x}_-^2/\omega^2 = (x_0 + \delta/\omega^2)^2$, the exact frequency for the single-degree-of-freedom system is found as

$$\Omega = \frac{\omega}{1 - \frac{2}{\pi}\sin^{-1}\left(\frac{\rho}{\rho + \omega^2}\right)} \tag{24}$$

where ω is the frequency in both discontinuous linear subregions and $\rho = \delta/x_0$. Fig. 11 shows the numerical simulations in configuration space of first and second NNMs for the 2 dof system with bang-bang nonlinearity at $\delta = 0, 0.25, 0.5$ and 0.875. The 1st case is linear.

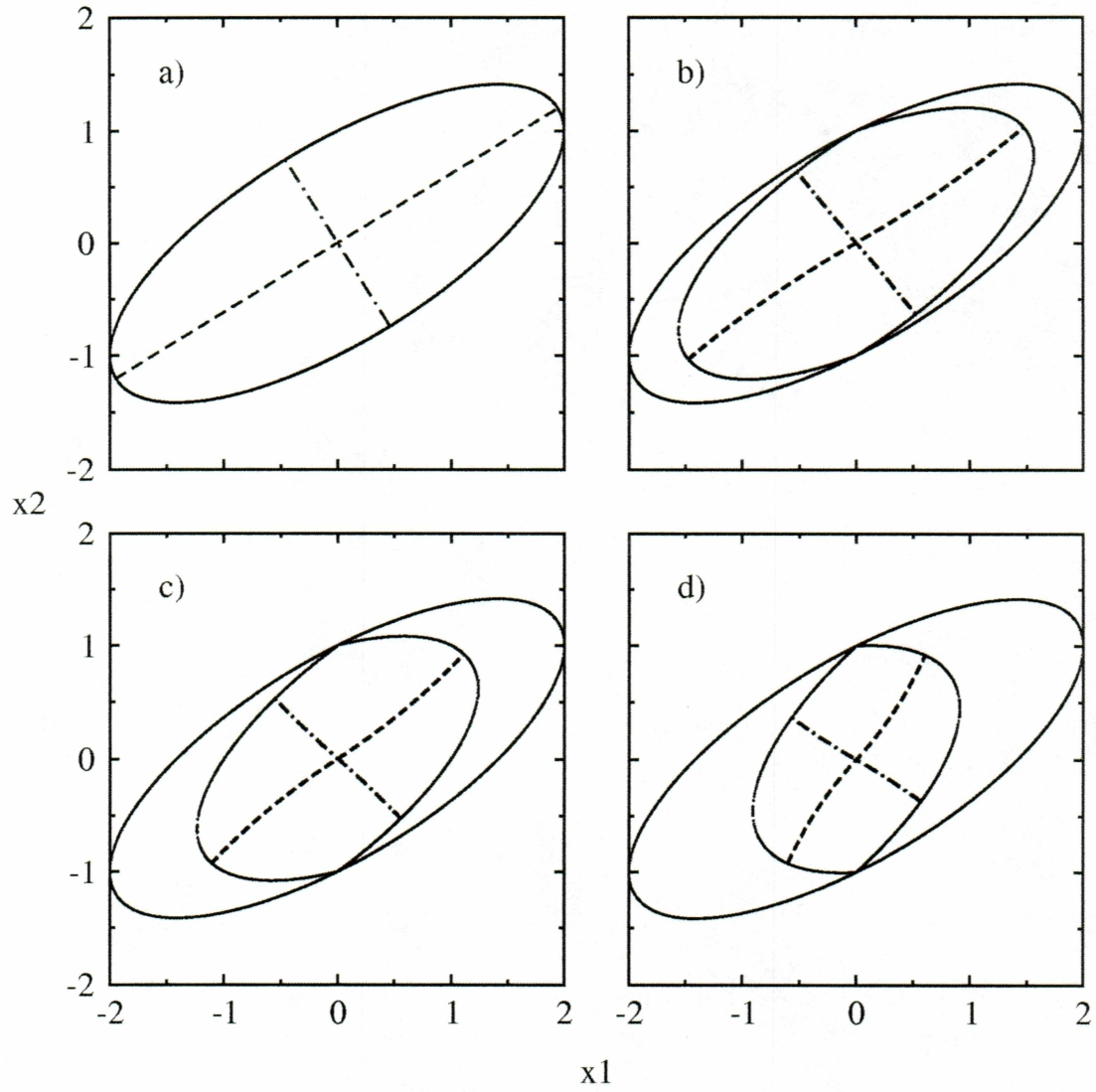

Figure 11: Numerical simulations in configuration space of NNMs for the two degree-of-freedom system with bang-bang nonlinearity with δ = a) 0.0 (linear) b) 0.25 c) 0.5 d) 0.875. The solid closed curves are the equipotential boundaries with and without the nonlinear spring.

CHAPTER 4

APPROXIMATION OF NNM FREQUENCIES AND MODE SHAPES

Two approximation techniques are used in this paper, Piecewise Modal Method (PMM) and Local Equivalent Linear Stiffness Method (LELSM).

4.1 Piecewise Model Method (PMM)

Chati *et al* (1997) first utilized the bilinear frequency relation (BFR), which is exact for only one degree-of-freedom, in order to approximate BNM frequencies of a multi-degree-of-freedom system. For this purpose, two separate sets of eigenfrequencies were computed (one set for each linear subregion) while the BFR was employed with each pair to approximate the BNM frequency in the *i*th mode via

$$\Omega_i = \frac{2\omega_{-i}\omega_{+i}}{\omega_{+i} + \omega_{-i}} \tag{25}$$

No clearance was present in that work. In a recent study, the effects of clearance and interference in BNM frequencies were investigated (Butcher, 1999). One method being used is called the *piecewise modal method*, which directly extended the use of the bilinear frequency relation as used in the prior paper in order to incorporate the effects of clearance. This technique approximates the BNM manifold as the piecewise union of the separate eigenvectors in the two linear subregions joined at the boundary.

For the multiple degree-of-freedom system, the approximate BNM frequency in the *i*th mode is found by direct analogy to equation (16) as

$$\Omega_i = 2\omega_{-i}\left[1+\frac{2}{\pi}\sin^{-1}\rho+\frac{1}{\gamma_i}\left(1-\frac{2}{\pi}\sin^{-1}\left(\frac{\rho}{\gamma_i\sqrt{1-\rho^2\left(1-\frac{1}{\gamma_i^2}\right)}}\right)\right)\right]^{-1} \tag{26}$$

where

$$\gamma_i = \frac{\omega_{+i}}{\omega_{-i}} \tag{27}$$

is the ratio of frequencies in the *i*th mode in the two linear subregions.

For deadzone, this relation is found by direct analogy to equation (20) as

$$\Omega_i = \omega_{-i}\left[\frac{2}{\pi}\sin^{-1}\frac{\rho}{\sqrt{\rho(2-\rho)+(\rho-1)^2\gamma_i^2}}+\frac{1}{\gamma_i}\left(1-\frac{2}{\pi}\sin^{-1}\frac{\rho}{\gamma_i^2-\rho(\gamma_i^2-1)}\right)\right]^{-1} \tag{28}$$

while for saturation it is found by analogy to equation (21) as

$$\Omega_i = \omega_{-i}\left[\frac{2}{\gamma_i\pi}\sin^{-1}\frac{\rho}{\sqrt{\rho(2-\rho)+\frac{(\rho-1)^2}{\gamma_i^2}}}+1-\frac{2}{\pi}\sin^{-1}\left(\frac{\rho}{\frac{1}{\gamma_i^2}-\rho\left(\frac{1}{\gamma_i^2}-1\right)}\right)\right]^{-1} \tag{29}$$

For bang-bang, the PMM relation for the *i*th NNM frequency is found by analogy with equation (24) as

$$\Omega_i = \frac{\omega_i}{1-\frac{2}{\pi}\sin^{-1}\left(\frac{\rho}{\rho+\omega_i^2}\right)} \tag{30}$$

4.2 Local Equivalent Linear Stiffness Method (LELSM)

The Local Equivalent Linear Stiffness Method (LELSM) is developed by Butcher (1999). It was suggested there that only a single element $k_{eq} = (\Omega/\omega_{-})^2$ (using the normalized frequency of equation (16), for example) on the main diagonal of an equivalent linear stiffness matrix $\boldsymbol{K}_{eq}$ should be affected by the presence of the nonlinearity while the remaining elements should remain unchanged from those in $\boldsymbol{K}$. The eigenvalue problem with matrices $\boldsymbol{M}$ and $\boldsymbol{K}_{eq}$ then yields the approximate NNM frequencies and mode shapes. For a n-degree-of-freedom system, since n different ρ values (and hence k_{eq} and $\boldsymbol{K}_{eq}$) result from each mode having a different initial condition for the same energy level, it is necessary to compute a $\boldsymbol{K}_{eq}$, which is valid for all modes, as

$$K_{eq} = U\ diag(\Omega_1^2, \ldots, \Omega_n^2)\ U^{-1} \tag{31}$$

from the n frequencies and eigenvectors which comprise U corresponding to the n individual equivalent stiffness matrices. The method can be easily implemented for higher dimensional systems.

For a normalized 2-degree-of-freedom system with clearance, deadzone, saturation, or bang-bang nonlinearity, we have

$$K_{eq} = \begin{bmatrix} k_{eq} - 1 \\ -1 \quad 2 \end{bmatrix} \tag{32}$$

where $k_{eq} = \Omega^2$. Here, Ω is the exact frequency of the single degree-of-freedom system with nonsmooth stiffness given by equations (16,20,21,24) in which ω_{-} or ω is set to the

frequency of this system in the first subregion while k_{eq} is the equivalent linear stiffness which causes that system to vibrate with the same frequency. The solution of the eigenvalue problem $\left| \boldsymbol{K}_{eq} - \Omega_i^2 \boldsymbol{I} \right| = 0$ then yields the approximate NNM frequencies Ω_i in each mode. For the limiting linear cases ($\rho = \pm 1$ for clearance; $\rho = 0, 1$ for deadzone and saturation; $\rho = 0$ for bang-bang) the results are exact.

CHAPTER 5

ORDER REDUCTION

5.1 Linear Based Order Reduction

Consider the system of n second order differential equations in structural form

$$M\ddot{x} + Kx + F(x) = 0 \tag{33}$$

where the nonsmooth nonlinearity $F(x)$ is isolated to the first m coordinates and m equations, i.e.

$$F(x) = \left[f_1(x_1) \ \ldots \ f_m(x_m) \ 0 \ \ldots \ 0\right]^T \tag{34}$$

where $f_i(x_i)$, $i=1,\ldots,m$ are piecewise linear functions. It is desired to reduce equation (33) to a set of m master coordinates, eliminating the $s=n-m$ slave coordinates. For this purpose, the displacement vector x is partitioned as $x = \left[x_m^T \ x_s^T\right]^T$. The linear part of (33) is

$$M\ddot{x} + Kx = 0 \tag{35}$$

whose eigenfrequencies ω_i and eigenvectors ϕ_i are easily obtained. Typically the modes with the lowest frequencies are retained in the reduced order model.

To construct the reduced model, let the n x m transformation matrix Φ be defined as

$$\Phi = \begin{bmatrix} I_m \\ T \end{bmatrix} \tag{36}$$

in which I_m is the m x m identity matrix and the (n-m) x m matrix T is found by iterating the following equation (Burton and Young, 1994; Burton and Rhee, 2000)

$$= -[k_{ss} - (m_{ss}T + m_{sm})(m_{ms}T + m_{mm})^{-1}k_{ms}]^{-1}[k_{sm} - (m_{ss}T + m_{sm})(m_{ms}T + m_{mm})^{-1}k_n \tag{37}$$

where the linear mass and stiffness matrices are partitioned as

$$\mathcal{M} = \begin{bmatrix} m_{mm} & m_{ms} \\ m_{sm} & m_{ss} \end{bmatrix} \qquad K = \begin{bmatrix} k_{mm} & k_{ms} \\ k_{sm} & k_{ss} \end{bmatrix} \tag{38}$$

Applying the transformation

$$x = \Phi x_m \tag{39}$$

to equation (33) and premultiplying by Φ^T yields

$$\tilde{M}\ddot{x}_m + \tilde{K}x_m + f(x_m) = 0 \tag{40}$$

in which the reduced m x m mass and stiffness matrices and m x 1 nonlinear vector are given by

$$\tilde{M} = \Phi^T M \Phi \qquad \tilde{K} = \Phi^T K \Phi \qquad f(x_m) = \left[f_1(x_1) \ \ldots \ f_m(x_m)\right]^T \tag{41}$$

It should be noted that equation (39) implies a relationship

$$x_s = Tx_m \tag{42}$$

between the master/slave coordinates and that the retained coordinates are a subset of the original physical coordinates. Also, it was shown in (Burton and Young, 1994; Burton and Rhee, 2000) that T preserves the exact eigenstructure of equation (35). Equation (39) is thus a Guyan-like order reduction transformation which accounts for the inertia as well as

stiffness effects. When the mass terms are set to zero in equation (37), the traditional Guyan reduction transformation $T = -k_{ss}^{-1}k_{sm}$ is produced (Guyan, 1965).

If only one master coordinate is retained (m=1), then $\Phi = \phi_i$ (the eigenvector corresponding to the retained mode normalized such that the first element is one) and equations (39) and (40) become

$$x = \phi_i x_1 \tag{43}$$

and

$$\ddot{x}_1 + \omega_i^2 x_1 + \beta_i f(x_1) = 0 \tag{44}$$

respectively where

$$\omega_i = \sqrt{\frac{\phi_i^T K \phi_i}{\phi_i^T M \phi_i}} \qquad \beta_i = \frac{1}{\phi_i^T M \phi_i} \tag{45}$$

are the ith modal frequency of equation (35) and the reduced nonlinear coefficient for the ith mode. It can be seen that the form of the nonsmooth nonlinearity is retained in the reduced model which utilizes a subset of the original physical coordinates. It is desirable that the dynamics of the reduced model are close to that of the ith nonlinear normal mode of the original full model (equation 33)). However, Rhee and Burton (2000) found that the nonlinear frequencies of equation (44) for deadzone and bang-bang nonlinearities in a two degree-of-freedom system differed from the NNM frequencies of the full model which were obtained by numerical integration. This error is shown later.

For a bilinear clearance nonlinearity, the ith linear frequency in the second subregion

is $\omega_{+i} = \sqrt{\omega_{-i}^2 + \beta_i k_c}$ in terms of the ith linear frequency in the first subregion, for linear-based order reduction at different modes, β_i is always a constant, which we can get from equation (45), so the approximate NNM frequency can be solved for equation (26). In Fig. 12, the approximate BNM frequencies in both modes of the 2-degree-of-freedom version of equation (10) obtained from the linear-based reduced model as well as the PMM and LELSM methods from (Butcher, 1999) are plotted versus ρ for $\alpha^2=2$ along with the exact BNM frequencies found by direct numerical simulation of the full 2-dof system. As was shown in (Butcher, 1999), for this value of α, two separate branches of NNMs exist for mode 1.

5.2 Improved Order Reduction via PMM

Although the linear based reduced order model has a similar oscillation amplitude as the x_1 coordinate in the full model, the frequency is not the same as the ith NNM frequency. An alternate value of β_i, however, could result in an improvement in the frequency. Let us try to find an improved value of β_i in the reduced model of equation (44) via PMM for each of these nonlinearities. Since both sets of linear frequencies can be easily determined, the improved value of β_i can be found easily as

$$\beta_i = \frac{1}{k_c}(\omega_{+i}^2 - \omega_{-i}^2) \tag{46}$$

which is independent of the value of ρ. Equation (44) along with the value of β_i computed above is the reduced model obtained from PMM for clearance, deadzone, and saturation nonlinearities. In Fig. 13 and 14, it is seen that PMM offers improvement for deadzone

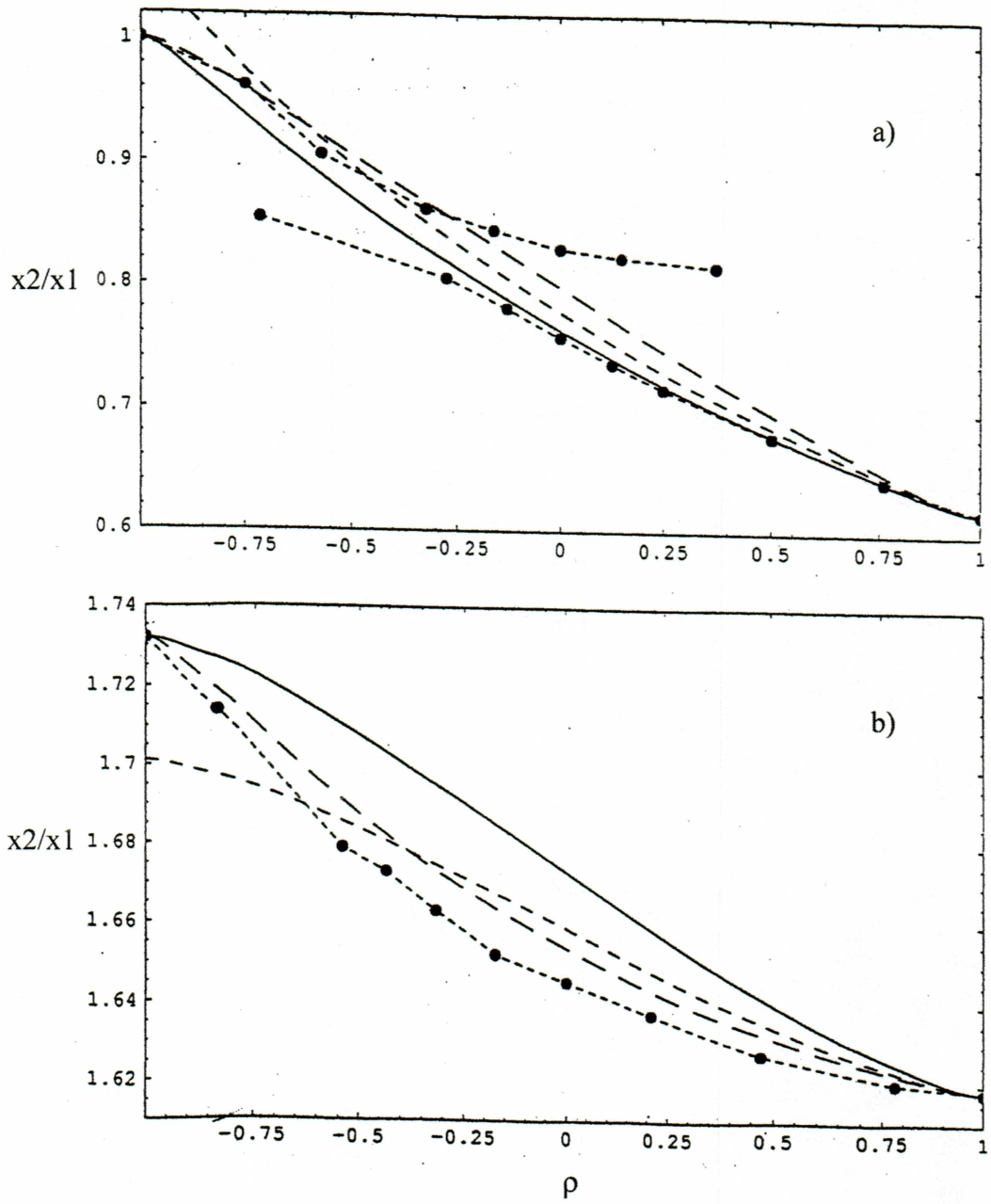

Figure 12: Frequencies of reduced order models of the 2-dof system with clearance nonlinearity in a) mode 1 and b) mode 2

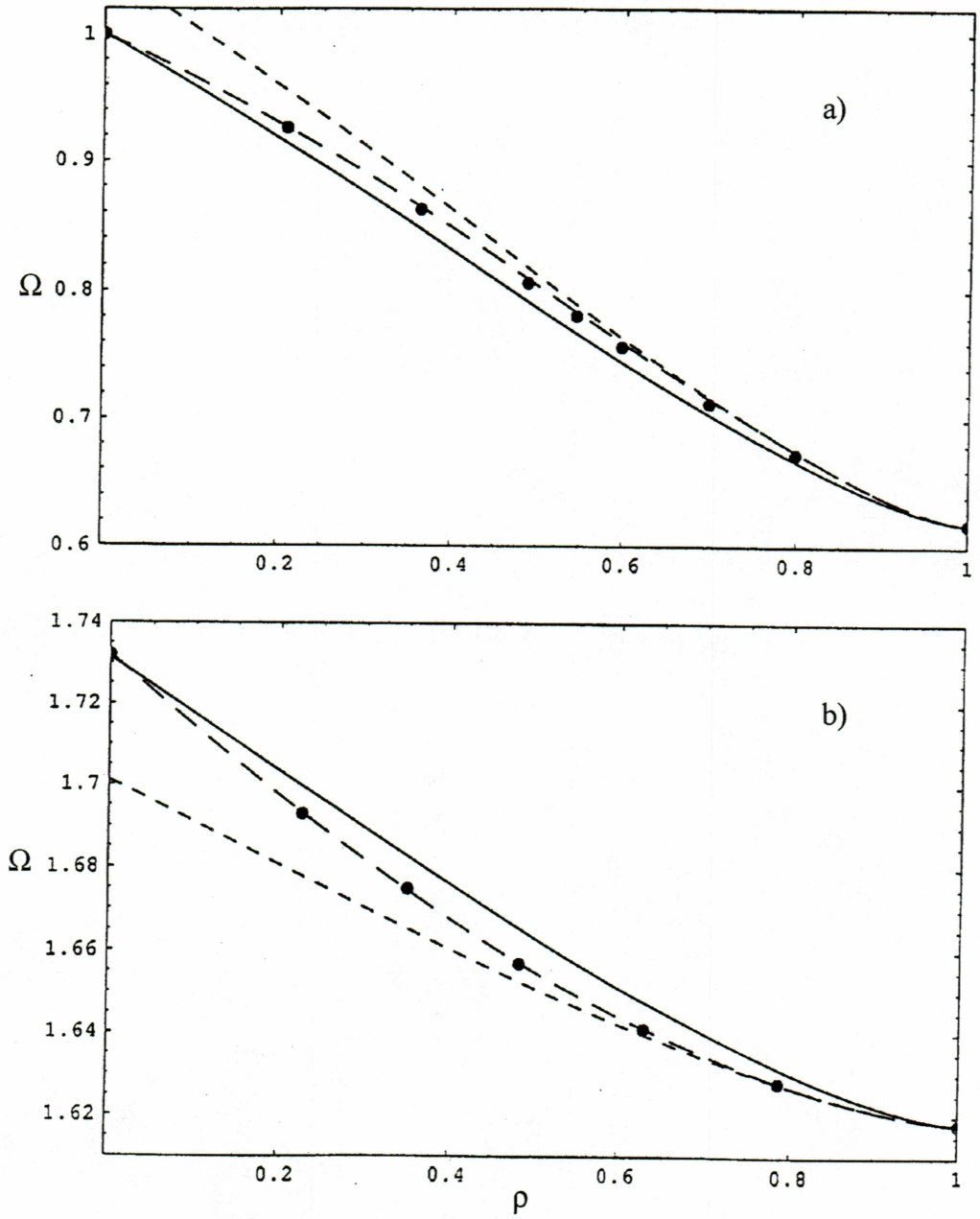

Figure 13: Frequencies of reduced order models of the 2-dof system with deadzone nonlinearity in a) mode 1 and b) mode 2 computed via the linear -based reduction (short-dashed), PMM (solid), LELSM (long-dashed), and numerical simulation of the full model (dots) for $\alpha^2 = 2$.

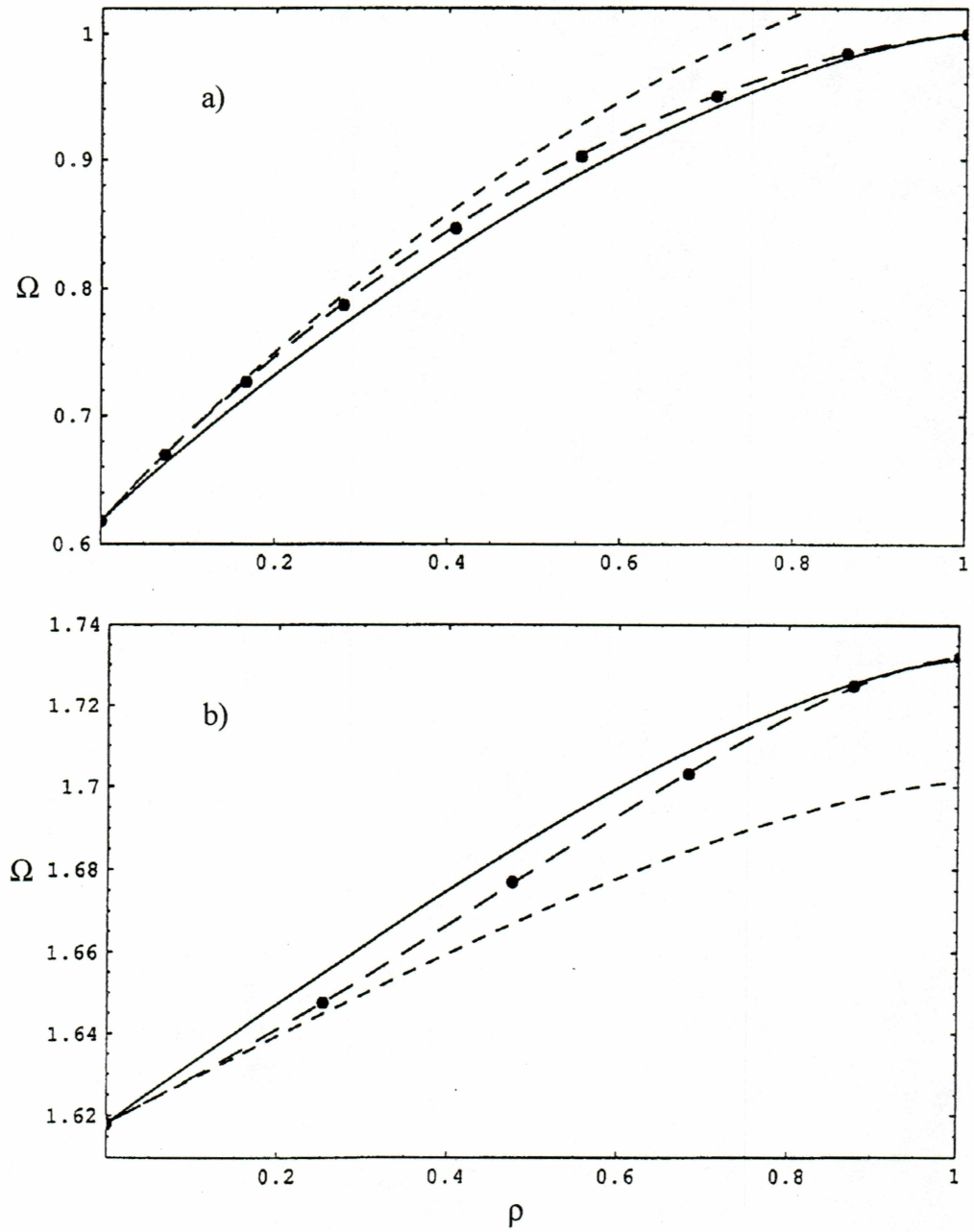

Figure 14: Frequencies of reduced order models of the 2-dof system with saturation nonlinearity in a) mode 1 and b) mode 2 computed via the linear -based reduction (short-dashed), PMM (solid), LELSM (long-dashed), and numerical simulation of the full model (dots) for $\alpha^2 = 2$.

and saturation over a limited range of ρ in both modes.

For bang-bang, equation (30) was used to estimate the NNM frequencies in Fig. 15 via PMM. To use PMM in the reduced model of equation (44), equation(30) becomes

$$\Omega_i = \frac{\omega_i}{1 - \frac{2}{\pi}\sin^{-1}\left(\frac{\beta_i \rho}{\beta_i \rho + \omega_i^2}\right)} \tag{47}$$

It is seen from equations (30) and (47) that we must set β_i=1 which again is independent of the value of ρ. It is seen in Fig.15 that the corresponding reduced models will be improved over the linear-based reduced models only in the first mode.

5.3 Improved Order Reduction via LELSM

In order to use another estimate of the NNM frequency Ω_i, let us solve for the first β_i in equation (26) using the relation $\gamma_i(\beta_i) = \sqrt{\omega_{-i}^2 + \beta_i k_c}/\omega_{-i}$. This yields

$$\beta_i = \frac{\omega_{-i}^2}{k_c}\left[\frac{\Omega_i^2\left(1 - \frac{2}{\pi}\sin^{-1}\left(\frac{\rho}{\gamma_i(\beta_i)\sqrt{1-\rho^2(1-1/(\gamma_i^2(\beta_i)))}}\right)\right)^2}{\left(2\omega_{-i} - \Omega_i\left(1 + \frac{2}{\pi}\sin^{-1}\rho\right)\right)^2} - 1\right] \tag{48}$$

for the clearance nonlinearity. Equation (48) is a transcendental equation for β_i which can be solved numerically once Ω_i is estimated in some way. (Note that in the case $\rho = 0$, the β_i's on the right disappear and equation (48) can be solved analytically). Similarly, equations (29) and (30) yield

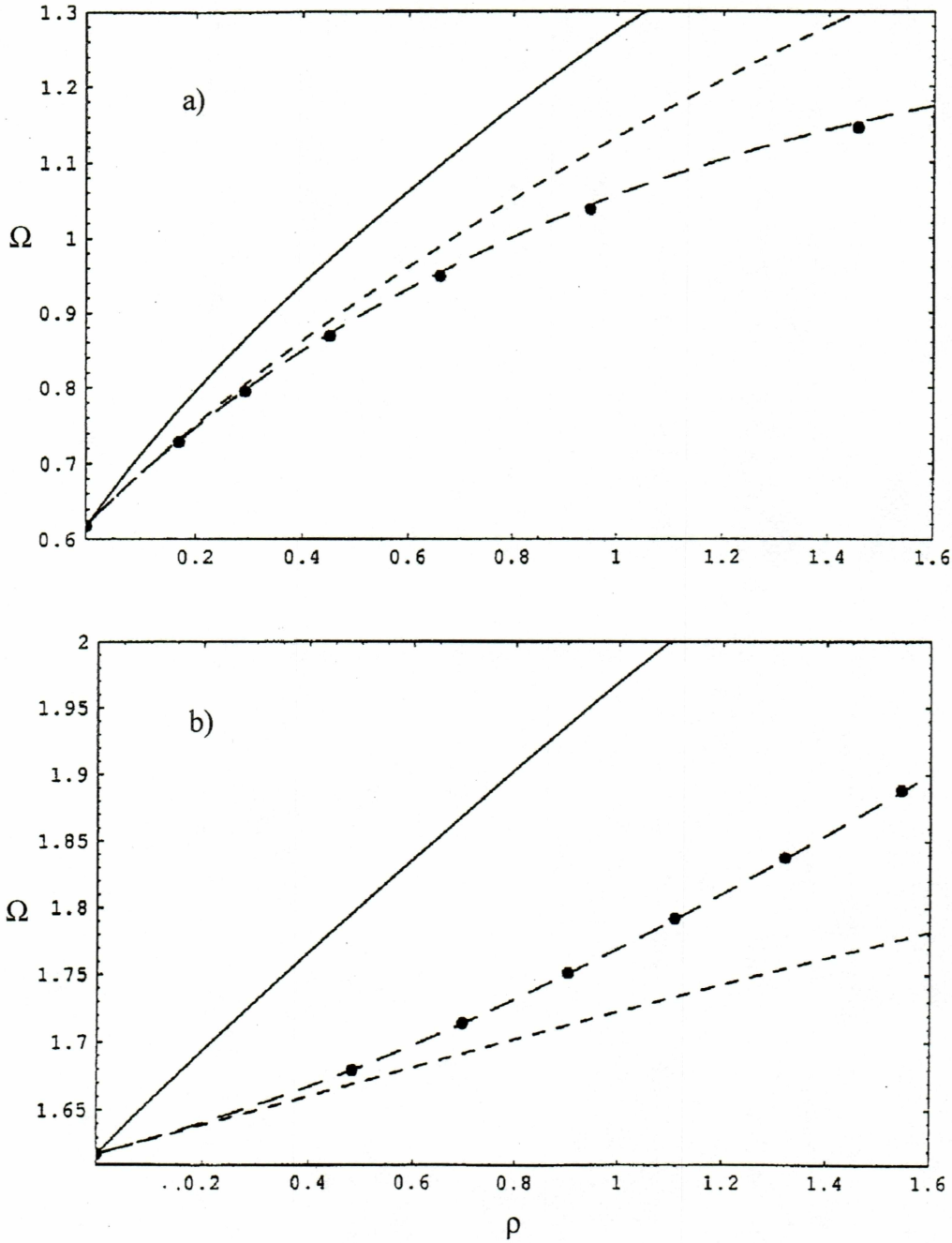

Figure 15: Frequencies of reduced order models of the 2-dof system with bang-bang nonlinearity in a) mode 1 and b) mode 2 computed via the linear-based reduction (short-dashed), PMM (solid), LELSM (long-dashed), and numerical simulation of the full model (dots).

$$\beta_i = \frac{\omega_{-i}^2}{k_c}\left[\frac{\Omega_i^2\left(1-\frac{2}{\pi}\sin^{-1}\left(\frac{\rho}{\gamma_i^2(\beta_i)-\rho(\gamma_i^2(\beta_i)-1)}\right)\right)^2}{\left(\omega_{-i}-\frac{2\Omega_i\sin^{-1}\frac{\rho}{\sqrt{\rho(2-\rho)+(\rho-1)^2\gamma_i^2(\beta_i)}}}{\pi}\right)^2}-1\right] \tag{49}$$

and

$$\beta_i = \frac{1}{k_c}\left(\left(\frac{2\left(\sin^{-1}\frac{\rho}{\sqrt{\rho(2-\rho)+\frac{(\rho-1)^2}{\gamma_i^2(\beta_i)}}}\right)}{\pi\left(\frac{1}{\Omega_i}-\frac{1}{\omega_{-i}}\left(1-\frac{2}{\pi}\sin^{-1}\left(\frac{\rho}{\frac{1}{\gamma_i^2(\beta_i)}-\rho\left(\frac{1}{\gamma_i^2(\beta_i)}-1\right)}\right)\right)\right)}\right)^2-\omega_{-i}^2\right) \tag{50}$$

for deadzone and saturation, respectively. For a bang-bang nonlinearity, equation (47) yields

$$\beta_i = \frac{\omega_{-i}^2}{\rho}\left[\frac{1}{1-\sin\left[\frac{\pi}{2}\left(1-\frac{\omega_{-i}}{\Omega_i}\right)\right]}-1\right] \tag{51}$$

As can be seen from Fig. 13, 14, 15, this method can possibly be used to obtain improved reduced order models whose frequencies are more accurate than those obtained

from the linear-based reduced models for clearance (mode 2), deadzone (both modes), saturation (both modes), and bang-bang (both modes) nonlinearities. For this purpose, equations (49-51) are used to find β_i once the NNM frequency Ω_i has been estimated via LELSM.

5.4 Examples

5.4.1 Deadzone Nonlinearity

As an example of a system with deadzone nonlinearity, the equations of motion for the two degree-of-freedom version of equation (18) are considered where $m_1=m_2=k_1=k_2=1$. The linear mode shapes are $\phi_1 = (1.0 \quad 0.618)^T$ and $\phi_2 = (1.0 \quad -1.618)^T$ and the modal frequencies are $\omega_1=0.618$ and $\omega_2=1.618$. The linear-based order reduction transformation of equation (43) was employed in Rhee and Burton (2000) which results in the reduced model of equation (44) where $\beta_1=0.724$ in the first mode and $\beta_2=0.276$ in the second. The effectiveness of the reduced order models was assessed in the former study by comparison of the frequency-amplitude dependence obtained by numerical integration of the reduced and full models. We compare the two models for equation (18a) by finding the exact BNM frequencies as well as the approximate frequencies from the various reduced order models.

To find the exact frequencies by numerical integration, the two BNMs can be located by simulating the motion for a variety of initial conditions along the equipotential boundary

$$E = \begin{cases} (x_2^2 + (x_1 - x_2)^2)/2; & |x_1| < x_c \\ (x_2^2 + (x_1 - x_2)^2 + \kappa_c (x_1 - x_c)^2)/2; & x_1 > x_c \\ (x_2^2 + (x_1 - x_2)^2 + \kappa_c (x_1 + x_c)^2)/2; & x_1 < -x_c \end{cases} \tag{52}$$

corresponding to some chosen energy level. Through trial and error, the correct initial conditions which yield periodic motion can be located by examining the motion in the configuration space. This is shown in Fig. 8 where the free spring has the same stiffness as the coupling springs (k_c=1 or α^2 = 2) and the total energy is E=1 for several different values for the clearance x_c. The first (a) and last (d) plots correspond to the two linear subregions ρ=0 and 1, respectively. Unlike the clearance case, the number of NNMs is equal to the number of degrees of freedom for all values of ρ.

For the case $x_c = 0.5$ (Fig.8b), the exact first modal frequency is found to be 0.862 rad/s. Using equation (20), the approximate nonlinear frequency obtained from the linear-based reduced model is 0.880 rad/s.

An improved reduced model can be obtained via LELSM. The equivalent linear stiffness matrix in this method is given by equation (32), where k_{eq} is found from

$$k_{eq} = \Omega^2 = \omega_-^2 \left[\frac{2}{\pi} \sin^{-1} \frac{\rho}{\sqrt{(\rho-1)^2 \alpha^2 + \rho(2-\rho)}} + \frac{1}{\alpha} \left(1 - \frac{2}{\pi} \sin^{-1} \left(\frac{\rho}{\alpha^2 - \rho(\alpha^2 - 1)} \right) \right) \right]^{-2} \tag{53}$$

with $\alpha^2 = 2$, ω_-=1, and ρ=0.363. The relation $\left| \boldsymbol{K}_{eq} - \Omega_i^2 \boldsymbol{I} \right| = 0$ results in an approximate frequency of Ω_1=0.864. Equation (49) is then used to obtain β_1=0.671 for the corresponding improved reduced order model. Comparisons of exact, linear-based, and improved results are in the time series plots in Fig. 16 for x_1 and Fig. 17 for x_2. As seen

Table 1: NNM frequencies for the Deadzone nonlinearity obtained from reduced order models and exact numerical simulations.

DOF n	mode i	k_c	ρ	β_i		Ω_i		
				linear based	improved	linear based	improved	exact
2	1	1	0	0.724	0.618	1.052	1.0	1.0
2	1	1	0.208	0.724	0.694	0.956	0.927	0.926
2	1	1	0.363	0.724	0.671	0.880	0.864	0.862
2	1	1	0.429	0.724	0.681	0.848	0.836	0.834
2	1	1	0.489	0.724	0.689	0.818	0.810	0.806
2	1	1	0.545	0.724	0.697	0.790	0.784	0.781
2	1	1	0.598	0.724	0.704	0.764	0.761	0.757
2	1	1	0.699	0.724	0.717	0.717	0.716	0.712
2	1	1	0.798	0.724	0.727	0.675	0.675	0.672
2	2	1	0	0.276	0.382	1.701	1.732	1.732
2	2	1	0.225	0.276	0.349	1.678	1.693	1.693
2	2	1	0.349	0.276	0.331	1.665	1.675	1.675
2	2	1	0.482	0.276	0.313	1.653	1.657	1.657
2	2	1	0.629	0.276	0.296	1.640	1.641	1.641
2	2	1	0.786	0.276	0.285	1.628	1.628	1.628

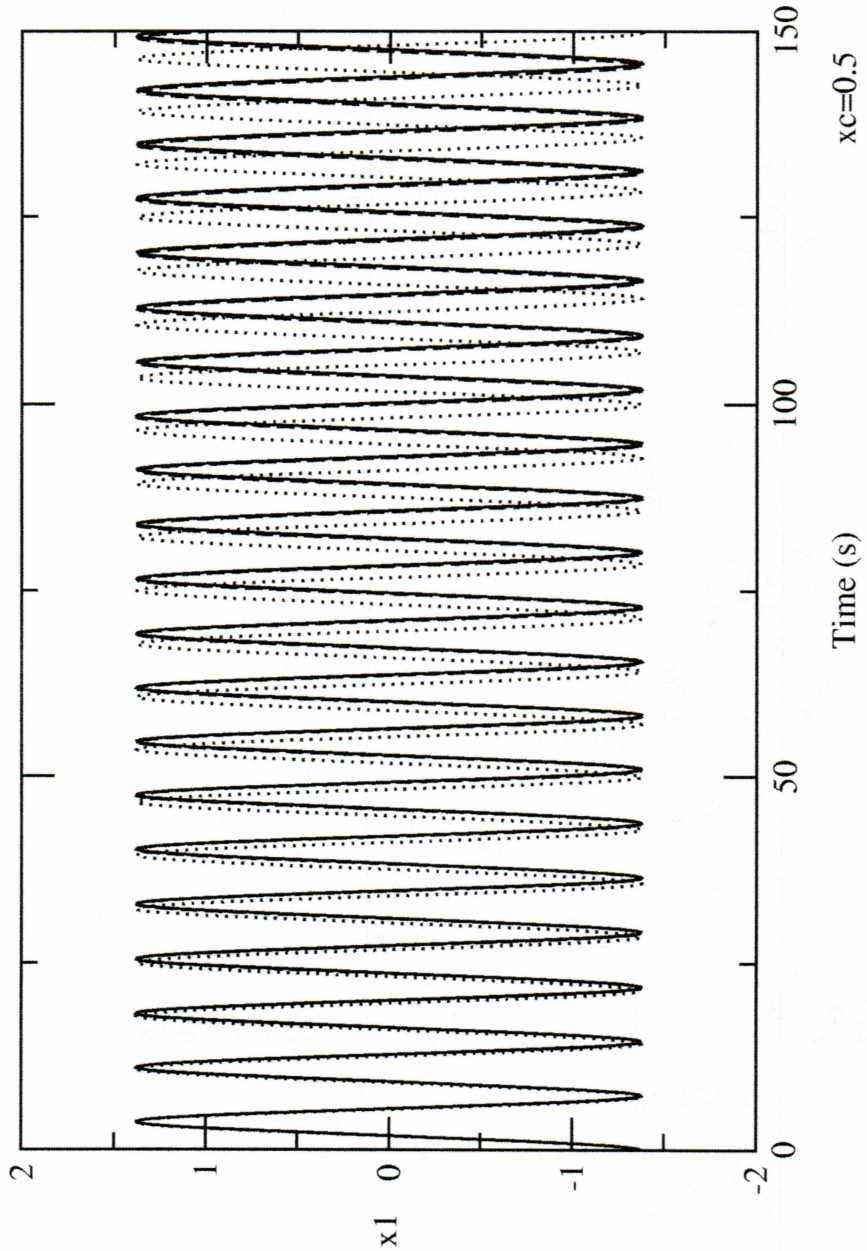

Figure 16: Time series of x1 of reduced order models of deadzone nonlinearity in the first mode computed via the linear-based reduction (dotted), LELSM (dashed), and numerical simulation of the full model (solid) for $\alpha^2 = 2$ and xc = 0.5.

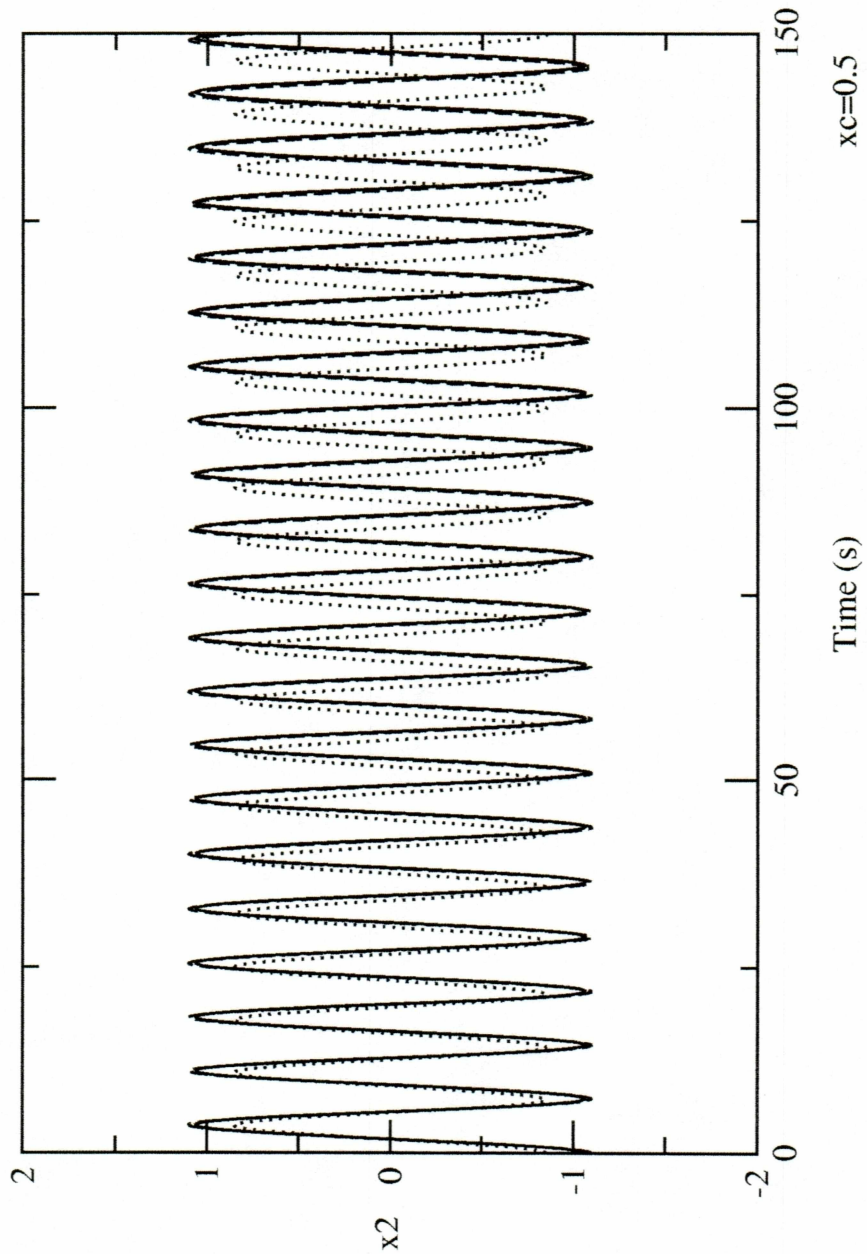

Figure 17: Time series of x2 of reduced order models of deadzone nonlinearity in the first mode computed via the linear-based reduction (dotted), LELSM (dashed), and numerical simulation of the full model (solid) for $\alpha^2 = 2$ and xc = 0.5.

here and in Table 1, the improved reduced model obtained via LELSM results in a significant improvement in the NNM frequency over the linear-based reduced model. Table 1 also lists the exact and approximate NNM frequencies (found via the linear-based reduction and LELSM) for several values of ρ along with the corresponding β values for the reduced models in first and second modes.

5.4.2 Saturation Nonlinearity

As an example of a system with saturation nonlinearity, the equations of motion for the two degree-of-freedom version of equation (11) and (18) are again considered where $m_1=m_2=k_1=k_2=1$. The linear mode shapes and frequencies are identical to the clearance and deadzone cases while the linear-based transformation results in the reduced model of equation (44) with the same values for β_1 and β_2. To find the exact frequencies by numerical integration, the two BNMs are located by simulating the motion for a variety of initial conditions along the equipotential boundary

$$E = \begin{cases} (x_2^2 + (x_1 - x_2)^2 + \kappa_c x_1^2)/2; & |x_1| < x_c \\ (x_2^2 + (x_1 - x_2)^2 + \kappa_c x_c^2)/2; & |x_1| > x_c \end{cases} \tag{54}$$

for E=1 and $\alpha^2 = 2$. In Fig. 9, The first (a) and last (d) plots correspond to the two linear subregions ρ=0 and 1, respectively. Again, the number of NNMs is equal to the number of degrees of freedom for all values of ρ as in the deadzone case.

For the case of x_c =0.75 (Fig. 9c), the exact first modal frequency is found to be 0.950 rad/s. Using equation (21), the approximate nonlinear frequency obtained from the linear-

based reduced model is 0.986 rad/s. An improved reduced model can be obtained via LELSM. The equivalent linear stiffness matrix in this method is given by equation (32) where k_{eq} is found from equation (21) as

$$k_{eq} = \Omega^2 = \omega_-^2 \left[\frac{2}{\pi\alpha}\sin^{-1}\frac{\rho}{\sqrt{\rho(2-\rho)+\frac{(\rho-1)^2}{\alpha^2}}} + 1 - \frac{2}{\pi}\sin^{-1}\left(\frac{\rho}{\frac{1}{\alpha^2}-\rho\left(\frac{1}{\alpha^2}-1\right)} \right) \right]^{-2} \quad (55)$$

with $\alpha^2 = 2$, $\omega_-=1$, and $\rho=0.709$. The relation $\left| \boldsymbol{K}_{eq} - \Omega_i^2 \boldsymbol{I} \right| = 0$ results in an approximate frequency of $\Omega_1=0.951$. Equation (50) is then used to obtain $\beta_1=0.640$ for the corresponding improved reduced order model. Comparisons of exact, linear-based, and improved results are in the time series plots in Fig. 18 for x_1 and Fig. 19 for x_2. As seen here and in Table 2, the improved reduced model obtained via LELSM represents a significant improvement in the NNM frequency over the linear-based reduced model. Table 2 also lists the exact and approximate NNM frequencies (found via the linear-based reduction and LELSM) for several values of ρ along with the corresponding β values for the reduced models in first and second modes.

5.4.3 Bang-bang Nonlinearity

For the bang-bang nonlinearity, the equations of motion for the two degree-of-freedom version of equations (11) and (22) are considered where $m_1=m_2=k_1=k_2=1$. The linear mode shapes and frequencies are identical to the previous cases while the linear-based order reduction transformation results in the reduced model of equation (44) with the same

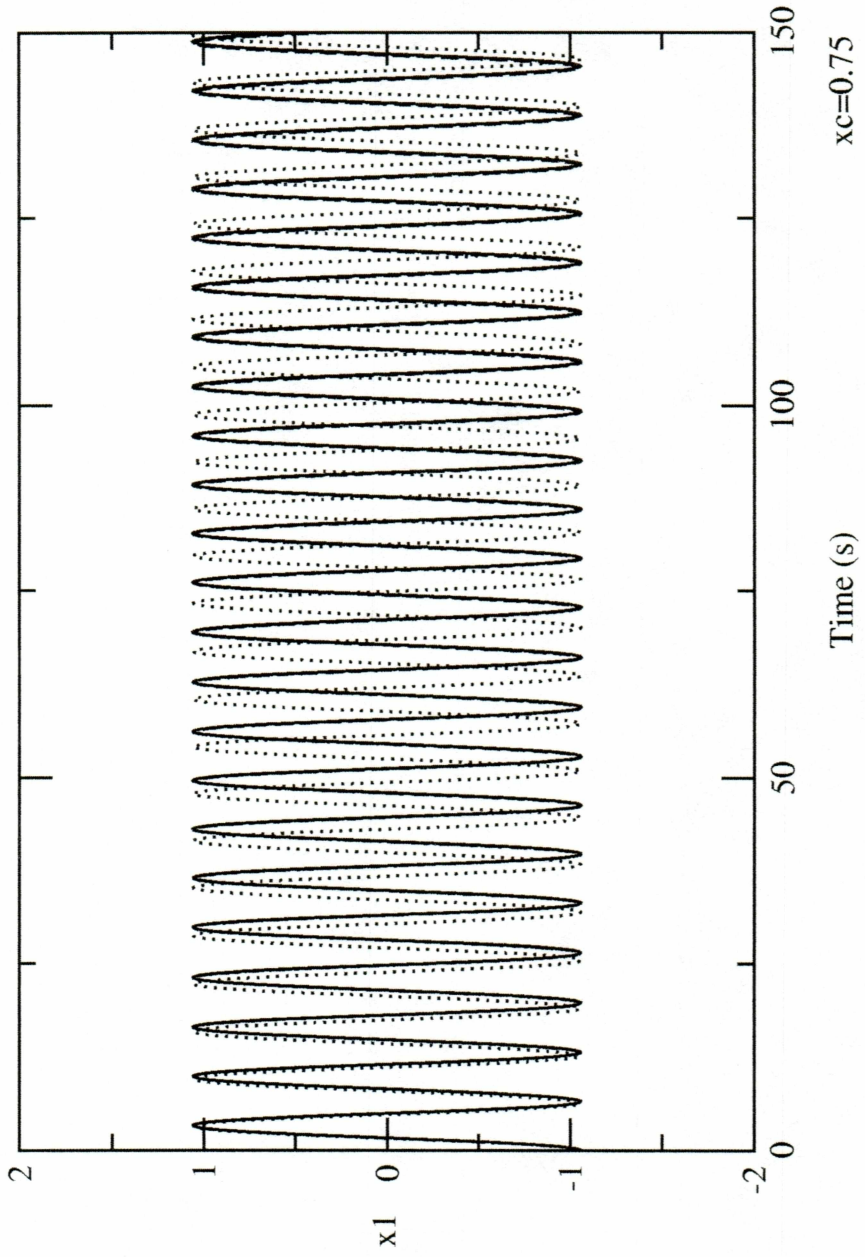

Figure 18: Time series of x1 of reduced order models of saturation nonlinearity in the first mode computed via the linear-based reduction (dotted), LELSM (dashed), and numerical simulation of the full model (solid) for $\alpha^2 = 2$ and xc = 0.75.

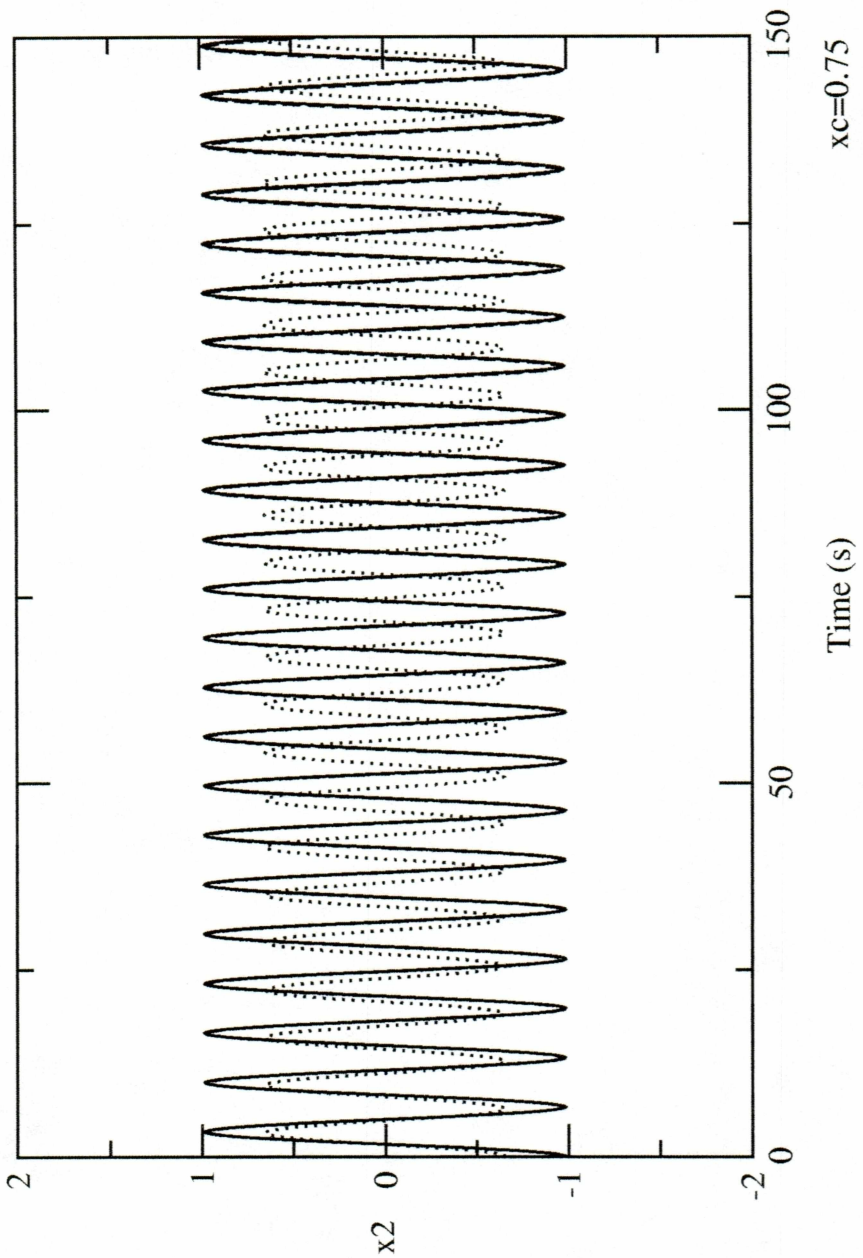

Figure 19: Time series of x2 of reduced order models of saturation nonlinearity in the first mode computed via the linear-based reduction (dotted), LELSM (dashed), and numerical simulation of the full model (solid) for $\alpha^2 = 2$ and xc = 0.75.

Table 2: NNM frequencies for the Saturation nonlinearity obtained from reduced order models and exact numerical simulations.

DOF n	mode i	k_c	ρ	β_i		Ω_i		
				linear based	improved	linear based	improved	exact
2	1	1	0.073	0.724	0.720	0.670	0.670	0.669
2	1	1	0.166	0.724	0.710	0.730	0.728	0.726
2	1	1	0.278	0.724	0.691	0.795	0.788	0.787
2	1	1	0.408	0.724	0.678	0.862	0.849	0.847
2	1	1	0.554	0.724	0.657	0.928	0.904	0.903
2	1	1	0.709	0.724	0.640	0.986	0.951	0.950
2	1	1	0.862	0.724	0.625	1.030	0.984	0.984
2	1	1	1.0	0.724	0.618	1.052	1.0	1.0
2	2	1	0.253	0.276	0.308	1.645	1.648	1.648
2	2	1	0.476	0.276	0.334	1.667	1.677	1.677
2	2	1	0.682	0.276	0.355	1.684	1.703	1.703
2	2	1	0.877	0.276	0.377	1.697	1.725	1.724
2	2	1	1.0	0.276	0.382	1.701	1.732	1.732

values for β_1 and β_2. The exact frequencies can be found by numerical simulation along with the equipotential boundary

$$E = \begin{cases} (x_2^2 + (x_1 - x_2)^2)/2 - \delta x_1; & x_1 < 0 \\ (x_2^2 + (x_1 - x_2)^2)/2 + \delta x_1; & x_1 > 0 \end{cases} \tag{56}$$

for E=1. In Fig. 11, the first (a) plot corresponds to the linear subregion ρ=0. Like the deadzone and saturation cases, the number of NNMs is equal to the number of degrees-of-freedom for the range of ρ shown.

For the case of δ=0.5 (Fig. 11c), the exact first modal frequency is found to be 0.868 rad/s. Using equation (47), the approximate nonlinear frequency obtained from the linear-based reduced model is 0.889 rad/s. As Fig. 15 shows, an improved reduced model can be obtained via LELSM. The equivalent linear stiffness matrix in this method is given by equation (32) where k_{eq} is found from equation (24) as

$$k_{eq} = \Omega^2 = \frac{\omega^2}{\left(1 - \frac{2}{\pi}\sin^{-1}\left(\frac{\rho}{\rho + \omega^2}\right)\right)^2} \tag{57}$$

with ω=1 and ρ=0.450. The relation $\left| \boldsymbol{K}_{eq} - \Omega_i^2 \boldsymbol{I} \right| = 0$ results in an approximate frequency of Ω_1=0.872. Equation (50) is then used to obtain β_1=0.672 for the corresponding improved reduced order model. Comparisons of exact, linear-based, and improved results are in the time series plots in Fig. 20 for x_1 and Fig. 21 for x_2. As seen here and in Table 3, which also lists the exact and approximate NNM frequencies (found

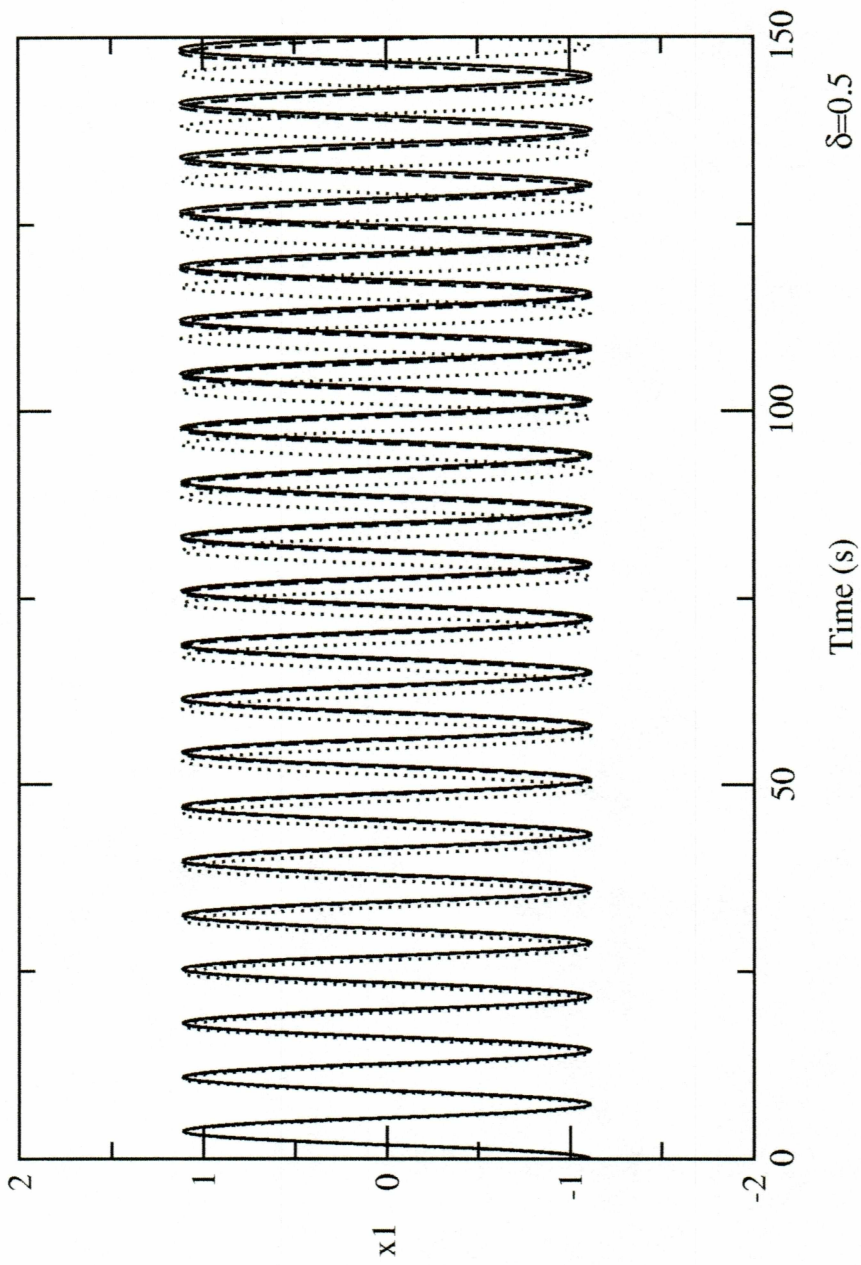

Figure 20: Time series of x1 of reduced order models of bang-bang nonlinearity in the first mode computed via the linear-based reduction (dotted), LELSM (dashed), and numerical simulation of the full model (solid) for δ=0.5.

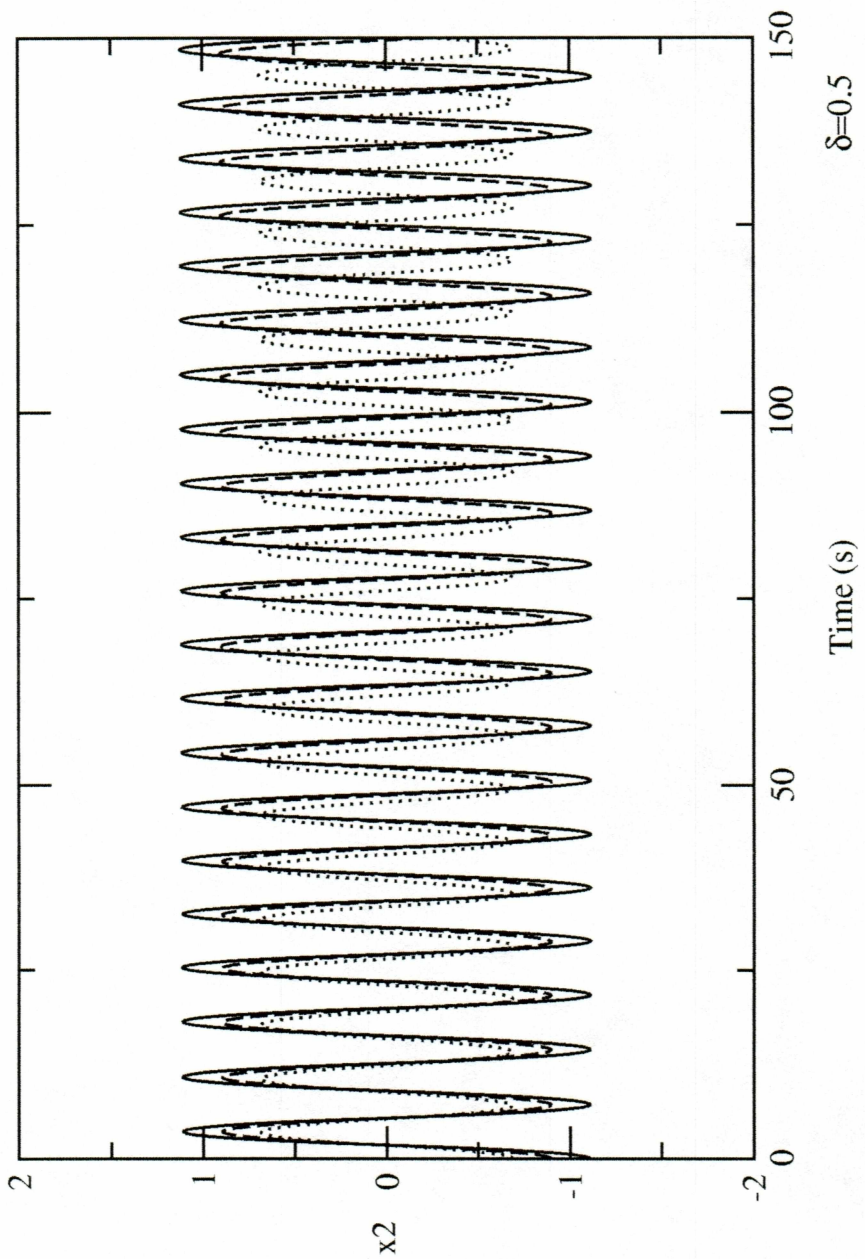

Figure 21: Time series of x2 of reduced order models of bang-bang nonlinearity in the first mode computed via the linear-based reduction (dotted), LELSM (dashed), and numerical simulation of the full model (solid) for δ=0.5.

Table 3: NNM frequencies for the Bang-bang nonlinearity obtained from reduced order models and exact numerical simulations.

DOF n	k_c	ρ	mode i	β_i		Ω_i		
				linear based	improved	linear based	improved	exact
2	1	0.074	1	0.724	0.717	0.671	0.670	0.670
2	1	0.169	1	0.724	0.706	0.733	0.730	0.729
2	1	0.292	1	0.724	0.691	0.805	0.797	0.795
2	1	0.450	1	0.724	0.670	0.889	0.872	0.868
2	1	0.658	1	0.724	0.641	0.988	0.953	0.949
2	1	0.948	1	0.724	0.598	1.112	1.043	1.038
2	1	1.456	1	0.724	0.522	1.300	1.152	1.145
2	1	2.180	1	0.724	0.427	1.529	1.241	1.234
2	1	0.131	2	0.276	0.291	1.632	1.633	1.633
2	1	0.254	2	0.276	0.305	1.645	1.648	1.648
2	1	0.370	2	0.276	0.319	1.658	1.664	1.664
2	1	0.482	2	0.276	0.334	1.669	1.680	1.680
2	1	0.694	2	0.276	0.363	1.692	1.714	1.714
2	1	0.901	2	0.276	0.392	1.713	1.751	1.752
2	1	1.108	2	0.276	0.423	1.734	1.792	1.793
2	1	1.320	2	0.276	0.454	1.755	1.837	1.838
2	1	1.543	2	0.276	0.485	1.777	1.888	1.889
2	1	1.783	2	0.276	0.518	1.800	1.944	1.94

via the linear-based reduction and LELSM) for several additional values of ρ along with the corresponding β values for the reduced models in first and second modes, the improved reduced model obtained via LELSM is extremely accurate. For all values of ρ in both modes, LELSM gives much better approximations than the linear-based model.

5.4.4 Reduction to Multi-Mode Reduced Models

While the examples discussed thus far involve obtaining a single degree-of-freedom reduced model corresponding to a single NNM, it is also possible to reduce a large-order system down to two or more degrees of freedom with dynamics approximating that of multiple NNMs. For this purpose, the LELSM method is used to obtain an equivalent linear stiffness matrix which approximates the NNM frequencies *and invariant manifolds* of the full model. Since the ability to approximate curved manifolds with straight eigenvectors (lines) becomes less accurate the more curved the manifold becomes, this procedure is more successful for symmetric nonlinearities such as deadzone, saturation, and bang-bang than for asymmetric ones such as a bilinear clearance. The approximate LELSM frequencies resulting from the 2 x 2 equivalent stiffness matrices has already been shown for a two degree-of-freedom system with these nonlinearities in Fig. 13,14, and 15. In Fig. 22-24 the slopes of the LELSM eigenvectors for the same systems are shown in both modes versus the parameter ρ along with the slopes of the best-fit lines determined by least-squares regression analysis of the numerically integrated NNM manifolds. It is seen in these figures that the LELSM matrix is very accurate in approximating the manifolds. This characteristic allows us to obtain a multi-mode reduced model which

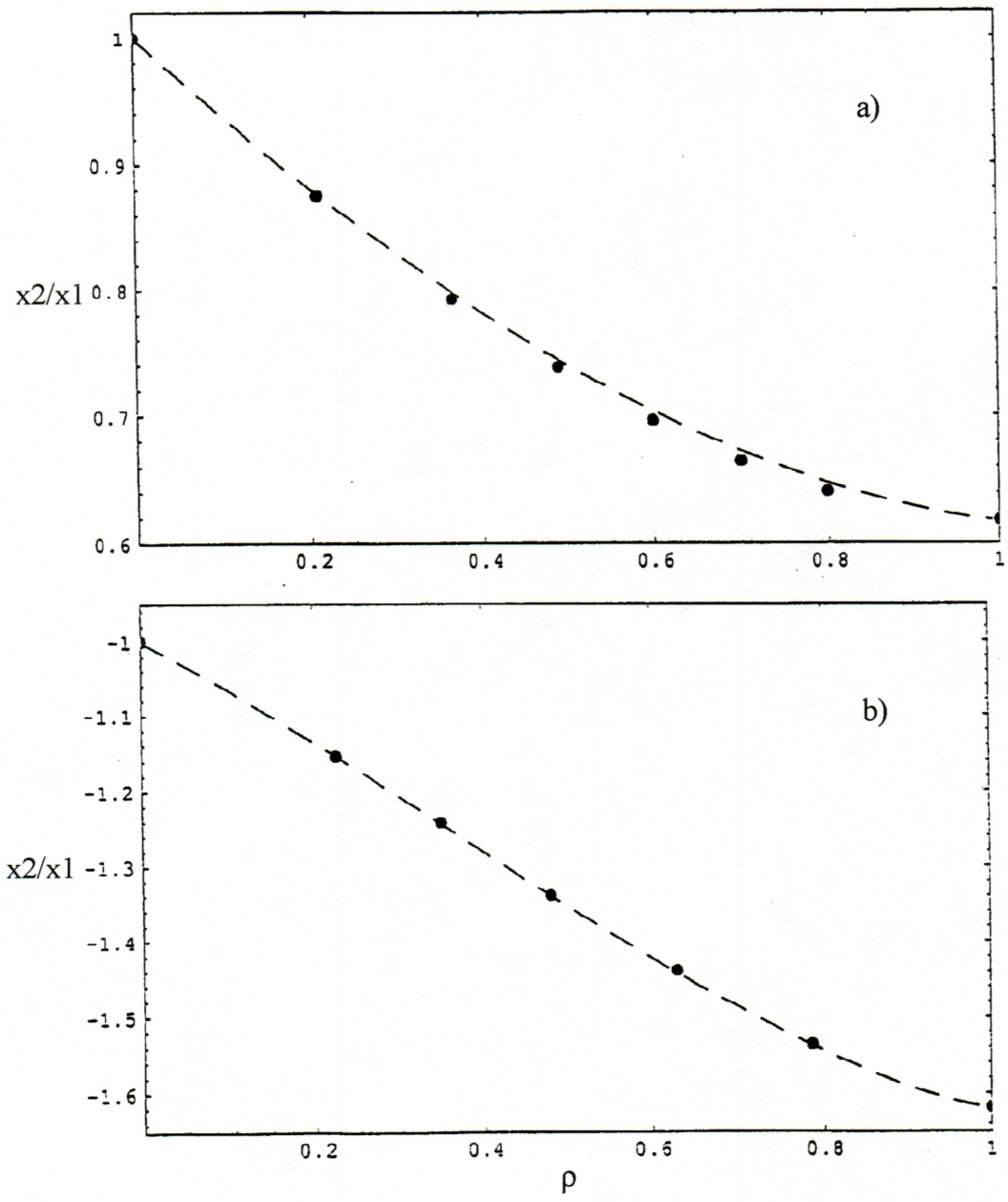

Figure 22: Slopes of the LELSM eigenvectors (long-dashed) of the 2-dof system with deadzone nonlinearity in a) mode 1 and b) mode 2 for $\alpha^2 = 2$ For comparison, the slopes of the best fit lines determined via least squares regression of the numerically simulated NNM manifolds are also shown (dots).

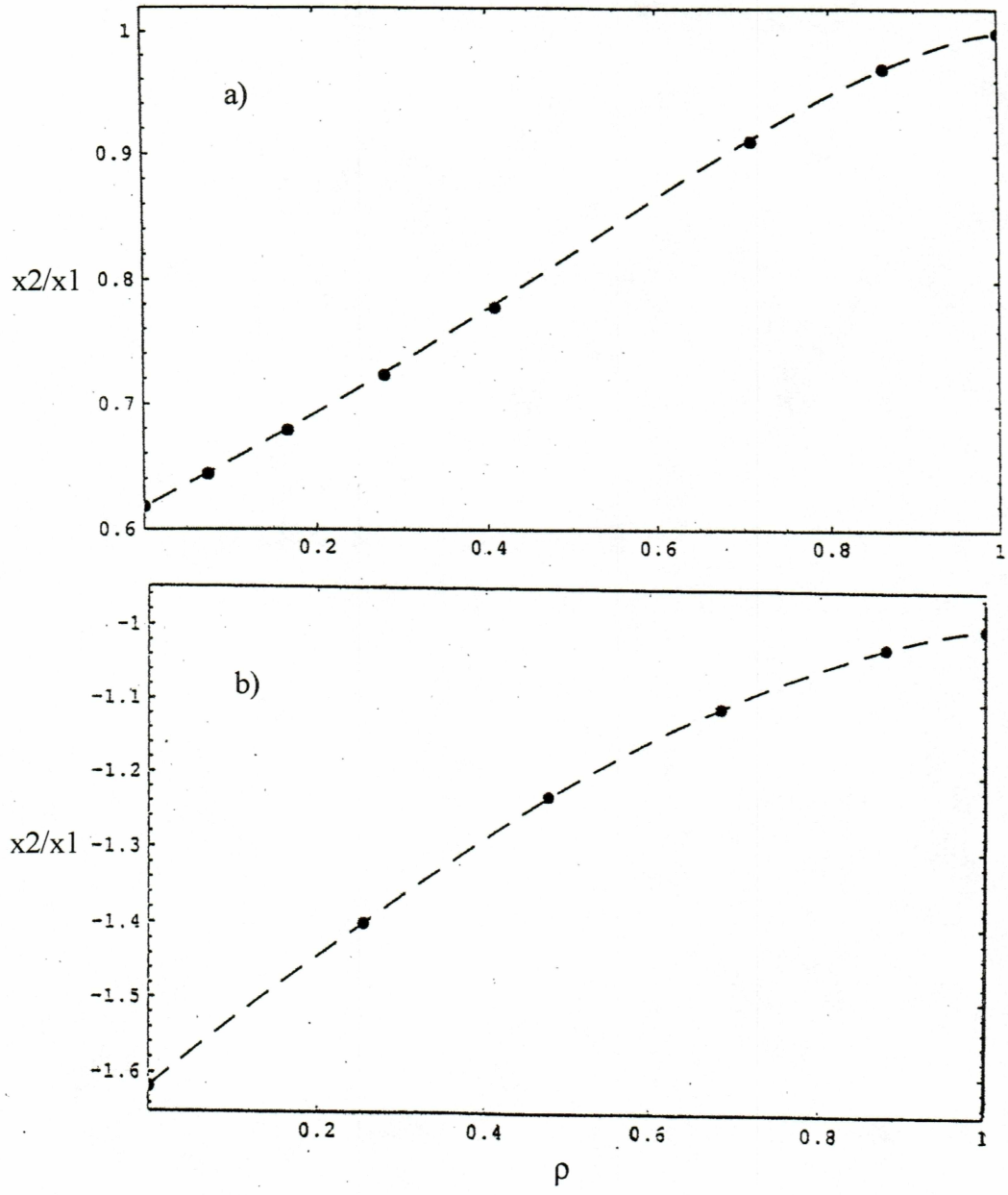

Figure 23: Slopes of the LELSM eigenvectors (long-dashed) of the 2-dof system with saturation nonlinearity in a) mode 1 and b) mode 2 for α^2 =2. For comparison, the slopes of the best fit lines determined via least squares regression of the numerically simulated NNM manifolds are also shown (dots).

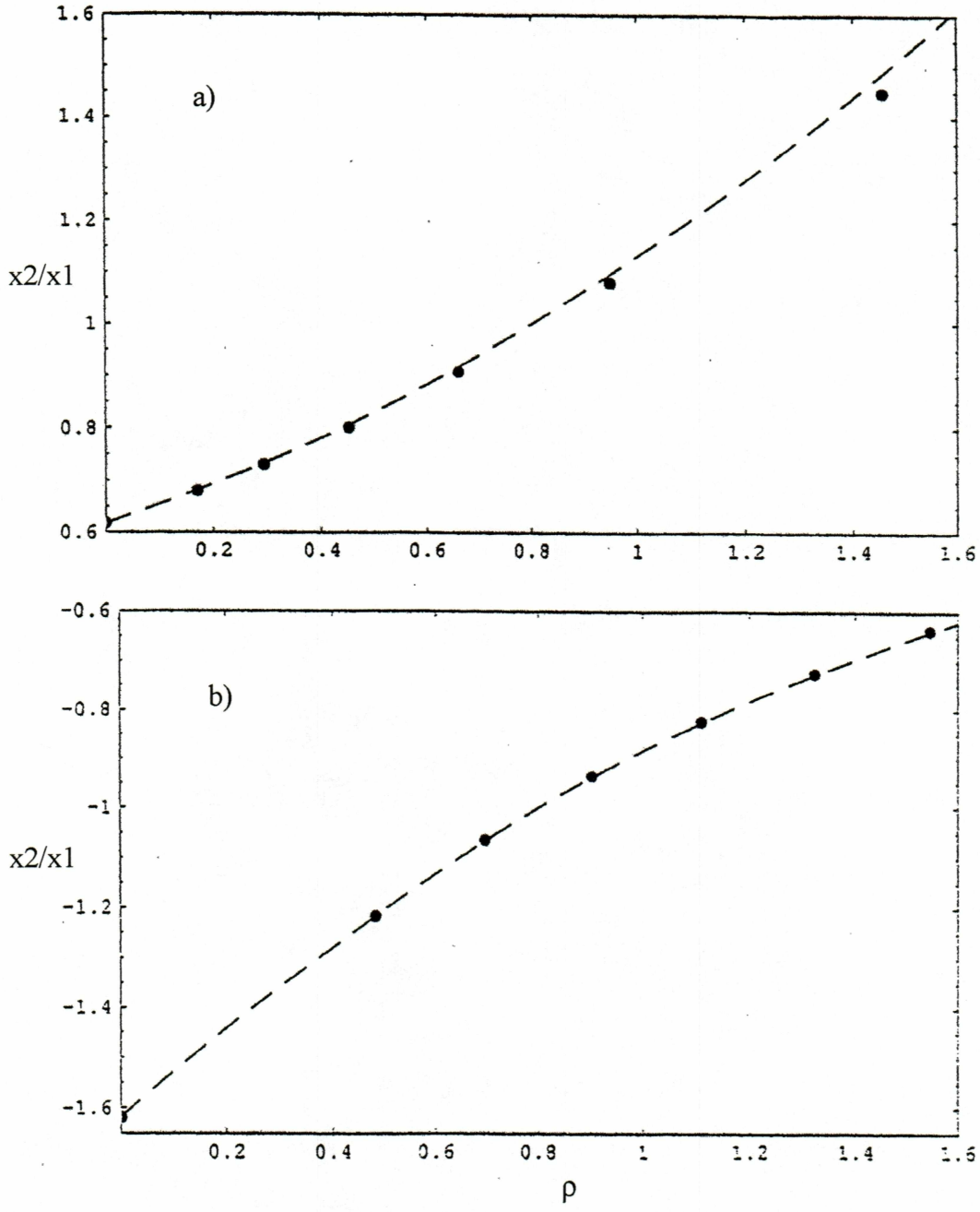

Figure 24: Slopes of the LELSM eigenvectors (long-dashed) of the 2-dof system with bang-bang nonlinearity in a) mode 1 and b) mode 2. For comparison, the slopes of the best fit lines determined via least squares regression of the numerically simulated NNM manifolds are also shown (dots).

accurately approximates the true NNM manifolds projected onto the space of retained coordinates.

As an illustration, we choose the four degree-of-freedom system with a deadzone nonlinearity of the form

$$\ddot{x} + \begin{bmatrix} 1 & -1 & 0 & 0 \\ -1 & 2 & -1 & 0 \\ 0 & -1 & 2 & -1 \\ 0 & 0 & -1 & 2 \end{bmatrix} x + \begin{bmatrix} f(x_1) \\ 0 \\ 0 \\ 0 \end{bmatrix} = 0 \tag{58}$$

where $f(x_1)$ is given by equation (18) with k_c=1 and x_c=1.25. It is desired to reduce equation (58) to two degrees-of-freedom. First, the linear-based order reduction in equations (36-39) is implemented by transforming equation (58) via

$$x = \begin{bmatrix} 1 & 0 \\ 0 & 1 \\ -1 & 1.8794 \\ -1 & 1.5321 \end{bmatrix} x_m \tag{59}$$

This results in the reduced order model

$$\begin{bmatrix} 3.0 & -3.4115 \\ -3.4115 & 6.8794 \end{bmatrix} \ddot{x}_m + \begin{bmatrix} 3.0 & -3.4115 \\ -3.4115 & 4.2412 \end{bmatrix} x_m + \begin{bmatrix} f(x_1) \\ 0 \end{bmatrix} = 0 \tag{60}$$

As explained previously, the transformation of equation (59) preserves the exact eigenstructure of the linear part of equation (58).

On the other hand, an equivalent linear stiffness matrix corresponding to the full model may be obtained *before the reduction process* by first computing the values of the

parameter ρ in each mode corresponding to a given energy level. Since the amplitude of coordinate x_1 depends on the mode for a given energy level, a separate ρ_i must be computed for the *i*th mode. By solving for the intersections of the eigenvectors of the stiffness matrix in equation (58) with the equipotential boundaries corresponding to a total energy of E=1 (which are computed similarly to equation (52)), the approximate amplitudes of x_1 in modes 1-4 are obtained as 2.115, 0.816, 0.396, and 0.172, respectively. It is thus apparent that only the first mode penetrates into the second linear subregion. Consequently, we obtain $\rho_{1\text{-}4}$ =0.591, 1.0, 1.0, 1.0. The equivalent stiffness matrix is then computed by assembling separate eigenvectors and eigenfrequencies as

$$K_{eq} = Udiag(0.4781^2, 1.0^2, 1.5321^2, 1.8794^2)U^{-1} \tag{61}$$

where the first frequency (0.4645) and the first eigenvector in U ((0.5640, 0.5982, 0.4957, 0.2798)^T) are found from those for the first mode in the approximate linear system

$$\ddot{x} + \begin{bmatrix} k_{eq} & -1 & 0 & 0 \\ -1 & 2 & -1 & 0 \\ 0 & -1 & 2 & -1 \\ 0 & 0 & -1 & 2 \end{bmatrix} x = 0 \tag{62}$$

where k_{eq} is obtained as 1.289 using the values ρ_1=0.591 and $\alpha^2 = 2$ in equation (20) in conjunction with the LELSM method. However, equation (62) represents *only the dynamics in the first mode*. Since it was seen that the other modes remain in the first subregion, the remaining frequencies (1.0, 1.5321, 1.8794) and eigenvectors in U ((0.5774, 0., -0.5774, -0.5774)^T; (0.4285, -0.5774, -0.2280, 0.6565)^T; (0.2280, -0.5774,

0.6565, -0.4285)^T) correspond to those in the stiffness matrix in equation (58).

Thus equation (58) can be replaced by an equivalent linear system with the stiffness matrix computed from equation (61) as

$$\ddot{x} + \begin{bmatrix} 1.080 & -0.9051 & 0.0705 & 0.0375 \\ -1 & 2 & -1 & 0 \\ 0 & -1 & 2 & -1 \\ 0 & 0 & -1 & 2 \end{bmatrix} x = 0 \tag{63}$$

The reason that K_{eq} is not symmetric is due to the fact that the eigenvector extracted from equation (62) is not orthogonal to the remaining ones extracted from the linear part of equation (58). Hence, this procedure accurately captures an important trait of NNMs of nonsmooth systems: *in general, they are not orthogonal at their intersection* (Zuo and Curnier, 1994). The eigenstructure-preserving transformation

$$x = \begin{bmatrix} 1 & 0 \\ 0 & 1 \\ -1 & 1.7714 \\ -1 & 1.4106 \end{bmatrix} x_m \tag{64}$$

then results in the reduced order linear system (with asymmetric stiffness matrix)

$$\begin{bmatrix} 3.0 & -3.1820 \\ -3.1820 & 6.1278 \end{bmatrix} \ddot{x}_m + \begin{bmatrix} 3.0 & -2.9094 \\ -3.1820 & 3.7151 \end{bmatrix} x_m = 0 \tag{65}$$

Thus, equation (65) has the exact lowest eigenfrequencies (0.4781 and 1.0) from equation (63) while the (non-orthogonal) mode shapes ((0.5640, 0.5982)^T and (0.5774, 0.0)^T) are exact projections of those in equation (63) onto the coordinates x_m. For comparison, the

LELSM method can be used to estimate the actual NNM frequency of equation (60) in the first mode as 0.4820 while the corresponding eigenvector $(0.5640, 0.5589)^T$ approximates the curved manifold as a straight line. Because the nonlinearity is not present in the second mode, its frequency and eigenvector are identical with those of equation (65).

While equation (65) is an accurate reduced model in the sense that the NNM frequencies and mode shapes are well-approximated by the linear eigenstructure, it may be preferable to obtain a reduced model in the form

$$\begin{bmatrix} 3.0 & -3.4115 \\ -3.4115 & 6.8794 \end{bmatrix} \ddot{x}_m + \begin{bmatrix} 3.0 & -3.4115 \\ -3.4115 & 4.2412 \end{bmatrix} x_m + \beta \begin{bmatrix} f(x_1) \\ 0 \end{bmatrix} = 0 \qquad (66)$$

which retains the linear part of equation (60) (obtained from the linear-based transformation) as well as a form of the original nonsmooth nonlinearity (multiplied by a parameter β) as did the single degree-of-freedom reduced models obtained previously. For such a model, it is desired to find a β which results in a model that more accurately represents the actual NNM dynamics that does the linear-based model (in which $\beta=1$). To accomplish this, at least two strategies are possible. First, equation (49) can be solved numerically for $\beta=0.3806$ in terms of $\Omega_1 = 0.4781$ and $\omega_{-1} = 0.3473$ (the lowest frequency of the linear part of equation (58)). The approximate frequency and mode shape of mode 1 in the resulting model in equation (66) can be approximated via LELSM as 0.4082 and $(0.5640, 0.5181)^T$, respectively, which are not as good as in the linear-based reduced model in this case.

The second approach is to try to find a stiffness matrix $\hat{K}_{eq}$ of the form

$$\hat{K}_{eq} = \begin{bmatrix} k_{eq} & -3.4115 \\ -3.4115 & 4.2412 \end{bmatrix} \tag{67}$$

which, when used in conjunction with the mass matrix in equation (60), results in (almost) the same eigenstructure as in equation (65). This is just the reverse of the LELSM method. In this case, k_{eq} was found as 3.281 which forces the lowest frequency to be identical with that (0.4781) from equation (65). Then, a value of β=**0.962** was found for which equation (66) has (nearly) the same NNM frequency in the first mode. The LELSM mode shape was determined as $(0.5640, 0.5562)^T$. Thus, the reduced model in equation (66) with this value of β is more accurate than with the previously computed value of β, and also more accurate than the linear-based reduced model in equation (60) when compared with the frequencies in equation (65).

CHAPTER 6

EIGENSTRUCTURE ASSIGNMENT

6.1 Linear System

For a linear system, two techniques are widely used for eigenstructure assignment.

6.1.1 Eigenvalue Placement

Consider the system of n second order differential equations in structural form

$$M\ddot{x} + Kx = Bu(t) \tag{68}$$

where the uncontrolled system is on the left hand side and ***Bu(t)*** is the control term. We assume that the controller has n actuators so that the matrix $\boldsymbol{B}$ has full rank. For simplicity we set it to $\boldsymbol{B} = \boldsymbol{I}$, the n-dimensional identity matrix. So for the uncontrolled part of (68), we can solve for the natural frequencies $\omega_1, \omega_2 \ldots \omega_i$. Suppose now that it is desired to change the natural frequencies to $\Omega_1, \Omega_2 \ldots \Omega_i$, The control force is chosen to be proportional to the displacements so that we have the constant gain feedback control law

$$u(t) = -Gx(t) \tag{69}$$

Furthermore, the gain matrix $\boldsymbol{G}$ is yielding n control gains to be found. So equation (68) becomes

$$M\ddot{x} + (K + G)x = 0 \tag{70}$$

where $G = \begin{bmatrix} g_1 & & & \\ & g_2 & & \\ & & \cdots & \\ & & & g_3 \end{bmatrix}$

we've already known that the natural frequencies are $\Omega_1, \Omega_2 \ldots \Omega_i$, so we can solve for G in (70), it's the controlled gain matrix.

6.1.2 Full Eigenstructure Placement

For the system represented by (68), not only we can change eigenvalues, we can also change eigenstructure.

For a desired system which has eigenstructure(eigenvalues and eigenvectors) that is designed

$$\ddot{x} + M_0^{-1} K_0 x = 0 \tag{71}$$

in equation (68), set

$$u(t) = -Gx(t) \tag{72}$$

where G is a full gain matrix.then we got

$$\ddot{x} + M^{-1}(K + BG)x = 0 \tag{73}$$

Comparing equations (71) and (73), solve for G, equation (44) becomes the designed system.

6.2 Nonsmooth Systems

6.2.1 Eigenvalue Placement via Pmm and N Constant Gains

Consider the system of n second order differential equations in structural form

$$M\ddot{x} + Kx + F(x) = Bu(t) \tag{74}$$

where the uncontrolled system is on the left hand side and the nonsmooth nonlinearity $F(x)$ is piecewise linear and isolated to the first coordinate and equation, i.e. $F(x)=(F(x_1)\ 0\ \ldots\ 0)^T$. We assume that the controller has n actuators so that the matrix $\boldsymbol{B}$ has full rank. For simplicity we set it to $\boldsymbol{B} = \boldsymbol{I}$, the n-dimensional identity matrix. The control force is chosen to be proportional to the displacements so that we have the constant gain feedback control law

$$u(t) = -Gx(t) \tag{75}$$

Furthermore, the gain matrix $\boldsymbol{G}$ is assumed to be diagonal thus yielding n control gains to be found.

In equation (26), if we divide the top and bottom by $\frac{2\omega_{+i}}{\pi}$, we obtain

$$\Omega_i = \omega_{-i} f(\rho_i, \gamma_i) \tag{76}$$

where

$$f(\rho_i, \gamma_i) = \pi \left[\frac{\pi}{2} + \sin^{-1}\rho_i + \frac{1}{\gamma_i}\left(\frac{\pi}{2} - \sin^{-1}\left(\frac{\rho_i}{\gamma_i \sqrt{1-\rho_i^2\left(1-\frac{1}{\gamma_i^2}\right)}} \right) \right) \right]^{-1} \tag{77}$$

The uncontrolled version of equation (74) has frequencies ω_{-i} and ω_{+i} in the first and second linear subregions, respectively, and overall NNM frequencies Ω_i. It is these which we desire to shift to some other specified values, denoted by $\hat{\Omega}_i$. If we can solve for the

corresponding shifted frequencies in either linear subregion, then it is straightforward to solve for the required control gains. To accomplish this, equation (76) is solved as

$$\hat{\omega}_{-i} = \frac{\hat{\Omega}_i}{f(\rho_i, \hat{\gamma}_i)} \tag{78}$$

where all terms with a hat represent the desired controlled values. However, because we do not know the value of $\hat{\gamma}_i$ (the ratio of the *controlled* linear *i*th mode frequencies in the two subregions) *a priori*, we must approximate by using the uncontrolled value, and equation (78) becomes

$$\hat{\omega}_{-i} \approx \frac{\hat{\Omega}_i}{f(\rho_i, \gamma_i)} \tag{79}$$

After solving for the controlled linear frequencies via equation (79), the control gains necessary to achieve them may be found from a variety of methods. The approach taken here is to write the characteristic equations of the desired system and the controlled system and to equate coefficients of like monomial powers to yield *n* algebraic equations for the *n* gains, which can then be solved. Then it is necessary to determine the updated value of $\hat{\gamma}_i$ so that one can determine the actual controlled frequencies via

$$\hat{\Omega}_i = \hat{\omega}_{-i} f(\rho_i, \hat{\gamma}_i) \tag{80}$$

Setting $\hat{\gamma}_i \rightarrow \gamma_i$, equation (79) may be iterated repeatedly until the control gains are found which result in NNM frequencies sufficiently close to the desired values via equation (80).

6.2.2 Eigenvalue Placement Via Order Reduction And One Constant Gain

Reconsider the system in equation (68) in which the matrix $\boldsymbol{B}=(1\ 0\ \ldots\ 0)^T$ corresponds to only one actuator. The scalar control force is chosen to be proportional to the displacement of x_1 as $u(t)=-gx_1$ where g is the unknown control gain to be found. To accomplish this, we reduce equation (68) to one master coordinate, eliminating the *n-1* slave coordinates. The linear uncontrolled part of (68) is

$$M\ddot{x} + Kx = 0 \tag{81}$$

whose eigenfrequencies ω_i and eigenvectors ϕ_i are easily obtained. Typically the mode with the lowest frequency is retained in the reduced order model. To construct the reduced model, we follow Burton and Young (1994), Burton and Rhee (2000), and Rhee and Burton (2000) and perform the transformation $x = \phi_i x_1$ to equation (68) where ϕ_i is the eigenvector corresponding to the retained mode normalized such that the first element is one. Premultiplying by ϕ_i^T and normalizing the mass to unity yields

$$\ddot{x}_1 + \omega_i^2 x_1 + \beta_i F(x_1) = \beta_i u(t) \tag{82}$$

where

$$\omega_i = \sqrt{\frac{\phi_i^T K \phi_i}{\phi_i^T M \phi_i}} \qquad \beta_i = \frac{1}{\phi_i^T M \phi_i} \tag{83}$$

It can be seen that the form of the nonsmooth nonlinearity is retained in the reduced model which utilizes a subset of the original physical coordinates.

For the single degree-of-freedom reduced model in equation (82) with $F(x_1)$ given in equation (13), the *uncontrolled* frequencies in the two linear subregions are $\omega_{-i} = \omega_i$ and

$$\omega_{+i} = \sqrt{\omega_{-i}^2 + \beta_i k_c} \tag{84}$$

(γ_i is the ratio of these) and NNM frequency Ω_i in the mode of interest. Again, we desire to shift the latter to some other specified value, denoted by $\hat{\Omega}_i$, by implementing feedback control. Equation (79) is used to solve for the corresponding *controlled* frequency in the first linear subregion while using the uncontrolled value for γ_i. Bringing the control force in equation (82) over to the left hand side, this frequency is also expressed as

$$\hat{\omega}_{-i} = \sqrt{\omega_{-i}^2 + \beta_i g} \tag{85}$$

from which the required gain is solved as

$$g = \frac{1}{\beta_i}(\hat{\omega}_{-i}^2 - \omega_{-i}^2) \tag{86}$$

One can then determine the updated value of $\hat{\gamma}_i$ and the actual controlled frequency via equation (80). Setting $\hat{\gamma}_i \to \gamma_i$, equations (89) and (86) may be iterated repeatedly until the control gain is found which results in a NNM frequency sufficiently close to the desired value.

6.2.3 Eigenstructure Assignment Via Lelsm And Full Gain Matrix

Again reconsider equation (74-75) in which no restrictions on the dimensions of $\boldsymbol{B}$ or $\boldsymbol{G}$ are made. It is desired to calculate the gain matrix $\boldsymbol{G}$ such that the controlled nonlinear

system has the approximate desired frequencies and mode shapes of a redesigned linear system

$$M_0\ddot{x} + K_0 x = 0 \tag{87}$$

Thus, this problem of eigenstructure assignment goes further than specifying the frequencies alone (eigenvalue placement). Also, although the NNM modes of the controlled and uncontrolled systems are not straight eigenvectors as in the linear case, the desired eigenvectors of equation (87) are usually quite similar to the actual curved NNM manifolds of the controlled system, while a regression analysis can be used to assess the accuracy.

In order to implement linear eigenstructure assignment, the Local Equivalent Linear Stiffness Method (LELSM) developed by Butcher (1999) is used to incorporate the effects of the nonlinear term *F(x)*. It was suggested there that only a single element $k_{eq} = (\Omega/\omega_{\_})^2$ (using the normalized frequency of equation (16), for example, on the main diagonal of an equivalent linear stiffness matrix $\boldsymbol{K}_{eq}$ should be affected by the presence of the nonlinearity while the remaining elements should remain unchanged from those in $\boldsymbol{K}$. The eigenvalue problem with matrices $\boldsymbol{M}$ and $\boldsymbol{K}_{eq}$ then yields the approximate NNM frequencies and mode shapes. Here, since n different ρ values (and hence k_{eq} and $\boldsymbol{K}_{eq}$) result from each mode having a different initial condition for the same energy level, it is necessary to compute $\boldsymbol{K}_{eq}$ as

$$K_{eq} = U\ diag(\Omega_1^2, \ldots, \Omega_n^2)U^{-1} \tag{88}$$

from the n frequencies and eigenvectors corresponding to the n individual equivalent stiffness matrices. The method can be easily implemented for higher dimensional systems.

Proceeding as in Inman (1989), the closed loop system becomes

$$\dot{x} + M^{-1}(K_{eq} + BG)x = 0 \tag{89}$$

Premultiplying equation (87) by M_0^{-1} and comparing with equation (89) yields the gain matrix as

$$G = B^I M(M_0^{-1}K_0 - M^{-1}K_{eq}) \tag{90}$$

in which B^I represents the left generalized inverse of $\boldsymbol{B}$. Thus, if this value of the gain matrix is implemented the resulting closed-loop system will have a response similar to that of the design set in equation (87). It should be pointed out that only mode shapes that satisfy certain criteria can be placed according to the linear theory (Andry *et al*, 1983).

6.2.4 Example: A 2-dof System With A Bilinear Clearance Nonlinearity

As an example of the first two strategies, the two-degree-of-freedom system with a bilinear clearance nonlinearity is considered. Equations (74-75) are given as

$$\begin{aligned} m_1\ddot{x}_1 + k_1(x_1 - x_2) + F(x_1) &= -g_1x_1 \\ m_2\ddot{x}_2 + (k_1 + k_2)x_2 - k_1x_1 &= -g_2x_2 \end{aligned} \qquad F(x_1) = \begin{cases} 0; & x_1 < x_c \\ k_c(x_1 - x_c); & x_1 > x_c \end{cases} \tag{91}$$

where g_1 and g_2 are the constant control gains. We consider the case of m_1=m_2=k_1=k_2=1 while x_c=0.5 and k_c=1 ($\alpha = \sqrt{2}$). The linear uncontrolled mode shapes in the first

subregion (with $F(x_1)$=0) are $\phi_1 = (1.0 \quad 0.618)^T$ and $\phi_2 = (1.0 \quad -1.618)^T$ and the modal frequencies are ω_{-1}=0.618 and ω_{-2}=1.618. The frequencies in the second subregion are ω_{+1}=1.0 and ω_{+2}=1.732.

To find the exact BNM frequencies for the uncontrolled system, the two BNMs can be located by simulating the motion for a variety of initial conditions along the equipotential boundary

$$E = \begin{cases} (x_2^2 + (x_1 - x_2)^2)/2; & x_1 < x_c \\ (x_2^2 + (x_1 - x_2)^2 + \kappa_c (x_1 - x_c)^2)/2; & x_1 > x_c \end{cases} \tag{92}$$

corresponding to some chosen energy level. Through trial and error, the correct initial conditions which yield periodic motion can be located by examining the motion in the configuration space. This is shown in Fig. 6(d) where the total energy of the uncontrolled system is E=1. For this case the first BNM has initial condition (x_1, x_2)=(-2.0,-1.0), ρ_1=0.25 and frequency Ω_1=0.717 while the second (ρ_2=1.0, Ω_2=1.618) is identical to the linear frequency. It is desired to shift these frequencies to $\hat{\Omega}_1$=0.85 and $\hat{\Omega}_2$=1.65 by implementing the position feedback control technique with two constant gains corresponding to the diagonal elements of the gain matrix $\boldsymbol{G}$ (with $\boldsymbol{B}=\boldsymbol{I}$) in equation (74). The Piecewise Modal Method (PMM) via equation (77) is used with the uncontrolled values for γ_1 =1.618 and γ_2 =1.070 to obtain $f(\rho_1, \gamma_1)$ =1.166 and $f(\rho_2, \gamma_2)$ =1. Following Section 6.2.1, the corresponding desired linear frequencies are found via equation (79) as $\hat{\omega}_{-1}$ =0.729 and $\hat{\omega}_{-2}$ =1.65.

To solve for the gains, the characteristic equations of the desired and controlled systems in the first linear subregion are equated as

$$det\begin{bmatrix} 1+g_1-\lambda & -1 \\ -1 & 2+g_2-\lambda \end{bmatrix} = (\lambda - 0.729^2)(\lambda - 1.65^2) \tag{93}$$

Collecting like powers in λ yields two equations for the gains:

$$\begin{aligned} -(3+g_1+g_2) &= -3.255 \\ 1+2g_1+g_2+g_1g_2 &= 1.450 \end{aligned} \tag{94}$$

from which g_1=0.182 and g_2=0.073 (the other solution results in negative gains and is ignored). To find the actual values for $\hat{\Omega}_i$, the controlled frequencies in the second subregion are found from

$$det\begin{bmatrix} 2.182-\omega_{+i}^2 & -1 \\ -1 & 2.073-\omega_{+i}^2 \end{bmatrix} = 0 \tag{95}$$

from which $\hat{\omega}_{+1,2}$ =1.061, 1.769 which yields $\hat{\gamma}_{1,2}$=1.455, 1.072. The actual controlled BNM frequencies are found from equation (80) to be $\hat{\Omega}_{1,2}$=0.823, 1.65.

It is seen that the first BNM frequency has shifted but is not the desired value, while the second frequency has become the desired value since it is a purely linear mode. To compute better gain values (and hence achieve a controlled frequency in the first mode that is closer to the desired value), we make the substitution $\hat{\gamma}_i \rightarrow \gamma_i$ and iterate equations (79-80) repeatedly until the desired accuracy is achieved. Table 4 shows the results for

Table 4: Comparison of theoretical and exact controlled NNM frequencies.

Controller	Iteration	g_i	$\hat{\Omega}_i$	Exact W_i
PMM/ 2 gains Uncontrolled frequencies: 0.717, 1.618 Desired frequencies: 0.850, 1.650	1	0.182, 0.073	0.823, 1.650	
	2	0.243, 0.046	0.843, 1.650	
	3	0.260, 0.039	0.848, 1.650	
	4	0.266 0.035	0.850, 1.650	0.865, 1.653
Order Red./ 1 gain Uncontrolled frequencies: 0.717, 1.618 Desired frequency: 0.850	1	0.187	0.827	
	2	0.227	0.847	
	3	0.233	0.849	
	4	0.235	0.850	0.846, 1.643

four iterations in which the final gain values are g_1=0.266 and g_2=0.035, resulting in NNM frequencies exactly equal to the desired values according to PMM. However, it must be recalled that PMM is an approximate technique, so in order to assess the accuracy the actual controlled BNM frequencies must be found by numerical integration. To this end, the control energy is computed as 0.55 (yielding a total energy of 1.55). Fig. 25 shows the controlled BNMs found in this way where the frequencies are 0.865 and 1.653. Hence the control strategy has succeeded in shifting the frequencies to within 11% of the desired values as compared with the uncontrolled system.

Next we control the same problem of equation (91) using the position feedback with order reduction and one constant gain. Referring to equation (68) in which the matrix $\boldsymbol{B}=(1\ 0\ \ldots\ 0)^T$ corresponds to one actuator and $u(t)=-gx_1$ where g is the unknown control gain to be found, it is obvious that we set $g_1=g$ and $g_2=0$ in equation (91). It is desired to design g in order to shift the first BNM frequency to $\hat{\Omega}_1=0.85$. Using the transformation

$$\begin{bmatrix} x_1 \\ x_2 \end{bmatrix} = \begin{bmatrix} 1.0 \\ 0.618 \end{bmatrix} x_1 \tag{96}$$

the single degree-of-freedom reduced order model of equation (82) is obtained where ω_1=0.618 and β_1=0.724. Following Section 4, the corresponding desired linear frequency is found via equation (79) with $\gamma_1 = \sqrt{0.618^2 + 0.724}/0.618 = 1.702$ as $\hat{\omega}_{-1}$=0.719.

The gain is found via equation (86) as $g=(0.719^2-0.618^2)/0.724=0.187$. The actual controlled value of $\hat{\gamma}_1 = \sqrt{0.719^2 + 0.724}/0.719 = 1.549$ is then used to compute the

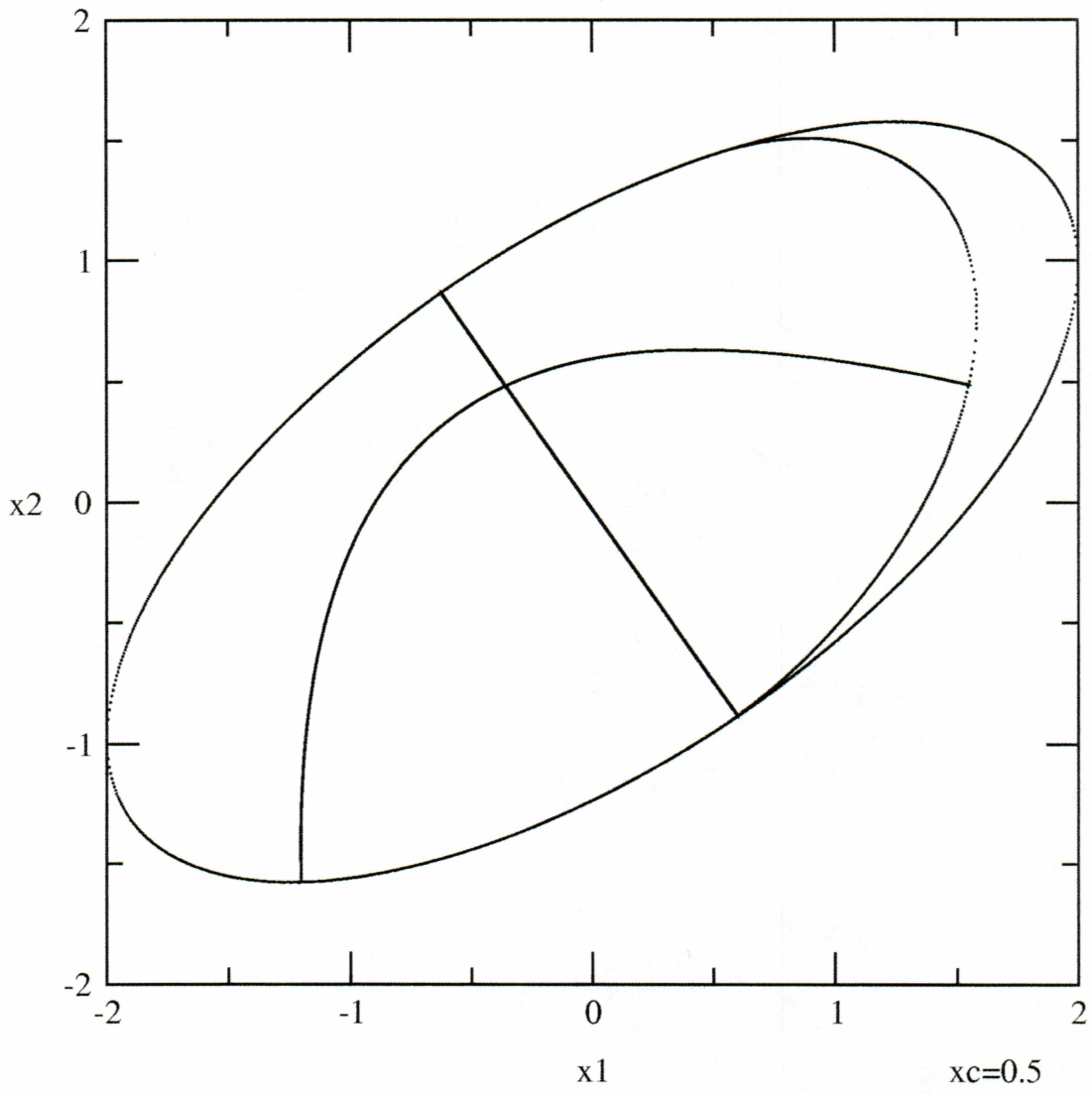

Figure 25: Numerical simulations in configuration space of the controlled BNMs (using the PMM strategy) for the system with a bilinear clearance nonlinearity.

actual BNM frequency of 0.827 via equation (80). Making the substitution $\hat{\gamma}_i \to \gamma_i$ and iterating equations (79) and (86), the desired frequency is achieved in four iterations as shown in Table 4. Although the final gain of g=0.235 causes the reduced model to have the desired frequency, the fact that the reduced model is an approximation to the dynamics in mode 1 means that the accuracy of the controlled BNM frequencies must be found by numerical integration. To this end, the control energy is computed as 0.47 (yielding a total energy of 1.47). Fig. 26 shows the controlled BNMs found in this way where the frequencies are 0.846 and 1.643. Hence the control strategy has succeeded in shifting the first BNM frequency to within 3% of the desired value as compared with the uncontrolled system. Finally, Fig. 27 contains time series of the uncontrolled, controlled via PMM, and controlled via order reduction systems along with a linear oscillation with the desired frequency for comparison.

6.2.5 Example 2: A 2-DOF System with a Symmetric Deadzone Nonlinearity

As an example of the last strategy for eigenstructure assignment, a two-degree-of-freedom system with a symmetric deadzone nonlinearity is considered. Equations (74-75) are given as

$$\begin{aligned} m_1\ddot{x}_1 + k_1(x_1 - x_2) + F(x_1) &= -g_{11}x_1 - g_{12}x_2 \\ m_2\ddot{x}_2 + (k_1 + k_2)x_2 - k_1x_1 &= -g_{21}x_1 - g_{22}x_2 \end{aligned} \qquad F(x_1) = \begin{cases} 0; & |x_1| < x_c \\ k_c(x_1 - x_c); & x_1 > x_c \\ k_c(x_1 + x_c); & x_1 < -x_c \end{cases} \tag{97}$$

where the full matrix of control gains is seen on the right hand side. Here, the case m_1=m_2=k_1=k_2=1, x_c=1.25, and k_c=1 ($\alpha = \sqrt{2}$) is considered. From equation (20), we can

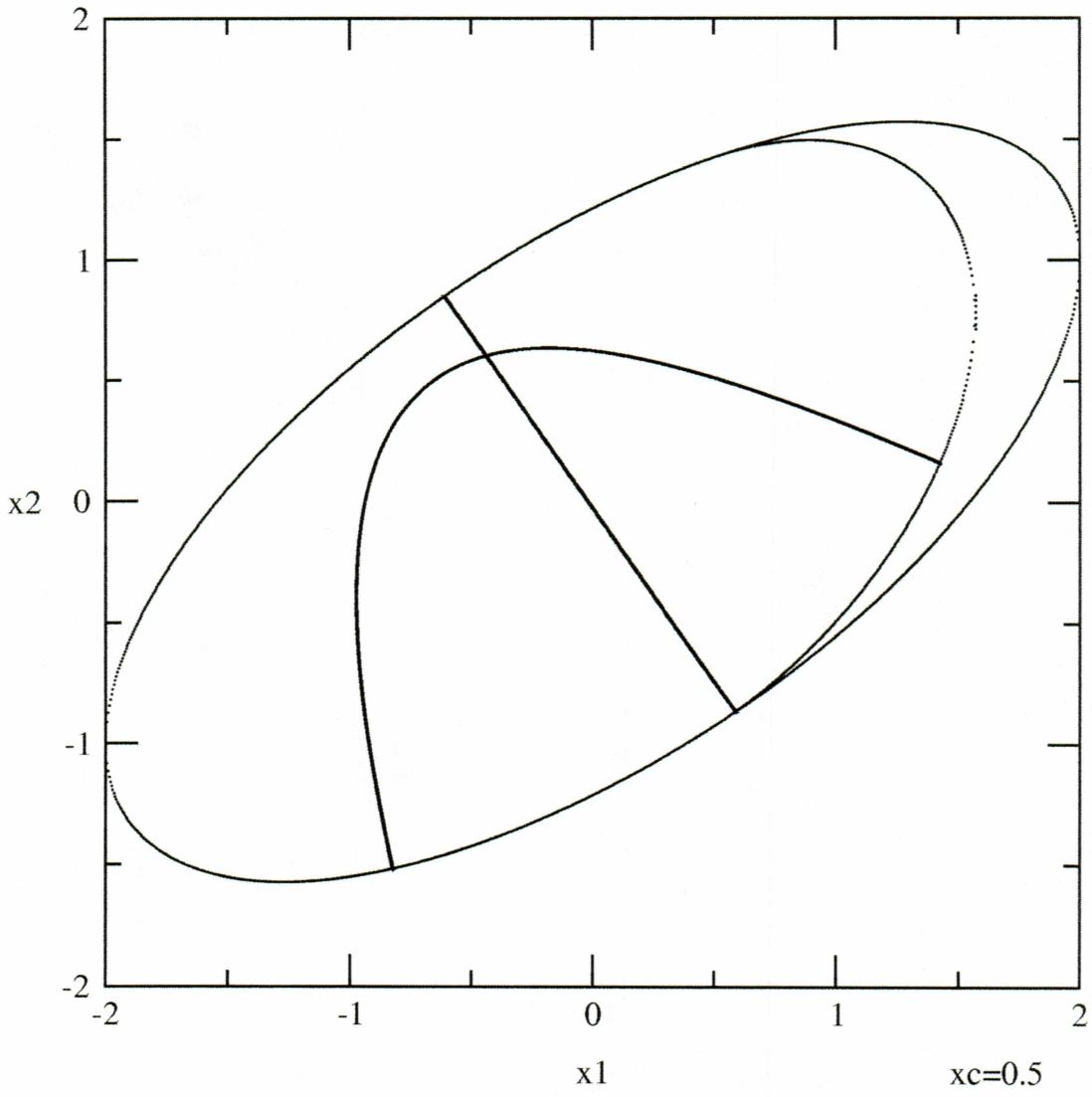

Figure 26: Numerical simulations in configuration space of the controlled BNMs (using the order reduction strategy) for the system with a bilinear clearance nonlinearity.

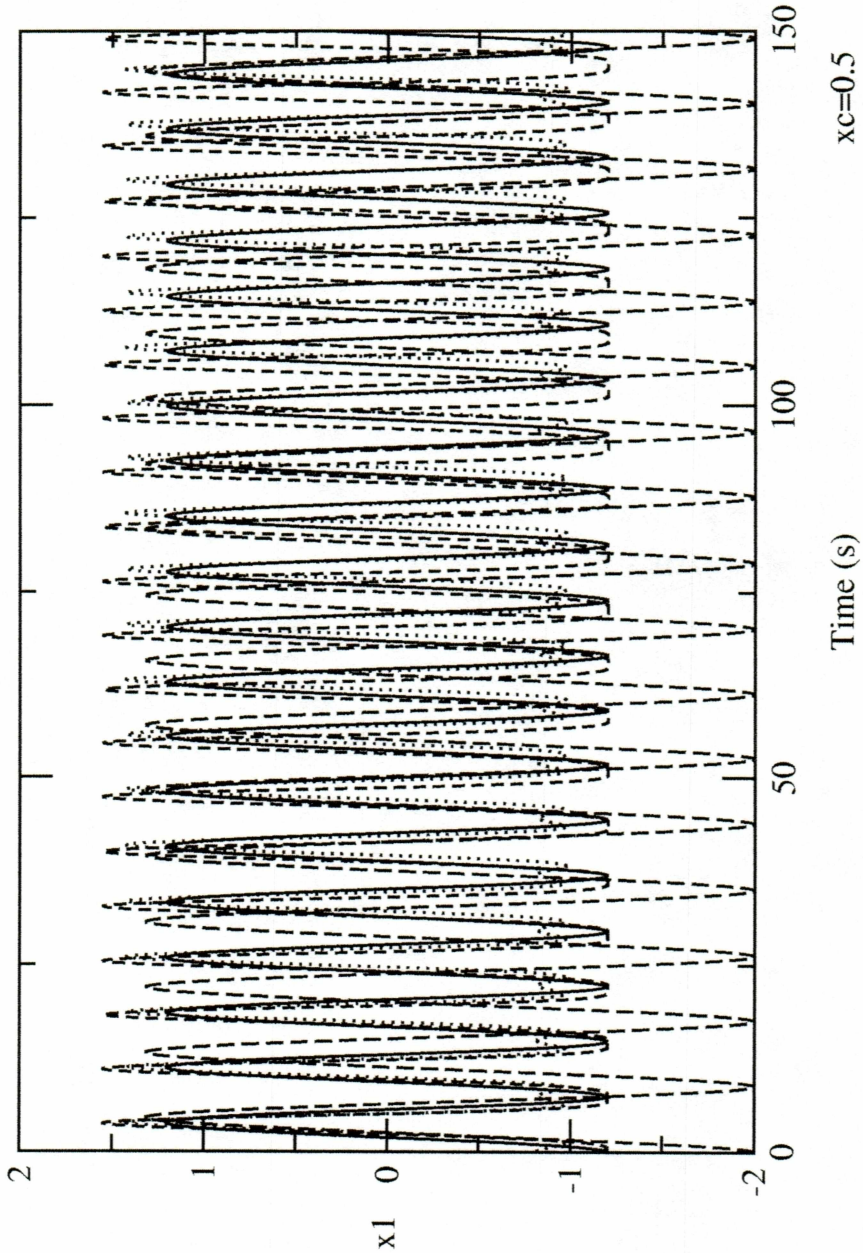

Figure 27: Time series of the uncontrolled (long-dashed), controlled via PMM (short-dashed), controlled via order reduction (dotted), and sinusoidal (with the desired frequency - solid) responses of the first NNM for the system with a bilinear clearance nonlinearity.

get the exact frequency of deadzone.

The normalized mode shapes in the first subregion are $\phi_1 = (0.851\ 0.526)^T$ and $\phi_2 = (0.526\ -0.851)^T$ and the modal frequencies are the same as those in the last example. Fig. 28 shows the numerically integrated NNMs of the uncontrolled system in the configuration space along with the equipotential boundaries for E=1. For this case the first BNM has initial condition (x_1, x_2)=(-1.789, -1.128), ρ_1=0.699 and frequency Ω_1=0.712. Using a regression analysis, the approximate slope of the curved NNM manifold in mode 1 was found as 0.665, which is 0.047 more than the linear slope of 0.618. The second mode (ρ_2=1.0, Ω_2=1.618) is identical to the linear frequency and mode shape. Assuming n actuators such that $\boldsymbol{B}=\boldsymbol{I}$ in equation (74), it is desired to shift the frequencies to $\hat{\Omega}_1$=0.85 and $\hat{\Omega}_2$=1.65 and the mode shapes to $\phi_1 = (1\ 1)^T$ and $\phi_2 = (1\ -1)^T$ by implementing the position feedback control technique with full gain matrix from Section 7.2.3.

The equivalent linear stiffness matrix $\boldsymbol{K}_{eq}$ is found from equation (87) where the frequencies ω_1=0.705, ω_2=1.618 and eigenvectors $\boldsymbol{u}_1$=(0.833, 0.554)^T, $\boldsymbol{u}_2$=(0.526 -0.851)^T (which comprise the columns of $\boldsymbol{U}$) are found from the eigenvalues and eigenvectors of

$$\begin{bmatrix} k_{eq} & -1 \\ -1 & 2 \end{bmatrix} \tag{98}$$

with k_{eq} found in equation (37). I.e. ω_1 and $\boldsymbol{u}_1$ are found with ρ_1=0.699 while ω_2 and $\boldsymbol{u}_2$ are found with ρ_2=1.0. (Note that the eigenvalues and eigenvectors of equation (102) are

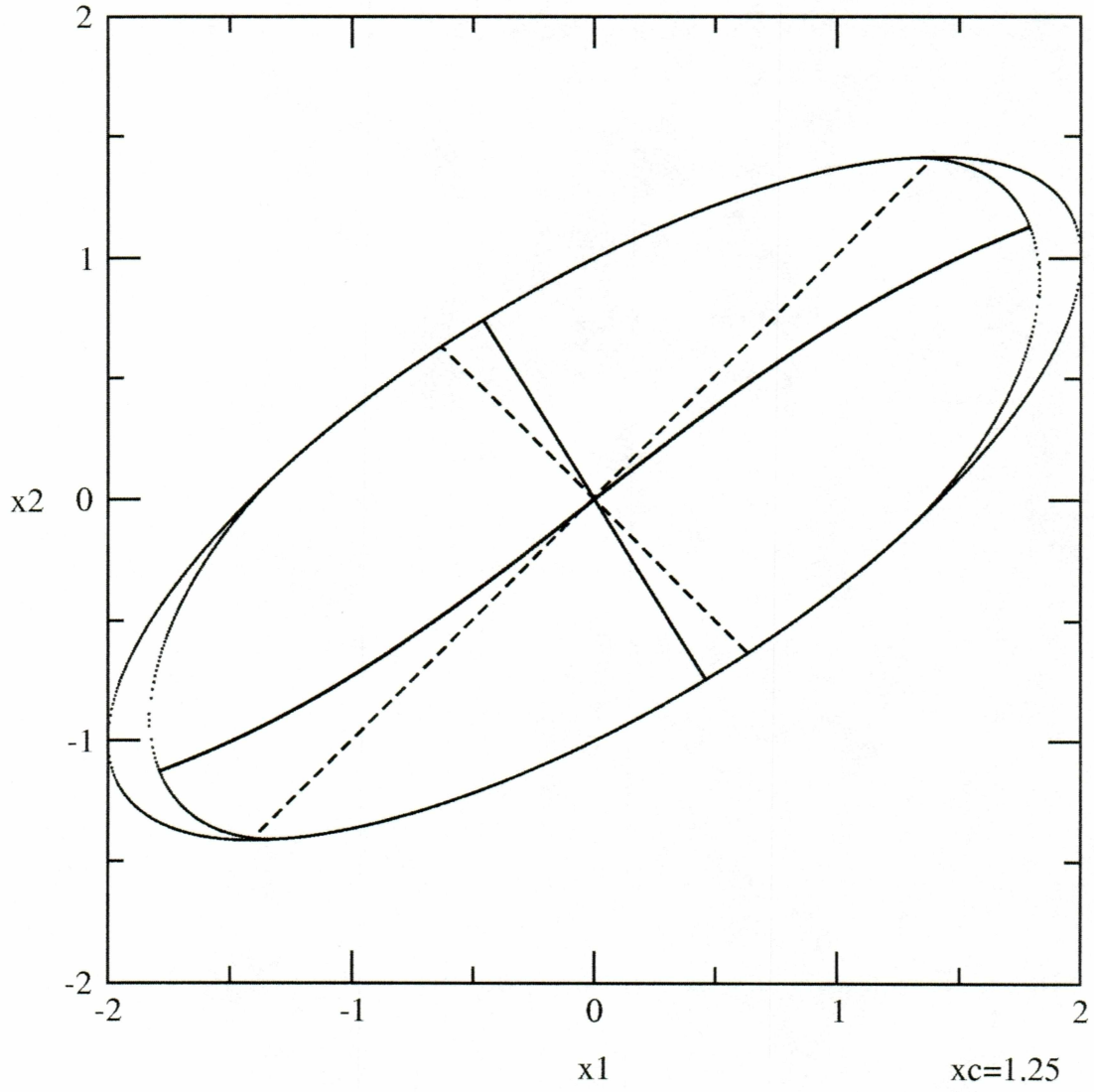

Figure 28: Numerical simulations in configuration space of the uncontrolled NNMs with $\alpha^2 = 2$ and xc = 1.25 for a two-degree-of-freedom system with a symmetic deadzone nonlinearity. The dashed lines indicate the desired mode shapes.

identical with those for the entire system found via LELSM since $\boldsymbol{M}=\boldsymbol{I}$ in this case.) Equation (88) then yields the equivalent stiffness matrix as

$$K_{eq} = \begin{bmatrix} 0.833 & 0.526 \\ 0.554 & -0.851 \end{bmatrix} \begin{bmatrix} 0.705^2 & 0 \\ 0 & 1.618^2 \end{bmatrix} \begin{bmatrix} 0.833 & 0.526 \\ 0.554 & -0.851 \end{bmatrix}^{-1} = \begin{bmatrix} 1.115 & -0.929 \\ -1.0 & 2.0 \end{bmatrix} \tag{99}$$

The desired system of equation (87) satisfies $\boldsymbol{M}_0=\boldsymbol{I}$ and

$$K_0 = \begin{bmatrix} 0.724 & 0.707 \\ 0.690 & -0.707 \end{bmatrix} \begin{bmatrix} 0.850^2 & 0 \\ 0 & 1.650^2 \end{bmatrix} \begin{bmatrix} 0.724 & 0.690 \\ 0.707 & -0.707 \end{bmatrix} = \begin{bmatrix} 1.740 & -1.0 \\ -1.0 & 1.705 \end{bmatrix} \tag{100}$$

Note that the first eigenvector has a slope of 0.953, which is 0.047 less than the desired slope of 1.0. (Recall that the approximate slope of the mode 1 manifold for the uncontrolled system was 0.047 more than the linear slope of 0.618.) Because only linearly orthogonal mode shapes can be placed (Andry *et al*, 1983), it is necessary to account for the effect of the nonlinearity as in the uncontrolled system. The gain matrix can therefore be found from equation (90) to be

$$G = \begin{bmatrix} 0.625 & -0.071 \\ 0 & -0.295 \end{bmatrix} \tag{101}$$

By finding the best fit lines through the curved NNM manifolds using least-squares regression, the accuracy of the controlled system may be found via numerical simulation. Table 5 shows how the results compare to the desired frequencies and mode shapes. The control energy is computed as 0.741 (yielding a total energy of 1.741) while Fig. 29 shows the controlled NNMs found via numerical integration with frequencies of 0.834 and 1.643.

Table 5: Controlled and uncontrolled NNM frequencies and mode shapes for Example 2

	Uncontrolled	Desired	Controlled
NNM Frequencies	$\Omega_1 = 0.712$ $\Omega_2 = 1.618$	$\Omega 1 = 0.85$ $\Omega 2 = 1.65$	$\Omega_1 = 0.834$ $\Omega_2 = 1.643$
NNM Mode shapes via regression	$\Phi_1 = \begin{pmatrix} 1 \\ 0.665 \end{pmatrix}$ $\Phi_2 = \begin{pmatrix} 1 \\ -1.618 \end{pmatrix}$	$\Phi_1 = \begin{pmatrix} 1 \\ 1 \end{pmatrix}$ $\Phi_2 = \begin{pmatrix} 1 \\ -1 \end{pmatrix}$	$\Phi_1 = \begin{pmatrix} 1 \\ 0.988 \end{pmatrix}$ $\Phi_2 = \begin{pmatrix} 1 \\ -1.004 \end{pmatrix}$

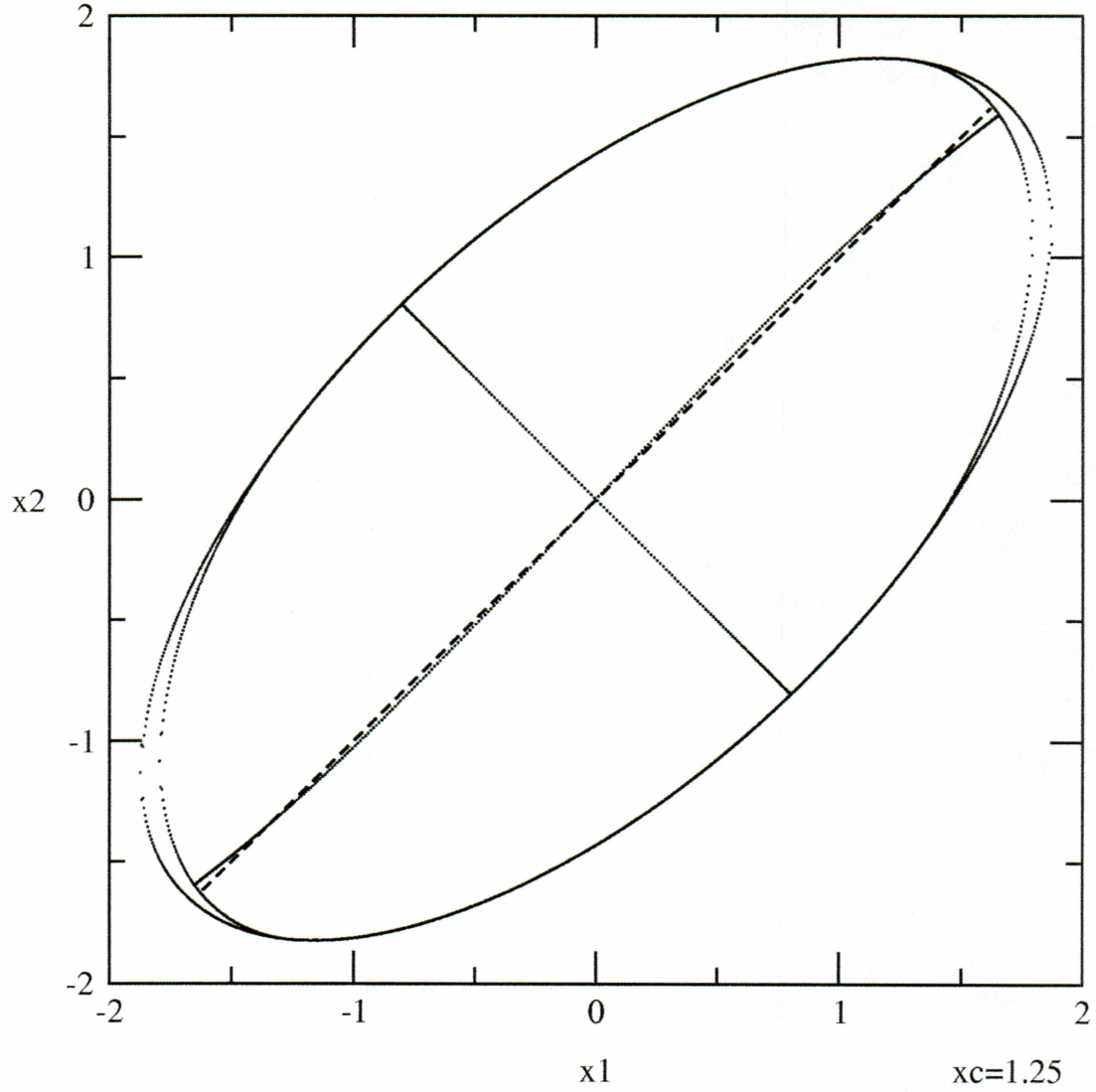

Figure 29: Numerical simulations in configuration space of the controlled NNMs (using the LELSM strategy) for the two-degree-of-freedom system with a symmetric deadzone nonlinearity. The dashed lines indicate the desired mode shapes.

Hence the control strategy has succeeded in shifting the first NNM frequency to within 12% of the desired value and the second mode's frequency to within 22% of the desired value. A regression analysis on the controlled first NNM yields the slope as 0.988 (a change of 4% of the desired value of 1.0) while the exact slope of the second mode is -1.004, which has changed from the desired value by less than 1%. Finally, Fig. 30 shows a time series of the uncontrolled and controlled system along with a linear oscillation with the desired frequency for comparison.

We should point out that the convergence of these techniques depends on the ability of PMM, order reduction, or LELSM to converge in approximating the NNM frequencies (see Butcher (1999) for further discussion). Thus, the best parameter choices to ensure convergence are those that result in weak nonlinearities (e.g. k_c small). However, the range of possible clearance (x_c) values is not limited by these methods, unlike in previous strategies (e.g. Chati *et al.* (1997); Zuo and Curnier (1994)). Finally, for nonlinearities such as bang-bang where acturator limits result in gain saturation, one must carry out the analysis to see if the desired poles are adequate or must be moved to a more realizable place. In such cases, several iterations of pole placement may be necessary.

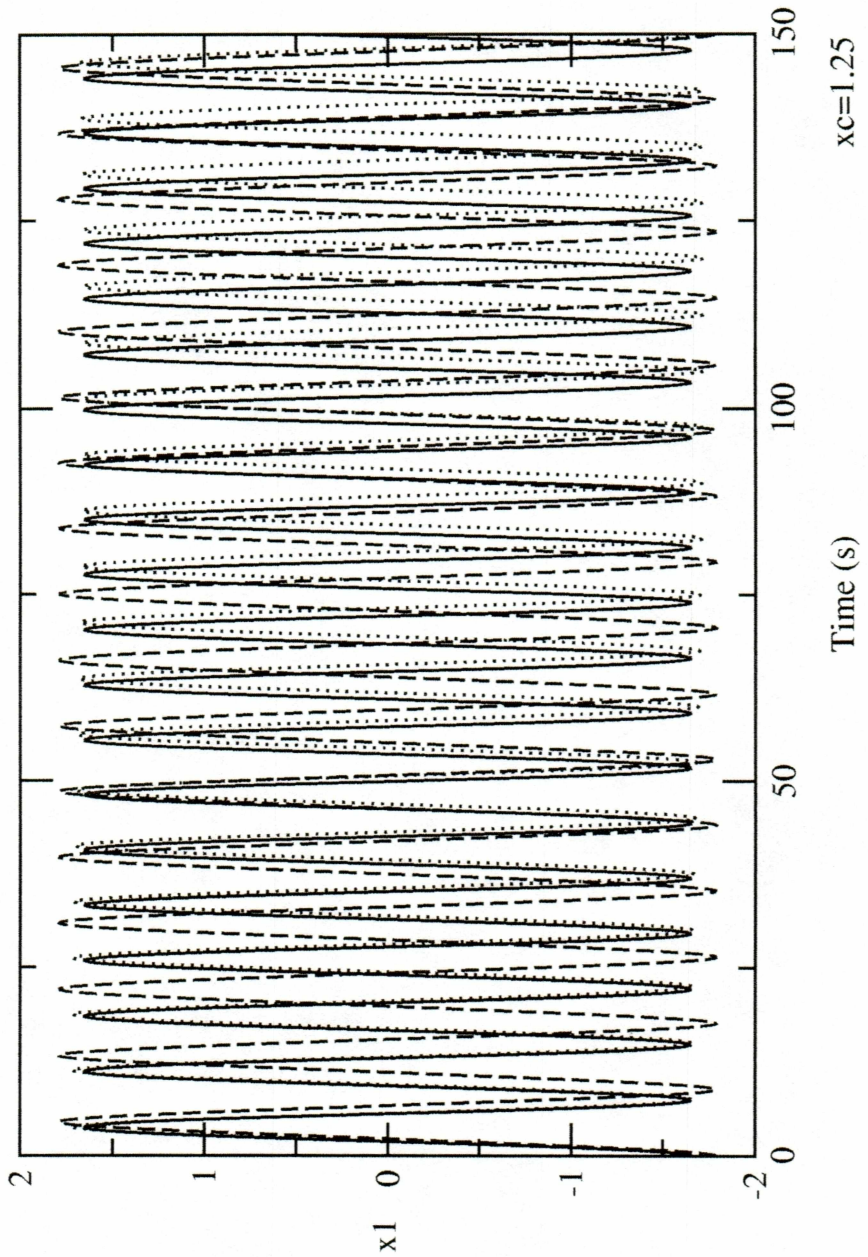

Figure 30: Time series of the uncontrolled (long-dashed), controlled via LELSM (dotted), and sinusoidal (with the desired frequency - solid) responses of the first NNM for the system with a deadzone nonlinearity.

CHAPTER 7

CONCLUSIONS

A technique for order reduction of nonsmooth trilinear systems with a deadzone and saturation nonlinearities and biliinear system with bangbang nonlinearity has been presented. First, a linear based order reduction transformation was applied to obtain a reduced order model whose frequency approximates the nonlinear normal mode (NNM) frequency of the full model. By employing the local equivalent linear stiffness method (LELSM), improved reduced order models whose frequencies are better approximations to those were obtained via linear-based order reduction. The frequencies of the resulting reduced order models were compared with those obtained from direct numerical simulations of the NNM dynamics in the configuration space and as a time series. The reduced order models obtained from the present technique use a subset of the original physical coordinates and contain the form of the nonsmooth nonlinearity of the full model.

Three techniques for eigenstructure assignment of multi-degree-of-freedom conservative vibrating systems with nonsmooth nonlinearities have been shown. By utilizing previous methods (PMM, LELSM, and order reduction) for approximating the NNM frequencies and mode shapes, these techniques result in either eigenvalue (pole) placement or full eigenstructure assignment. The strategies utilize either one actuator gain for the mode to be controlled (for order reduction), n actuator gains for n degrees of freedom (using PMM), or a full $n \times n$ matrix of actuator gains (using LELSM). These strategies are implemented via constant-gain proportional position feedback and thus do

not require the use of gain switching or a nonlinear control law. The techniques were applied to a two degree-of-freedom system with a bilinear clearance nonlinearity.

Future work will be considering more vibrating systems with different nonlinearities, and also extend the method to make it get better approximations for multi-degree of freedom systems.

REFERENCES

A. F. Vakakis, L. I. Manevitch, Y.V. Mikhlin, V. N. Pilipchuk and A. A. Zevin 1996, "Normal Modes and Localization in Nonlinear Systems". New York: John Wiley

Andronov, A. A.(Aleksandr Aleksandrovich), 1966, "Theory of Oscillators".

Andry, A.N., Jr., Shapiro, E.Y., and Chung, J.C., 1983, "Eigenstructure assignment for linear systems," IEEE *Trans. Aerospace and Electronic Systems* AES-19(5), 713-729.

Brogliato, Bernard, 1963, "Nonsmooth Mechanics: Models, Dynamic and Control."

Burton, T. D. and Rhee, W., 2000, "On the reduction of nonlinear structural dynamic models," *J. Vibration and Control* 6, 531-556.

Burton, T. D. and Young, M. E., 1994, "Model reduction and nonlinear normal modes in structural dynamics, " *Proc. ASME IMECE*, Chicago, IL, AMD 192, 9-16.

Butcher, E. A., 1999, "Clearance effects on bilinear normal mode frequencies," *J. Sound and Vibration* 224, 305-328.

Butcher, E. A.,2001, "Order Reduction of Bilinear Systems Containing a Clearance," proceedings of *18th Biennial Conference on Mechanical Vibration and Noise*, September 9-12, 2001, Pittsburgh, PA.

Chati, M., Rand, R., and Mukherjee, S., 1997, "Modal analysis of a cracked beam," *Journal of Sound and Vibration* 207, 249-270.

Chen, S.-L., and Shaw, S. W., 1996, "Normal Modes for Piecewise Linear Vibratory Systems," *Nonlinear Dynamics* 10, 135-164.

Choy, P. K., Padovan, J., and Batur, C., 1989, "Rub interactions of flexible casing rotor systems," ASME *J. Engr. for Gas Turbines and Power* 111, 652-658.

D. Dane Quinn, 1999, "An Impact Oscillator with Finite Time Collisions", Proceedings of DETC '99, 1999 ASME *Design Engineering Technical Conferences*, September 12-15, 1999, Las Vegas, Nevada, USA

Flowers, G. T. and Wu, F., 1996, "Disk shaft vibration induced by bearing clearance effects: analysis and experiments," ASME *J. Vibration and Acoustics*, 204-208.

Gaul, L. and Lenz, J., 1997, "Nonlinear dynamics of structures assembled by bolted joints," *Acta Mechanica* 125, 169-181.

Guyan, R.J., 1965, "Reduction of stiffness and mass matrices," *AIAA Journal* 3, 380.

Inman, D. J., 1989, *Vibration with Control, Measurement, and Stability*, Prentice Hall, NJ.

Jiang, D., Pierre, C., Soumier, V., and Shaw, S., 2001, "Amplitude Nonlinear Normal Modes of Piecewise Linear Systems," proceedings of *18th Biennial Conference on Mechanical Vibration and Noise*, September 9-12, 2001, Pittsburgh, PA.

M.D. Todd and L. N. Virgin, 1996, "Natural Frequency Considerations of An Impact

Oscillantor", *Journal of Sound and Vibration,* 194(3), 452-460.

Month, L.A. and Rand, R.H.,1977, "The Stability of Bifurcating PeriodicSolutions in a Two-Degree-of-Freedom Nonlinear System," Journal of Applied Mechanics, pp.782-783 .

Nayfeh, A.H. and Balachandran, B., 1995, *Applied Nonlinear Dynamics*, Wiley, New York.

Pesheck, E., Pierre, C., and Shaw, S., 2002, "Modal Reduction of a Nonlinear Rotating Beam through Nonlinear Normal Modes," ASME *Journal of Vibration and Acoustics* 124, 229-236.

Rhee, W. and Burton, T. D., 2000, "Model reduction in structures with non-analytic nonlinearities," presented at *8th Conf. on Nonlinear Vibrations, Stability, and Dynamics of Structures*, July 23-27, 2000, Virginia Polytechnic Institute and State University.

R. J. Comparin and R. Singh, 1990, "Frequency Response Characteristics Of A Multi-Degree-of-Freedom System with Clearances", *Journal of Sound and Vibration*142(1), 191-124.

R.M. Rosenberg 1962, *Journal of Applied Mechanics* 30, 7-14. "The normal modes of nonlinear *n*-degrees-of-freedom-systems".

Shaw, S. W. and Holmes, P. J., 1983, "A Periodically Forced Piecewise Linear Oscillator," *Journal of Sound and Vibration* 90, 129-155.

Shaw, S. W. and Pierre, C., 1993, "Normal modes for non-linear vibratory systems,"*J. Sound and Vibration* 164, 85-124.

Shaw, S. W., Pierre, C., and Pesheck, E., 1999, "Modal analysis-based reduced-order models for nonlinear structures- an invariant manifold approach,"*Sound and Vibration Digest* 31, 3-16

Slotine, J.-J. E. and Li, W., 1991, *Applied Nonlinear Control*, Prentice Hall, NJ.

Stengel, R. F., 1994, *Optimal Control and Estimation*, Dover, New York.

V. I. Babitsky, 1998, "Theory of Vibro-Impact Systems with Applications".

W. Weaver, Jr. and S. P. Timoshenko, D. H. Young, 1929, "Vibration Problems in Engineering", Fifth Edition.

Zuo, L. and Curnier, A., 1994, "Non-linear Real and Complex Modes of Conewise Linear Systems," *Journal of Sound and Vibration* 174, 289-313.

APPENDICES

```
                                PROGRAM DEADZONE
* THIS PROGRAM USES A RK(4,4) SUBTROUTINE TO INTEGRATE THE
   EQUATIONS
* FOR A PIECEWISE LINEAR SPRING-MASS SYSTEM.
*
      IMPLICIT DOUBLE PRECISION(A-H,O-Z)
      DIMENSION X(6), D1(6), D2(6), D3(6), TS1(100)
      PI=4.D0*DATAN(1.D0)
*
* INITIALIZE TIME, READ INPUT FILE, AND OPEN OUTPUT FILE
*
      T=0.D0
      DT1=0.01D0
      NEQ=6
      NO=0
      ener=1.d0
          alsq=2.d0
          OPEN(UNIT=9,FILE='deadzone.in')
      READ(9,*)X(1),X(3),X(2),X(4),XC,ALPHA
      CLOSE(9)
      *K1*XA=(K1+KC)*X(1) ; K1=1 ; KC=(ALPHA**2-1)*K1
      *XA IS THE AMPLITUDE WITHOUT XC
      *XA=(K1+KC)*X(1)/K1
      KC=ALPHA**2-1
      XA=(1+KC)*X(1)
      RHO=-XC/XA
      DT2=DT1/ALPHA
      DPLUS=DSQRT(1.D0-RHO**2*(1.D0-1.D0/ALPHA**2))/ALPHA-RHO/
      ALPHA**2
      DTV=DSQRT(1.D0-RHO**2*(1.D0-ALPHA**2))/ALPHA-RHO
      TOUT=1.d0*50.0D0

      IF((X(1).LE.XC).AND.(X(1).GE.(-XC)))THEN
        STIFF=1.D0
        F1=0.D0
        DT=DT1
      ELSEIF(X(1).LT.(-XC))THEN
        STIFF=ALPHA**2
        F1=-(ALPHA**2-1.D0)*XC
        DT=DT2
      ELSE
```

```
          STIFF=ALPHA**2
          F1=(ALPHA**2-1.D0)*XC
          DT=DT2
        ENDIF

        ITOP=1
        ICT=1
        OPEN(UNIT=7,FILE='deadzone.out',STATUS='UNKNOWN')
        WRITE(7,*)X(1),X(3)

*
* CHECK FOR PIECEWISE STIFFNESS BOUNDARY CLOSURE AND INTEGRATE
EQUATIONS
*
        B=1
 60CDT=ABS((XC-X(1))/X(2))
        ECDT=ABS((-XC-X(1))/X(2))
        A=X(2)
        C=A*B
        IF                                                    (((XC.EQ.2.D0).OR.(XC.EQ.(-
2.D0))).AND.(((C.LT.0.D0).AND.(A.GT.B)).OR.((A.EQ.0.D0).AND.(B.LT.0.D0))))
THEN
          TS1(ICT)=T
          ICT=ICT+1
        ENDIF
        B=A

        IF((STIFF.NE.1.D0).AND.(ECDT.LT.DT).AND.(X(2).GT.0.D0)) THEN
          CALL SWITCH2TH(T,ECDT,NEQ,X,D1,STIFF,F1)
          STIFF=1.D0
          F1=0.D0
          DT=DT1
          ITOP=1
        ELSEIF((STIFF.EQ.1.D0).AND.(CDT.LT.DT).AND.(X(2).GT.0.D0)) THEN
          CALL SWITCH(T,CDT,NEQ,X,D1,STIFF,F1)
          TS1(ICT)=T
          ICT=ICT+1
          STIFF=ALPHA**2
          F1=(ALPHA**2-1.D0)*XC
          ITOP=0
          DT=DT2
        ELSEIF((STIFF.NE.1.D0).AND.(CDT.LT.DT).AND.(X(2).LT.0.D0)) THEN
          CALL SWITCH(T,CDT,NEQ,X,D1,STIFF,F1)
```

```
          STIFF=1.D0
          F1=0.D0
          DT=DT1
          ITOP=1
        ELSEIF((STIFF.EQ.1.D0).AND.(ECDT.LT.DT).AND.(X(2).LT.0.D0)) THEN
          CALL SWITCH2TH(T,ECDT,NEQ,X,D1,STIFF,F1)
          STIFF=ALPHA**2
          F1=-(ALPHA**2-1.D0)*XC
          DT=DT1
          ITOP=1
        ELSE
           CALL RK4(T,DT,NEQ,X,D1,D2,D3,STIFF,F1)
        ENDIF
        NO=NO+1
        WRITE(7,*)X(1),X(3)
*
* LOOP TO FINAL TIME
*
        IF (T.GE.TOUT) THEN
          CLOSE(7)
          OPEN(UNIT=11,FILE='SPLS.LOG')

          AVFREQ=6.D0*PI/(TS1(4)-TS1(1))
          WRITE(11,*)TS1(1),TS1(2),TS1(3),TS1(4)
          WRITE(11,*)TS1(2)-TS1(1),TS1(3)-TS1(2),TS1(4)-TS1(3)
          WRITE(11,*)'AVFREQ=',AVFREQ
          CLOSE(11)
          STOP'PROGRAM COMPLETE'
        ELSE
          GOTO 60
        ENDIF
        END


        SUBROUTINE SWITCH(T,CDT,NEQ,X,D1,STIFF,F1)
*
* EULER INTEGRATION OF EQUATIONS AT THE SWITCHING PLANE
*
        IMPLICIT DOUBLE PRECISION (A-H, O-Z)
        DIMENSION X(6), D1(6)
*
        CALL DERIV(T,X,D1,STIFF,F1)
*
```

```
* MOVE THE STATES FORWARD ONE INTEGRATION STEP
*
      DO 88 I=1,NEQ
 88   X(I)=X(I)+CDT*D1(I)
      T=T+CDT
      RETURN
      END

      SUBROUTINE SWITCH2TH(T,ECDT,NEQ,X,D1,STIFF,F1)
*
* EULER INTEGRATION OF EQUATIONS AT THE SWITCHING PLANE
*
      IMPLICIT DOUBLE PRECISION (A-H, O-Z)
      DIMENSION X(6), D1(6)
*
      CALL DERIV(T,X,D1,STIFF,F1)
*
* MOVE THE STATES FORWARD ONE INTEGRATION STEP
*
      DO 88 I=1,NEQ
 88   X(I)=X(I)+ECDT*D1(I)
      T=T+ECDT
      RETURN
      END


      SUBROUTINE RK4(T,DELTAT, NEQ, X,D1,D2,D3,STIFF,F1)
*
* 4TH ORDER RK INTEGRATOR -- FIXED STEP SIZE -- TAKES
* INTEGRATION STEPS OF SIZE DELTAT.
*
      IMPLICIT DOUBLE PRECISION (A-H, O-Z)
      DIMENSION X(6), D1(6), D2(6), D3(6)
*
* TAKE ONE INTEGRATION STEP - REQUIRES 4 CALLS TO DERIV
*
      CALL DERIV(T,X,D1,STIFF,F1)
      DO 101 I = 1,NEQ
        D1(I)=D1(I)*DELTAT
       101   D2(I) = X(I) + 0.5D0 * D1(I)
*
      TT = T + 0.5D0 * DELTAT
      CALL DERIV(TT,D2,D3,STIFF,F1)
```

```
      DO 102 I = 1,NEQ
        D3(I)=D3(I)*DELTAT
        D1(I)=D1(I)+2.D0*D3(I)
102   D2(I)=X(I)+0.5D0*D3(I)
*
      DO 103 I = 1,NEQ
        D3(I)=D3(I)*DELTAT
        D1(I)=D1(I)+2.D0*D3(I)
103   D2(I)=X(I)+D3(I)
*
      T=T+DELTAT
      CALL DERIV(T,D2,D3,STIFF,F1)
*
* MOVE THE STATES FORWARD ONE INTEGRATION STEP
*
      DO 104 I=1,NEQ
       104  X(I)=X(I)+(D1(I)+D3(I)*DELTAT)/6.D0
*
      RETURN
      END
*
      SUBROUTINE DERIV(T,X,DX,STIFF,F1)
*
* THIS SUBROUTINE GENERATES THE EQUATIONS OF MOTION.
*
      IMPLICIT DOUBLE PRECISION (A-H,O-Z)
      DIMENSION X(6), DX(6)
*
      DX(1) = X(2)
      DX(2) = -STIFF*X(1)+X(3)+F1
      DX(3) = X(4)
      DX(4) = X(1)-2.D0*X(3)
      DX(5) = 0.
      DX(6) = 0.
      CWRITE(7,*)"V1=",DX(1), "   A1=",DX(2), "   V2=",DX(3), "   A2=",DX(4)
*
      RETURN
      END
```

program potential for deadzone

```
      IMPLICIT DOUBLE PRECISION(A-H,O-Z)
      ener=1.d0
      alsq=2.d0
      xc=0.625d0
      dx=0.005d0


      open(unit=7,file='pot.out',status='unknown')
      xmax=(2.d0*(alsq-1.d0)*xc+dsqrt(4.d0*(2.d0*alsq-1.d0)*ener
     >-2.d0*(alsq-1.d0)*xc**2))/(2.d0*alsq-1.d0)
      xmin=-xmax
      x=xmin
      write(7,*)(x-dx),(x-dx)/2.d0
      write(7,*)(x-dx),(x-dx)/2.d0+(5.d0*dx)
      write(7,*)(x-dx),(x-dx)/2.d0-(5.d0*dx)
5     y1=-(-x+dsqrt(4.d0*ener-2.d0*(alsq-1.d0)*(-x-xc)**2-(-x)**2))/2.d0
      y2=-(-x-dsqrt(4.d0*ener-2.d0*(alsq-1.d0)*(-x-xc)**2-(-x)**2))/2.d0
      write(7,*)x,y1
      write(7,*)x,y2
      x=x+dx
      if (x.le.(-xc)) goto 5

10    y1=(x-dsqrt(4.d0*ener-x**2))/2.d0
      y2=(x+dsqrt(4.d0*ener-x**2))/2.d0
      write(7,*)x,y1
      write(7,*)x,y2
      x=x+dx
      if (x.le.xc) goto 10

20    y1=(x+dsqrt(4.d0*ener-2.d0*(alsq-1.d0)*(x-xc)**2-x**2))/2.d0
      y2=(x-dsqrt(4.d0*ener-2.d0*(alsq-1.d0)*(x-xc)**2-x**2))/2.d0
      write(7,*)x,y1
      write(7,*)x,y2
      x=x+dx
      if (x.le.xmax) goto 20
      write(7,*)x,x/2.d0
      write(7,*)x,x/2.d0+(5.d0*dx)
      write(7,*)x,x/2.d0-(5.d0*dx)
      write(7,*)x,x/2.d0+(10.d0*dx)
      write(7,*)x,x/2.d0-(10.d0*dx)
      write(7,*)x,x/2.d0+(14.d0*dx)
```

```
        write(7,*)x,x/2.d0-(14.d0*dx)

        close(7)

        open(unit=8,file='eigvec1.out',status='unknown')
        open(unit=9,file='eigvec2.out',status='unknown')

        write(8,*)-1.9465,-1.2030
        write(8,*)xc,0.61803d0*xc
        write(8,*)1.9465,1.9465-0.381966*xc

        if(xc.gt.0.4595) then
          write(9,*)-0.4595,0.7435
          write(9,*)0.4595,-0.7435
        elseif(xc.lt.-0.4595) then
          write(9,*)-1.,1.-0.61803*xc
          write(9,*)1.,-1.-0.61803*xc
        else
          write(9,*)-0.4595,0.7435
          write(9,*)xc,-1.61803*xc
          write(9,*)1.,-1.-0.61803*xc
        endif

stop'complete'
end
```

```
                        PROGRAM deadzonecontrol
*
* THIS PROGRAM USES A RK(4,4) SUBTROUTINE TO INTEGRATE THE
EQUATIONS
* FOR A PIECEWISE LINEAR SPRING-MASS SYSTEM.
*
      IMPLICIT DOUBLE PRECISION(A-L,M-Z)
      DIMENSION X(6), D1(6), D2(6), D3(6), TS1(100)
      PI=4.D0*DATAN(1.D0)
*
* INITIALIZE TIME, READ INPUT FILE, AND OPEN OUTPUT FILE
*
      T=0.D0
      DT=0.001D0
      NEQ=6
      OPEN(UNIT=9,FILE='deadzone.in')
      READ(9,*)X(1),X(2),X(4),XC
      CLOSE(9)
          ener=1.666d0
          alsq=2.d0
      TOUT=5.D0*10.D0
      ITOP=1
      ICT=1
      OPEN(UNIT=7,FILE='deadzonecontrol.out',STATUS='UNKNOWN')
c     X(3)=0.5*(1.19153*X(1)+2.11252*dsqrt(1.71-X(1)**2-1.02641*X(1)*
C      XC-0.513204*XC**2))
          X(3)=0.5*(1.19153*X(1)+1.47392*dsqrt(3.51278-X(1)**2))
          WRITE(7,*)X(1),X(3)
*
* CHECK FOR PIECEWISE STIFFNESS BOUNDARY CLOSURE AND INTEGRATE
EQUATIONS
*
* GET SEVERAL PERIOD TO CALCULATE FREQUENCY
      XX1=X(1)
60    XX2=XX1
      XX1=X(1)
      IF  (((XX1*XX2).LT.0.D0).AND.(XX1.GT.0.D0))THEN
        TS1(ICT)=T
        ICT=ICT+1
    ELSEIF(((XX1*XX2).EQ.0.D0).AND.(XX1.EQ.0.D0).AND.(XX2.LT.0.D0))THEN
        TS1(ICT)=T
        ICT=ICT+1
      ENDIF
```

```
      CALL RK4(T,DT,NEQ,X,D1,D2,D3,XC)

      WRITE(7,*)X(1),X(3)

*
* LOOP TO FINAL TIME
*
      IF (T.GE.TOUT) THEN
        CLOSE(7)
        OPEN(UNIT=11,FILE='deadzone.log')
        AVFREQ=6.D0*PI/(TS1(4)-TS1(1))
        WRITE(11,*)TS1(2)-TS1(1),TS1(3)-TS1(2),TS1(4)-TS1(3)
        WRITE(11,*)'AVFREQ=',AVFREQ
        CLOSE(11)
        STOP'PROGRAM COMPLETE'
      ELSE
        GOTO 60
      ENDIF
      END


      SUBROUTINE RK4(T,DELTAT, NEQ, X,D1,D2,D3,XC)
*
* 4TH ORDER RK INTEGRATOR -- FIXED STEP SIZE -- TAKES
* INTEGRATION STEPS OF SIZE DELTAT.
*
      IMPLICIT DOUBLE PRECISION (A-L, M-Z)
      DIMENSION X(6), D1(6), D2(6), D3(6)
*
* TAKE ONE INTEGRATION STEP - REQUIRES 4 CALLS TO DERIV
*
      CALL DERIV(T,X,D1,XC)
      DO 101 I = 1,NEQ
        D1(I)=D1(I)*DELTAT
101   D2(I) = X(I) + 0.5D0 * D1(I)
*
      TT = T + 0.5D0 * DELTAT
      CALL DERIV(TT,D2,D3,XC)
      DO 102 I = 1,NEQ
        D3(I)=D3(I)*DELTAT
        D1(I)=D1(I)+2.D0*D3(I)
102   D2(I)=X(I)+0.5D0*D3(I)
```

```
*
      CALL DERIV(TT,D2,D3,XC)
      DO 103 I = 1,NEQ
        D3(I)=D3(I)*DELTAT
        D1(I)=D1(I)+2.D0*D3(I)
103   D2(I)=X(I)+D3(I)
*
      T=T+DELTAT
      CALL DERIV(T,D2,D3,XC)
*
* MOVE THE STATES FORWARD ONE INTEGRATION STEP
*
      DO 104 I=1,NEQ
104   X(I)=X(I)+(D1(I)+D3(I)*DELTAT)/6.D0
*
      RETURN
      END

      SUBROUTINE DERIV(T,X,DX,XC)
*
* THIS SUBROUTINE GENERATES THE EQUATIONS OF MOTION.
*
      IMPLICIT DOUBLE PRECISION (A-L,M-Z)
      DIMENSION X(6), DX(6)
*
      IF(X(1).LE.(-XC))THEN
        DX(2)=-2.56843D0*X(1)+1.10507*X(3)-XC
      ELSEIF((X(1).GT.(-XC)).AND.(X(1).LE.XC))THEN
        DX(2)=-1.56843D0*X(1)+1.10507*X(3)
      ELSE
        DX(2)=-2.56843D0*X(1)+1.10507*X(3)+XC
      ENDIF
*
      DX(1) = X(2)
      DX(3) = X(4)
      DX(4) = 0.975934D0*X(1)-1.74657D0*X(3)
      DX(5) = 0.D0
      DX(6) = 0.D0
*
RETURN
END
```

```
                                PROGRAM SATURATION
*
* THIS PROGRAM USES A RK(4,4) SUBTROUTINE TO INTEGRATE THE
EQUATIONS
* FOR A PIECEWISE LINEAR SPRING-MASS SYSTEM.
*
      IMPLICIT DOUBLE PRECISION(A-L,M-Z)
      DIMENSION X(6), D1(6), D2(6), D3(6), TS1(100)
      PI=4.D0*DATAN(1.D0)
*
* INITIALIZE TIME, READ INPUT FILE, AND OPEN OUTPUT FILE
*
      T=0.D0
      DT=0.001D0
      NEQ=6
      OPEN(UNIT=9,FILE='SATURATION.IN')
      READ(9,*)X(1),X(3),X(2),X(4),XC
      CLOSE(9)
      TOUT=6.D0*7.3D0
      ITOP=1
      ICT=1
      OPEN(UNIT=7,FILE='SATURATION.OUT',STATUS='UNKNOWN')
      WRITE(7,*)X(1),X(3)

*
* CHECK FOR PIECEWISE STIFFNESS BOUNDARY CLOSURE AND INTEGRATE
EQUATIONS
*

* GET SEVERAL PERIOD TO CALCULATE FREQUENCY

      XX1=X(1)
60    XX2=XX1
        XX1=X(1)
        IF(((XX1*XX2).LT.0.D0).AND.(XX1.GT.0.D0))THEN
          TS1(ICT)=T
          ICT=ICT+1

ELSEIF(((XX1*XX2).EQ.0.D0).AND.(XX1.EQ.0.D0).AND.(XX2.LT.0.D0))THEN
          TS1(ICT)=T
          ICT=ICT+1
        ENDIF
```

```
      WRITE(7,*)X(1),X(3)
      *
* LOOP TO FINAL TIME
*
      IF (T.GE.TOUT) THEN
        CLOSE(7)
        OPEN(UNIT=11,FILE='SATURATION.LOG')
        AVFREQ=6.D0*PI/(TS1(4)-TS1(1))
        WRITE(11,*)TS1(2)-TS1(1),TS1(3)-TS1(2),TS1(4)-TS1(3)
        WRITE(11,*)'AVFREQ=',AVFREQ
        CLOSE(11)
        STOP'PROGRAM COMPLETE'
      ELSE
        GOTO 60
      ENDIF
      END

      SUBROUTINE RK4(T,DELTAT, NEQ, X,D1,D2,D3,XC)
*
* 4TH ORDER RK INTEGRATOR -- FIXED STEP SIZE -- TAKES
* INTEGRATION STEPS OF SIZE DELTAT.
*
      IMPLICIT DOUBLE PRECISION (A-L, M-Z)
      DIMENSION X(6), D1(6), D2(6), D3(6)
*
* TAKE ONE INTEGRATION STEP - REQUIRES 4 CALLS TO DERIV
*
      CALL DERIV(T,X,D1,XC)
      DO 101 I = 1,NEQ
        D1(I)=D1(I)*DELTAT
101   D2(I) = X(I) + 0.5D0 * D1(I)
*
      TT = T + 0.5D0 * DELTAT
      CALL DERIV(TT,D2,D3,XC)
      DO 102 I = 1,NEQ
        D3(I)=D3(I)*DELTAT
        D1(I)=D1(I)+2.D0*D3(I)
102   D2(I)=X(I)+0.5D0*D3(I)
*
      CALL DERIV(TT,D2,D3,XC)
      DO 103 I = 1,NEQ
        D3(I)=D3(I)*DELTAT
        D1(I)=D1(I)+2.D0*D3(I)
```

```
103     D2(I)=X(I)+D3(I)
*
        T=T+DELTAT
        CALL DERIV(T,D2,D3,XC)
*
* MOVE THE STATES FORWARD ONE INTEGRATION STEP
*
        DO 104 I=1,NEQ
 104    X(I)=X(I)+(D1(I)+D3(I)*DELTAT)/6.D0
*
RETURN
END

        SUBROUTINE DERIV(T,X,DX,XC)
*
* THIS SUBROUTINE GENERATES THE EQUATIONS OF MOTION.
*
        IMPLICIT DOUBLE PRECISION (A-L,M-Z)
        DIMENSION X(6), DX(6)
*
        IF(X(1).LE.(-XC))THEN
          DX(2)=-X(1)+X(3)+XC
        ELSEIF((X(1).GT.(-XC)).AND.(X(1).LE.XC))THEN
          DX(2)=-2.D0*X(1)+X(3)
        ELSE
          DX(2)=-X(1)+X(3)-XC
        ENDIF
*
        DX(1) = X(2)
        DX(3) = X(4)
        DX(4) = X(1)-2.D0*X(3)
        DX(5) = 0.D0
        DX(6) = 0.D0
*
RETURN
END
```

```
                                PROGRAM BANGBANG
*
* THIS PROGRAM USES A RK(4,4) SUBTROUTINE TO INTEGRATE THE
EQUATIONS
* FOR A PIECEWISE LINEAR SPRING-MASS SYSTEM.
*
      IMPLICIT DOUBLE PRECISION(A-L,M-Z)
      DIMENSION X(6), D1(6), D2(6), D3(6), TS1(100)
      PI=4.D0*DATAN(1.D0)
*
* INITIALIZE TIME, READ INPUT FILE, AND OPEN OUTPUT FILE
*
      T=0.D0
      DT=0.0005D0
      NEQ=6
      OPEN(UNIT=9,FILE='bangbang.in')
      READ(9,*)X(1),X(3),X(2),X(4),DELTA
      CLOSE(9)
      TOUT=5.D0*7.3D0
      ITOP=1
      ICT=1
      OPEN(UNIT=7,FILE='BANGBANG.OUT',STATUS='UNKNOWN')
      WRITE(7,*)X(1),X(3)
*
* CHECK FOR PIECEWISE STIFFNESS BOUNDARY CLOSURE AND INTEGRATE
EQUATIONS
*

* GET SEVERAL PERIOD TO CALCULATE FREQUENCY

      XX1=X(1)
60    XX2=XX1
      XX1=X(1)
      IF(((XX1*XX2).LT.0.D0).AND.(XX1.GT.0.D0))THEN
        TS1(ICT)=T
        ICT=ICT+1

ELSEIF(((XX1*XX2).EQ.0.D0).AND.(XX1.EQ.0.D0).AND.(XX2.LT.0.D0))THEN
        TS1(ICT)=T
        ICT=ICT+1
      ENDIF
* CHANGE THE VALUE OF DEL AT THE MOMENT X1 CROSS ZERO
      IF(X(1).LE.0.D0)THEN
```

```
          DEL=-DELTA
        ELSEIF(X(1).GT.0.D0)THEN
          DEL=DELTA
        ENDIF

CALL RK4(T,DT,NEQ,X,D1,D2,D3,DEL)
WRITE(7,*)X(1),X(3)
*
* LOOP TO FINAL TIME
*
        IF (T.GE.TOUT) THEN
          CLOSE(7)
          OPEN(UNIT=11,FILE='BANGBANG.LOG')
          AVFREQ=6.D0*PI/(TS1(4)-TS1(1))
          WRITE(11,*)TS1(2)-TS1(1),TS1(3)-TS1(2),TS1(4)-TS1(3)
          WRITE(11,*)'AVFREQ=',AVFREQ
          CLOSE(11)
          STOP'PROGRAM COMPLETE'
        ELSE
          GOTO 60
        ENDIF
        END

SUBROUTINE RK4(T,DELTAT, NEQ, X,D1,D2,D3,DEL)
*
* 4TH ORDER RK INTEGRATOR -- FIXED STEP SIZE -- TAKES
* INTEGRATION STEPS OF SIZE DELTAT.
*
        IMPLICIT DOUBLE PRECISION (A-L, M-Z)
        DIMENSION X(6), D1(6), D2(6), D3(6)
*
* TAKE ONE INTEGRATION STEP - REQUIRES 4 CALLS TO DERIV
*
        CALL DERIV(T,X,D1,DEL)
        DO 101 I = 1,NEQ
          D1(I)=D1(I)*DELTAT
101     D2(I) = X(I) + 0.5D0 * D1(I)
*
        TT = T + 0.5D0 * DELTAT
        CALL DERIV(TT,D2,D3,DEL)
        DO 102 I = 1,NEQ
          D3(I)=D3(I)*DELTAT
          D1(I)=D1(I)+2.D0*D3(I)
```

```
102      D2(I)=X(I)+0.5D0*D3(I)
*
         CALL DERIV(TT,D2,D3,DEL)
         DO 103 I = 1,NEQ
           D3(I)=D3(I)*DELTAT
           D1(I)=D1(I)+2.D0*D3(I)
103      D2(I)=X(I)+D3(I)
*
         T=T+DELTAT
         CALL DERIV(T,D2,D3,DEL)
*
* MOVE THE STATES FORWARD ONE INTEGRATION STEP
*
         DO 104 I=1,NEQ
104      X(I)=X(I)+(D1(I)+D3(I)*DELTAT)/6.D0
*
RETURN
END

         SUBROUTINE DERIV(T,X,DX,DEL)
*
* THIS SUBROUTINE GENERATES THE EQUATIONS OF MOTION.
*
         IMPLICIT DOUBLE PRECISION (A-L,M-Z)
         DIMENSION X(6), DX(6)
*
         DX(1) = X(2)
         DX(2) = -X(1)+X(3)-DEL
         DX(3) = X(4)
         DX(4) = X(1)-2.D0*X(3)
         DX(5) = 0.D0
         DX(6) = 0.D0
*
RETURN
END
```

PROGRAM REGRESSION

```
*
IMPLICIT DOUBLE PRECISION(A-H,O-Z)
DIMENSION X(600), Y(600)
*
* INITIALIZE TIME, READ INPUT FILE, AND OPEN OUTPUT FILE
*
      OPEN(UNIT=9,FILE='deadzoneregression.in')
      N=444
      N1=0
5     N1=N1+1
      READ(9,*)X(N1),Y(N1)
      IF(N1.LT.N) THEN
       GOTO 5
      ENDIF
      CLOSE(9)
*
      SUMX=0
      SUMY=0
      SUMXY=0
      SUMX2=0
      ST=0
      SR=0
*
      N2=0
10    N2=N2+1
      SUMX=SUMX+X(N2)
      SUMY=SUMY+Y(N2)
      SUMXY=SUMXY+X(N2)*Y(N2)
      SUMX2=SUMX2+X(N2)**2
      IF(N2.LT.N) THEN
       GOTO 10
      ENDIF
*
      XM=SUMX/N
      YM=SUMY/N
      A1=(N*SUMXY-SUMX*SUMY)/(N*SUMX2-SUMX**2)
      A0=YM-A1*XM
      N3=0
20    N3=N3+1
      ST=ST+(Y(N3)-YM)**2
      SR=SR+(Y(N3)-A1*X(N3)-A0)**2
      IF(N3.LT.N)THEN
```

```
          GOTO 20
        ENDIF
        SYX=(SR/(N-2))**0.5
        R2=(ST-SR)/ST
*
        OPEN(UNIT=7,FILE='deadzoneregression.out',STATUS='UNKNOWN')
        WRITE(7,*)'A1=',A1,'    ','A0=',A0,'    ','ST=',ST,'    ','SR=',SR,'    ','SYX=',SYX,'
','R2=',R2
CLOSE(7)
*
END
```